

# **COMBINING CYCLIC PEPTIDES WITH METAL COORDINATION**

A Thesis  
Presented to  
The Academic Faculty

by

Kimberly Ann Arrowood

In Partial Fulfillment  
of the Requirements for the  
Master's Degree in Chemistry in the  
School of Chemistry and Biochemistry

Georgia Institute of Technology  
August 2009

# COMBINING CYCLIC PEPTIDES WITH METAL COORDINATION

Approved by:

Dr. Marcus Weck, Advisor  
School of Chemistry and Biochemistry  
*Georgia Institute of Technology*

Dr. David Collard  
School of Chemistry and Biochemistry  
*Georgia Institute of Technology*

Dr. Julia Kubanek  
School of Chemistry and Biochemistry  
*Georgia Institute of Technology*

Date Approved: May 14, 2009

## **ACKNOWLEDGEMENTS**

I wish to thank my advisor, Marcus Weck for his support during these past few years. I would like to thank all the current and former Weck group members that have helped me out during my time at the Georgia Institute of Technology. Thanks especially to Dr. Gerhardt for teaching me what I needed to know to carry on the lactide and peptide projects. Also thanks to Trey Pinon and Si Kyung Yang for their help as we made it through each of the different hurdles of our time as graduate students. I also need to thank Dr. Madhavan for her guidance on the peptide project. Finally, I would like to thank my husband for his loving support and encouragement during the time I was in school. In addition, my family provided much encouragement and support during my time in graduate school.

# TABLE OF CONTENTS

	Page
ACKNOWLEDGEMENTS	iii
LIST OF FIGURES	v
LIST OF ABBREVIATIONS	viii
SUMMARY	x
<u>CHAPTER</u>	
1 Introduction	1
Supramolecular Chemistry and Peptides	2
Prior Use of Cyclic Peptides in Supramolecular Chemistry	6
2 Cyclic Peptide Synthesis Design and Results	13
Research Design	13
Solution Phase	14
Solid Phase	18
Experimental Section	28
Future Work	31
APPENDIX A: 2-Dimensional NMR data of Cyclic Peptides	34
APPENDIX B: An Alkyne Functionalized Lactide Monomer	53
Introduction	53
Results and Discussion	53
Conclusions	57
Experimental Section	58
Raw Data	62
REFERENCES	74



## LIST OF FIGURES

	Page
Figure 1.1: Cyclic peptide vertical self-assembly through hydrogen bonding	7
Figure 1.2: Bis-pincer molecule	9
Figure 1.3: Pincer molecule joining two cyclic peptides together	9
Figure 1.4: Alignment of peptide nanotubes in lipid membrane	10
Figure 1.5: Monopyridyl cyclic peptide species with bis-pincer	12
Figure 2.1: Initial linear octapeptide to be synthesized by Warren Gerhardt	13
Figure 2.2: Di-substituted pyridylalanine cyclic peptide	14
Figure 2.3: Initial solution phase synthetic scheme	15
Figure 2.4: Di-substituted pyridylalanine cyclic octapeptide route containing two N-methylated phenylalanines	17
Figure 2.5: Wang resin	19
Figure 2.6: Solid-phase approach with N(methylated) alanines and phenylalanines	20
Figure 2.7: Kenner “Safety-catch” Resin synthesis	21
Figure 2.8: Monosubstituted pyridylalanine coordinated to bis-pincer compound	22
Figure 2.9: $^1\text{H}$ NMR spectrum of compound 6	23
Figure 2.10: Mass spectrum of compound 6	23
Figure 2.11: $^1\text{H}$ NMR spectrum of cyclic peptide and bis-pincer complex	24
Figure 2.12: Linear octapeptide containing N-methylated alanines	25
Figure 2.13: Mass spectrum for compound 7	27
Figure 2.14: $^1\text{H}$ NMR spectrum of compound 7	28
Figure A.1: COSY data of mono-substituted pyridylalanine cyclic peptide	34
Figure A.2: COSY 7.2-9.0 ppm range	35
Figure A.3: COSY 7.2-9.0, 4.0-5.5 ppm	36

Figure A.4: COSY 1.0-6.0 ppm	37
Figure A.5: TOCSY data of compound 6	38
Figure A.6: TOCSY 4.0-9.0, 4.0-0.0 ppm	39
Figure A.7: ROESY data of compound 6	40
Figure A.8: COSY data of di-substituted pyridylalanine cyclic peptide	42
Figure A.9: COSY 7.0-9.0 ppm	43
Figure A.10: COSY 5.5-0.0 ppm	44
Figure A.11: COSY 9.0-7.0, 5.5-4.5 ppm	45
Figure A.12: COSY 5.5-4.3, 2.4-3.4ppm	46
Figure A.13: COSY 5.6-4.2, 0.5-1.5 ppm	47
Figure A.14: HSQC data of di-substituted pyridylalanine cyclic peptide	48
Figure A.15: HSQC 150-120, 7.0-9.0 ppm	49
Figure A.16: HSQC 57-44, 4.3-5.7 ppm	50
Figure A.17: HSQC 50-5, 0-3.5 ppm	51
Figure B.1: Lactide monomer	53
Figure B.2: Synthesis of lactide monomer	54
Figure B.3: Ring opening polymerization of functionalized monomer and subsequent post-polymerization reaction	55
Figure B.4: $^1\text{H}$ NMR spectrum for 2-hydroxypent-4-ynoic acid (300 MHz)	62
Figure B.5: $^{13}\text{C}$ NMR spectrum for 2-hydroxypent-4-ynoic acid (300 MHz)	63
Figure B.6: $^1\text{H}$ NMR spectrum for 2-(2-bromopropanolyoxy)pent-4ynoic acid (300 MHz)	64
Figure B.7: $^1\text{H}$ NMR spectrum for 2-(2-iodopropanolyoxy)pent-4ynoic acid (300 MHz)	65

Figure B.8: $^1\text{H}$ NMR spectrum of 3-methyl-6-(pro-2-ynyl)-1,4-dioxane-2,5-dione (300 MHz)	66
Figure B.9: $^{13}\text{C}$ NMR spectrum for 3-methyl-6-(pro-2-ynyl)-1,4-dioxane-2,5-dione (300 MHz)	67
Figure B.10: $^{13}\text{C}$ NMR spectrum for 3-methyl-6-(pro-2-ynyl)-1,4-dioxane-2,5-dione 10ppm-170ppm (300 MHz)	68
Figure B.11: $^1\text{H}$ NMR spectrum of lactide copolymer	69
Figure B.12: $^{13}\text{C}$ NMR spectrum of lactide copolymer (300 MHz)	70
Figure B.13: $^{13}\text{C}$ NMR spectrum of lactide copolymer region 15ppm-31ppm (300 MHz)	71
Figure B.14: $^{13}\text{C}$ NMR spectrum Lactide Copolymer region 66-80ppm (300 MHz)	72
Figure B.15: $^{13}\text{C}$ NMR spectrum Lactide Copolymer 165-171ppm (300 MHz)	73

## LIST OF ABBREVIATIONS

Boc	<i>tert</i> -Butyl dicarbamate
COSY	CORrelation SpectroscopY
DCC	dicyclohexylcarbodiimide
DIEA	diisopropylethylamine
DMAP	Dimethylaminopyridine
DMF	<i>N,N</i> -dimethylformamide
Fmoc	9-Fluorenyl methyl carbamate
HATU	Tetramethyluronium hexafluorophosphate
HOAt	Hydroxy-7-azabenzotriazole
HOBt	1-Hydroxy-benzotriazole
HPLC	High Perfomance Liquid Chromatography
HSQC	Heteronuclear Single Quantum Coherence
MALDI-MS	Matrix Assisted Laser Desorption/ Ionization- Mass Spectrometry
MeOH	Methanol
NMR	Nuclear Magnetic Resonance
PLA	Poly(lactide)
PyBOP	Benzotriazole-1-ly-oxytrispyrrolidinophosphonium
Pyr	L-4-pyridylalanine
ROESY	Rotating frame Overhauser Effect SpectroscopY
TFA	Trifluoroacetic acid
TIPS	Thermally induced phase separation
TLC	Thin Layer Chromatography

TOCSY

Total COrrrelation SpectroscopY

## SUMMARY

This thesis targets cyclic peptide supramolecular structures for biomaterial applications. The introduction gives a brief insight into supramolecular interactions, peptides, and their application in biomaterials. These supramolecular interactions range from the weak forces of electrostatics and van der Waals interactions, to hydrogen bonding and metal-coordination. The application of peptides and supramolecular interactions has become a highly studied area of chemistry, which has quickly gotten attention in the area of biomaterials. The use of peptides in biomaterials seems obvious since *in vivo* rejection of this material might be limited. Nature can be used as a blue print to direct the path for hydrogen bonding motifs and metal-coordinating interactions and can be applied potentially towards supramolecular biomaterials. Finally, the introduction reviews the use of cyclic peptides and accounts for the synthetic design of the cyclic octapeptide to be used throughout the thesis work.

The second chapter of the thesis provides the details by which the synthetic scheme for creating the linear peptides of interest and ultimately the cyclic peptides is described in detail. Many synthetic challenges were met and overcome during this thesis work; the most notable was overcoming purification challenges and poor amino acid coupling reactions that resulted in low yields. This thesis focuses primarily on the di-substituted pyridylalanine cyclic octapeptide, however much of the initial work on the mono-substituted cyclic octapeptide was carried out in tandem allowing for comparison of the two peptides necessary for future work.

# CHAPTER 1

## INTRODUCTION

Throughout the past few centuries chemists have become increasingly competent with making and breaking chemical bonds. With each passing year, more is learned about covalent bonding, orbitals, and how to manipulate a compound and reaction to obtain the desired result. A recent growing area of chemistry is supramolecular chemistry. This area is a multidisciplinary field that focuses on electrostatics, hydrogen bonding, van der Waals interactions, donor-acceptor interactions, metal coordination, and  $\pi$ - $\pi$  interactions.<sup>1,2</sup> Often, these interactions are just thought of as stabilizing interactions and less often about how to use these interactions to benefit a desired application. Until recently most of the focus has been on covalent interactions, however the intermolecular and intramolecular interactions of molecules have become an increasingly popular area of research. The focus of how these interactions can be modified and exploited to chemically do new things or to mimic nature has provided a vast array of different applications for many different types of materials.<sup>3</sup> Supramolecular chemistry has a unique impact in chemistry because the different interactions that are available for a chemist to choose from can be tailored for the application and environment for which the final compound will be used. Unlike covalent bonding, however, the weak interactions that hold the supramolecular architectures together are solvent dependent which must be kept in mind especially when the architecture employs hydrogen bonding in an aqueous or polar protic environment. Considering for example that the hydrogen bond is weaker than most metal coordination interactions, knowing how to optimize the hydrogen bonding arrays using appropriate solvents may be just as effective synthetically as using a metal coordinated species.

Supramolecular architectures have numerous applications in all areas of science; however, one of the fastest growing areas of research uses supramolecular architectures for biomaterials purposes.<sup>4</sup> Biomaterials are materials that should be compatible with the body, generally the final application is for use in the human body, however many applications use mice or rabbits as test subjects.<sup>5</sup> Some of the most widely proposed uses for the supramolecular biomaterials are as delivery applications of drugs or genes.<sup>6, 7</sup> One benefit of drug delivery by this route is a targeted applications where the drug is administered right into the intended area where then the supramolecular architecture can break down releasing the drug.<sup>6</sup> Another interesting application uses three strands of self-complementary peptides to create a collagen-like triple helix that is said to be highly biocompatible and biostable.<sup>8</sup> Other peptides have also been used for various biomaterials applications including nanowires, scaffolds, channels or pores.<sup>9, 10</sup> The use of peptides in this area of chemistry is a natural choice since these materials need to be biocompatible and the human body already employs peptides and amino acids for its daily uses. Another aspect that makes peptides an excellent choice is that they are responsive to stimuli; thus, a change in environmental pH, temperature, or polarity can affect the manner in which the biomaterial responds. A review by Stevens *et al.* nicely highlights the different aspects of peptide biomaterials in reference to their supramolecular interactions and applications.<sup>11</sup> The use of peptides can offer many different advantages to biomaterials in the area of supramolecular chemistry.

### **Supramolecular Chemistry and Peptides**

On a daily basis many chemists struggle to synthesize compounds that nature designs and synthesizes, in unique ways. Some of the most stunning compounds that nature designs are peptides, with the secondary, tertiary and even quaternary structures that lead to different functions. With small changes in the primary structure of the



peptide, the other structures are all affected leading to a rise in differences of hydrophobicity, overall structure, and function.<sup>12</sup> The primary sequence of amino acids can be used to tailor the outcome of the peptide's structure and potentially its function. Since nature does use peptides so frequently it seems natural to take advantage of the many aspects of peptides and amino acids in supramolecular chemistry to create new applications for biomaterials.

Peptides offer many advantages for biomaterials applications. One major advantage is the vast array of functional groups that are available or synthesized on a peptide backbone. Another major advantage of utilizing peptides is that using the twenty common amino acids enables the body to not see the biomaterial as a foreign object, thus reducing the likelihood of it rejecting or attacking the device. This is increasingly important as much money and time is spent on research to ensure that a device is both safe and effective inside the body. In addition, the route by which peptides are created, by joining amino acids together, allows for the primary structure to be changed and unnatural amino acids to be incorporated. Unnatural or D-amino acids are becoming more and more commercially available as well as other synthetically interesting amino acids that can be used immediately or undergo further chemical reactions to create new peptides. Another advantage that proteins and peptides utilize is the many different stabilizing interactions to create the larger structures that are necessary for biological function. Covalently, peptides use disulfide bonds which can introduce strain or lock the peptide into a specific conformation.<sup>13</sup> As mentioned previously, peptides can also take advantage of supramolecular interactions like self-association, hydrogen bonding, and metal-coordination to create elaborate structures. Each of these interactions has its own advantages and disadvantages that enable different applications to be more appropriate for certain types of interactions.

Self-associating peptides often have different domains which are very dissimilar in their hydrophobic properties. For example one domain of an  $\alpha$ -helix may be very

hydrophobic, whereas a  $\beta$ -sheet located close to the helix can be more hydrophilic in nature. These interactions become much more important in the overall structure once domains have been established. Many supramolecular architectures that use hydrophobic interactions appear as micelles, vesicles, or bilayers.<sup>14</sup> Applications for such architectures include scaffolding, drug delivery, tissue engineering, and lipid membrane surfactants.<sup>15-19</sup> This type of self-assembly is more of a non-directed route as opposed to hydrogen bonding or metal-coordination that are a directed route because the bonding interactions can be tailored to promote binding in a certain direction or orientation.

One of the most widely known uses of hydrogen bonding exists among DNA base pairs, which have been studied extensively since the 1950's.<sup>20</sup> The bond between a hydrogen atom attached to an electronegative atom and the lone pair of another electronegative atom in itself is a weak interaction, however nature and more recently chemists have learned how to maximize these interactions based on donor acceptor placement.<sup>21</sup> The hydrogen bond donor is the hydrogen attached to an electronegative atom and the hydrogen bond acceptor is the electronegative atom with a lone pair. By knowing how to properly arrange donors and acceptors on a molecule the strength of the overall intermolecular forces can be tuned.<sup>22</sup> Peptides are unique in that they have many different ways to hydrogen bond both using the main-chain and side-chains. In main-chain hydrogen bonding, the amide hydrogen often serves as donor while the oxygen on the carbonyl group is often the acceptor. Side-chains of peptides also contribute to hydrogen bonding motif both in bonding and directing the conformation of the domain. One of the most unique aspects of hydrogen bonding is that based on the conformation of the amino acids there are different types of secondary structures that arise. Pauling and Corey lead the way with their work in the area of determining how the different hydrogen bonding domains were comprised.<sup>23, 24</sup> There are helical as well as planar hydrogen bonding domains. Each  $\alpha$ -helix is comprised of 3.7 amino acids where the carbonyl oxygen hydrogen bonds with the amide hydrogen on an amino acid four residues away,

thus giving rise to the  $n+4$  notation. These can be either right-handed or left-handed helices and tend to have different hydrophobicities on the faces of the helix. The planar or sheet motifs are referred to as  $\beta$ -sheets or  $\beta$ -strands. These are extended lengths of polypeptides that can hydrogen bond with each other. Based on how the sheets align gives rise to the parallel versus antiparallel hydrogen bonding.

However, hydrogen bonding is not just limited to peptide chains; their use in the biomaterials realm can be combined with polymers to increase their effectiveness. One such application is for poly(ethylene urethane) to be used as a cardiovascular device in which two polymers of different mechanical moduli are hydrogen bonded together to create the necessary elastomeric properties needed for the application.<sup>25</sup> Hydrogen bonding is also being used in caprolactone polymers to obtain the thermoplastic properties necessary for other cardiovascular applications.<sup>26</sup> Potential drug delivery applications also arise from using a sacrificial template along with hydroxypropylcellulose and poly(acrylic acid) in a layer by layer method to create an hollow microsphere based on hydrogen bonding interactions.<sup>27</sup> Other methods also rely on encapsulation but the hydrogen bonding interaction is involved in hydrogen bonding the drug and material together not the material and the body.<sup>28</sup> Peptide nanotubes that are used for transport or even for electronically active biomaterials are also being designed using hydrogen bonding and peptide-based biomaterials.<sup>29</sup>

The last supramolecular interaction to discuss is metal coordination, though solvent dependent, it can be amongst the strongest of all the supramolecular interactions. The predominate advantage of metal-coordination is the highly directional binding that occurs between the metal and the desired ligand. Whereas, with hydrogen bonding there may be multiple donors and acceptors, using metal-coordination interactions there is a clearly defined metal center and binding ligand(s), which can be optimized over other metal ligand interactions to be thermodynamically favorable. Chemists take their inspiration from nature in proteins like the zinc finger in which cysteine and histidine

bind the zinc ion to make the protein active for RNA transcription.<sup>30, 31</sup> However, the science of supramolecular architectures and metal coordination really grew in the area of rotaxanes, calixarenes, calixcrowns, and other larger coordinating ligands.<sup>32-35</sup> The area of biomaterials using metal coordination, while synthetically challenging, is not new for peptide chemistry. To date one of the most elegant uses of metal peptide interactions is the ruthenium and peptide coils.<sup>36</sup> This research has inspired part of the design of this thesis' supramolecular architecture, which will be discussed in greater detail later. In addition there are other systems that use different peptide ligands to mimic collagen and receptors.<sup>37, 38</sup> Unfortunately, most applications that employ metal-peptide coordination still lie outside the realm of biomaterials.

Each of the different supramolecular interactions has their own place within the world of biomaterials, as well as helping to contribute to this thesis. Their relationship will be further elaborated on later on during this work to show how each type of interaction, no matter how small, plays a large role in helping cyclic peptides find its place within biomaterials applications.

### **Prior Use of Cyclic Peptides in Supramolecular Chemistry**

Ghadiri has pioneered the work in the area of cyclic peptides along with metal-peptide coordination since the early 1990's.<sup>39-41</sup> These peptides are small cyclic peptides that have even numbers of alternating D- and L-amino acids that allow the backbone of the ring to be planar.<sup>41</sup> This planar ring allows for the amide proton and the carbonyl of another ring to intermolecularly hydrogen bond allowing for vertical self-assembly of peptide nanotubes, see Figure 1.1.

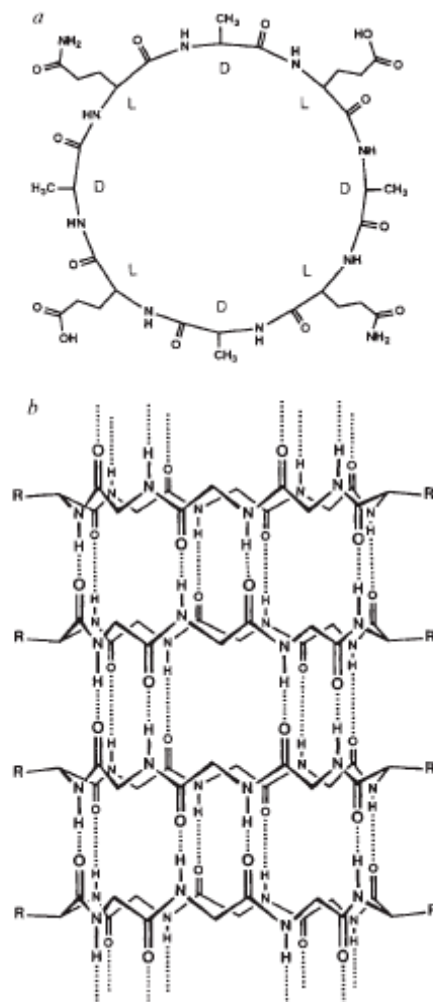


**Figure 1.1** Cyclic peptide vertical self-assembly through hydrogen bonding. Image taken from reference<sup>41</sup>

This antiparallel  $\beta$ -sheet stacking produces a highly ordered peptide nanotube that allows for the amino acid side-chains to exist on the periphery of the cyclic peptide. This is important to remember for application purposes because the peptide's hydrophobicity can easily be changed by changing the amino acids. Since the residues of the amino acids lie on the outside of the cyclic peptide structure the inner core of the nanotube is hollow. The diameter of the hollow nanotube can be tuned by changing the number of amino acids within the cyclic peptide. For example a cyclic octapeptide has an inner diameter of 7.5 Å, while an cyclic dodecapeptide has an inner diameter of 13 Å.<sup>42, 43</sup> The

inner diameter of the nanotube plays a critical role in its applications. The predominant application for peptide nanotubes is as transmembrane channels, where the membrane is imbedded into a lipid bilayer and allows for the passage of small molecules or ions through the nanotube. Water molecules, glucose, glutamic acid, sodium and potassium ions have all been shown to pass through different sized transmembrane nanotubes.<sup>44-48</sup> Furthermore, cyclic peptides can be used inside an existing pore for binding.<sup>49</sup> In contrast to using the inner core for transport, a 1,4,5,8-naphthalenetetracarboxylic diimide side-chain attached to a cyclic peptide has been used to create an electronically active peptide nanotube.<sup>29</sup> Another cyclic peptide system takes advantage of the close side-chain interactions to control fluorescent signal between homo and heterodimers.<sup>50</sup> Cyclic peptides have also shown to be active as antiviral and antibacterial agents.<sup>51, 52</sup> Biosensors have also been proposed by supporting a cyclic peptide nanotube onto a self-assembled monolayer.<sup>53</sup>

The biomaterial applications of cyclic peptides provide the motivation for this thesis: to improve the transport of small molecules across a lipid bilayer with cyclic peptides and metal-coordination. A well-designed system in which a cyclic peptide species can undergo metal-coordination with a metal complex could potentially allow for a well-defined supramolecular arrays consisting of peptide nanotubes that effectively maximize the transport of small molecules or ions across a lipid bilayer. The hydrophobic nature of amino acids can be used to make the periphery of the cyclic peptides hydrophobic, thus allowing for better interaction with the hydrophobic lipid bilayer. Hydrogen bonding between cyclic peptides allows for the vertical self-assembly of the nanotubes and minimizes defects. The last supramolecular interaction used is metal coordination which can tether two cyclic peptide nanotubes to one another. The proposed route to joining the cyclic peptides together is through a pincer molecule. A pincer, as shown in Figure 1.2, can coordinate to a cyclic peptide through nitrogen containing amino acids, which will be discussed later. This pincer complex has been

studied by the Weck group and others and has shown to be effective due to being quantitative, fast, and reversible in different solvents.<sup>54, 55</sup>

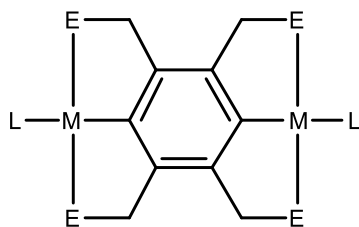


**Figure 1.2** Bis-pincer molecule: M= metal center (Pd, Pt), L= Ligand, E=neutral electron donor (S, N, P).

Each metal center of the pincer complex takes advantage of the platinum or palladium's preference to be square planar with four ligands. The nomenclature comes from what atom occupies the two electron donor positions labeled E. If, for example they are occupied by sulfur the resulting complex is called a SCS-pincer complex, while the use of a nitrogen would lead to an NCN-pincer complex.<sup>56</sup> Figure 1.3 shows how a single bis-pincer molecule can coordinate to two cyclic peptides.

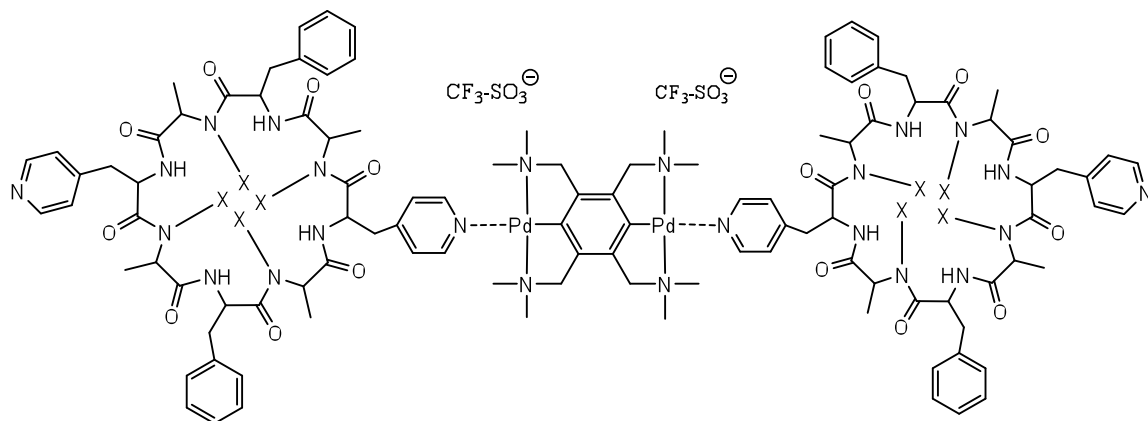


**Figure 1.3** Pincer molecule joining two cyclic peptides together. (X=H or CH<sub>3</sub>)

By aligning the peptide nanotubes in a vertical fashion with one another the transport across the membrane is thought to be greater because the nanotubes can align the plane of the peptide ring parallel with the air-water interface.<sup>57</sup>

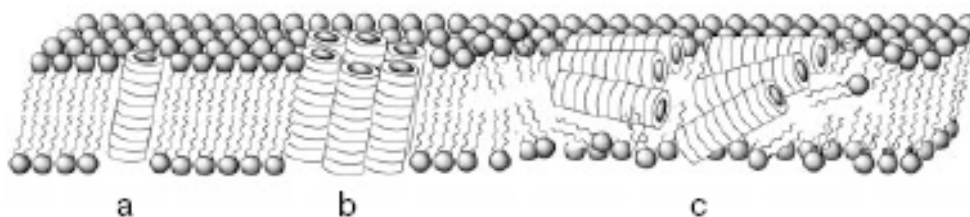


**Figure 1.4** Alignment of peptide nanotubes in a lipid membrane. A) A single nanotube in a membrane matrix, B) Multiple peptide nanotubes arranged in an orderly fashion, C) Random arrangement of peptide nanotubes within the lipid bilayer.<sup>58</sup>

Theoretically, there are many different orientations of peptide nanotubes within a lipid bilayer. Figure 1.4 shows that the peptides can be parallel with the lipid bilayer (a and b) randomly scattered within the bilayer itself (c). By having the nanotubes metal-coordinated to one another it could be possible to achieve an arrangement more like (b) in that the peptide nanotubes are closely packed and run parallel with each other, thus allowing for maximized transport through the lipid bilayer. Ghadiri has explored the use of a hydrogen bond motif using glutamic acid side-chains to hold peptide nanotubes together, however a metal-coordinated system would have stronger association constants.<sup>59</sup> Another advantage that metal-coordinated systems might have over hydrogen bound systems is that inserting the metal-coordinated nanotubes might be entropically favorable since glutamic acid and hydrophobic tails of the lipid bilayer would not want to associate together. While the targeted research would not yield the first metal-coordinated peptide nanotubes, it would be the first peptide nanotubes that are joined together to form a complex array of peptide nanotubes using metal-coordination. Previously, Kimura and coworkers used three terpyridine ligands on a cyclic peptide to complex copper, however the copper can only accommodate one terpyridine ligand per copper ion thus it is not useful for joining two peptide nanotubes together.<sup>60</sup> Another method that has been described to tether peptide nanotubes together uses a covalently



bound azobenzene between two cyclic peptides, much like the pincer would do; however this azobenzene is UV active and when irradiated with UV light it folds one cyclic peptide onto the other which defeats the purpose of tethering together for this thesis' application.<sup>61, 62</sup>

The research design for this thesis is based on the work by Ghadiri. The material described in this thesis focuses on the efforts of the peptide synthesis to include an alternating amino acid sequence that consisted of D-alanines and L-phenylalanines. One aspect of peptide nanotubes that must be taken into account is the characterization of the cyclic peptide supramolecular structures. Initially, it would be too overwhelming and insoluble in most solvents to work strictly with the vertically self-assembled peptides. Therefore, N-methylation of the amide backbone on one face of the molecule effectively blocks hydrogen bonding on one face, allowing only for dimerization of the cyclic peptides.<sup>63</sup> Once the amino acid sequence was set, the focus turned towards the ligand for metal-coordination. Turning towards nature, we see that nitrogen based amino acids are capable of binding to metal centers. It has also been shown that pyridine is an established ligand for the pincer complex. Furthermore, pyridine is structurally similar to the phenylalanine residues in the peptide species helping it to be more symmetrical.<sup>56, 64</sup> Therefore, a prior graduate student in the group, Warren Gerhardt, tested the position of the nitrogen and the effect of the linker to the amino acid on the pyridine containing amino acid to determine which had the highest binding constant with the pincer metal center.<sup>65</sup> It was determined that a 4-pyridylalanine was the best ligand for the pincer during the study, therefore the final cyclic peptide would consist of D-N-methylated-alanine, L-phenylalanine, and L-4-pyridylalanine residues. Fortunately, all of those amino acids are commercially available albeit expensive. Initial synthetic routes towards the cyclic peptide species called for one L-4-pyridylalanine per cyclic peptide molecule. This would allow characterization to be easier by having just one site for binding to a metal center. Using a mono-pincer and a tripeptide containing the L-4-pyridylalanine,

initially, gave a  $K_a$  value  $>1200\text{ M}^{-1}$ .<sup>65</sup> However, to join more than one nanotube together, a bis-pincer would need to be used

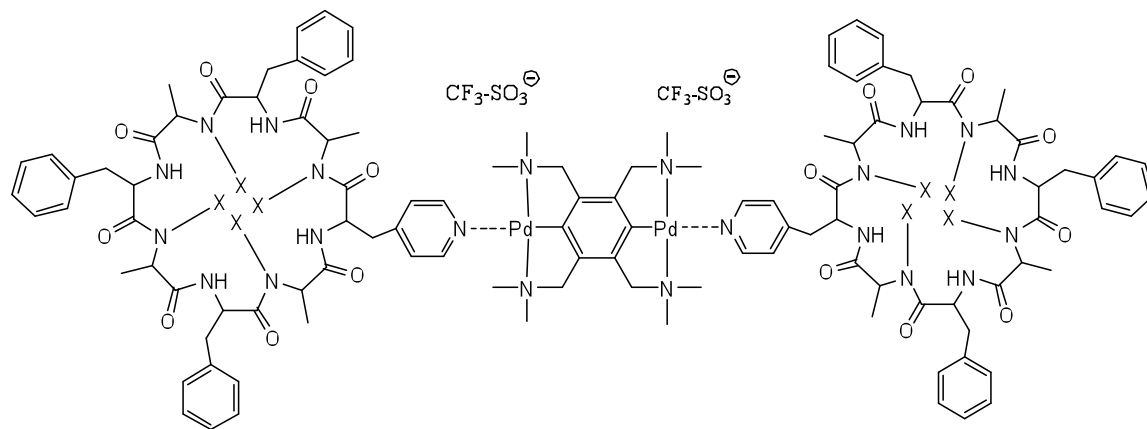


**Figure 1.5** Monopyridyl cyclic peptide species with bis-pincer

and would create the “sunglasses” peptide similar to Figure 1.5 where the X’s represent methyl groups blocking hydrogen bonding on one face. After the mono-pyridyl system had been explored the dipyrindyl cyclic peptide species shown in Figure 1.3 could be investigated.

This system would be much more complex to characterize but is ultimately one of the first major steps in showing that long range supramolecular arrays based on peptide nanotubes are feasible. Once the characterization is complete on the N-methylated alanines of the cyclic peptide species, the system can be extended to explore the non-methylated cyclic peptide species that would self-assemble vertically through hydrogen bonding forming the desired peptide nanotubes, while being able to self-assemble horizontally using metal-coordination. Furthermore, the transport of small molecules across the membrane could be investigated using the dipyrindyl cyclic peptide nanotubes.

## CHAPTER 2

### CYCLIC PEPTIDE SYNTHESIS AND RESULTS

#### Research Design

Throughout the years, the synthetic design for the peptide project has changed. The foundation of alternating D-alanine and L-phenylalanine residues has always been the primary goal of the cyclic peptide, along with the L-4-pyridylalanine as the metal coordinating species. However, the positions of the methyl groups on the amide nitrogens, along with the route to synthesis of the cyclic peptide, have been varied. Initial studies by Warren Gerhardt began by creating the mono-substituted pyridylalanine.

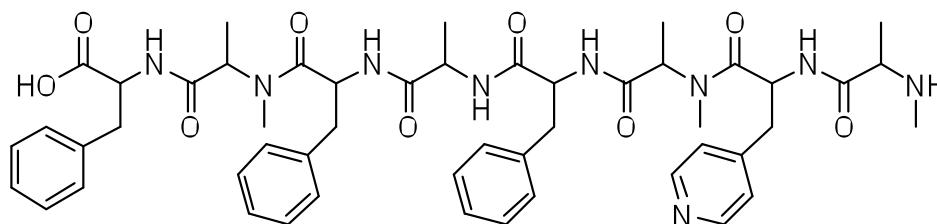


**Figure 2.1** Initial linear octapeptide to be synthesized by Warren Gerhardt (compound 1)

The goal of this thesis, however, is the synthesis of the di-substituted pyridylalanine cyclic peptide, as shown in Figure 2.2. Depending on the synthetic route explored, the X's in Figure 2.2 can represent hydrogen or a methyl group. The last synthetic route taken placed methyl groups in the amide positions of the D-alanines. As previously stated the methyl groups prevent hydrogen bonding on one face of the molecule allowing for better characterization. The methyl groups also require that the subsequent coupling be completed twice to ensure that the following amino acid in the sequence does indeed get fully coupled to each position on the resin; without this an incomplete linear sequence is made and alters the final compound.

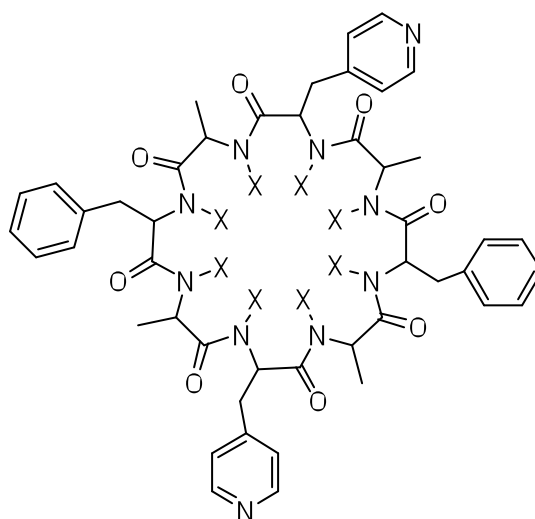


**Figure 2.2** Di-substituted pyridylalanine cyclic peptide (X=H, Me) (compound 2)

Different synthetic routes were explored to obtain the purified cyclic peptides. Some routes involved a solution phase approach and others involved a solid phase approach with utilizes a polymer based resin.

### Solution Phase

Solution phase synthesis offers many advantages over the solid phase approach. The first advantage is the scale on which the reactions can be carried out (gram scale) as opposed to the milligram scale for solid phase approaches. Often solution phase synthesis can offer higher yields and fewer steps. Since the di-substituted peptide has a repeating unit it can be synthesized as a tetra-peptide in the solution phase approach and be coupled to itself, rather than coupling eight amino acid units together. This saves time and money since there are fewer coupling and purification steps. This approach also uses fewer equivalents of starting material, usually just one equivalent to ensure full coupling. However, the drawbacks of this approach are more difficult purification steps and solubility issues. The peptide has to be recrystallized or chromatographed over silica gel between coupling steps to remove any remaining amino acids and coupling agents.

Solution phase peptide chemistry can use different types of protecting groups, however this thesis focused on using a benzyl protecting group for the carboxylic acid on the C-terminus of the peptide and a Boc (*tert*-butyl dicarbamate) protecting group for the N-terminus of the peptide. The amino acids used for this synthesis are purchased with the Boc group already in place. When treated with the trifluoroacetic acid the Boc group leaves the peptide as 2-methylprop-1-ene, which is a gas at room temperature eliminating other purification steps during the synthesis.

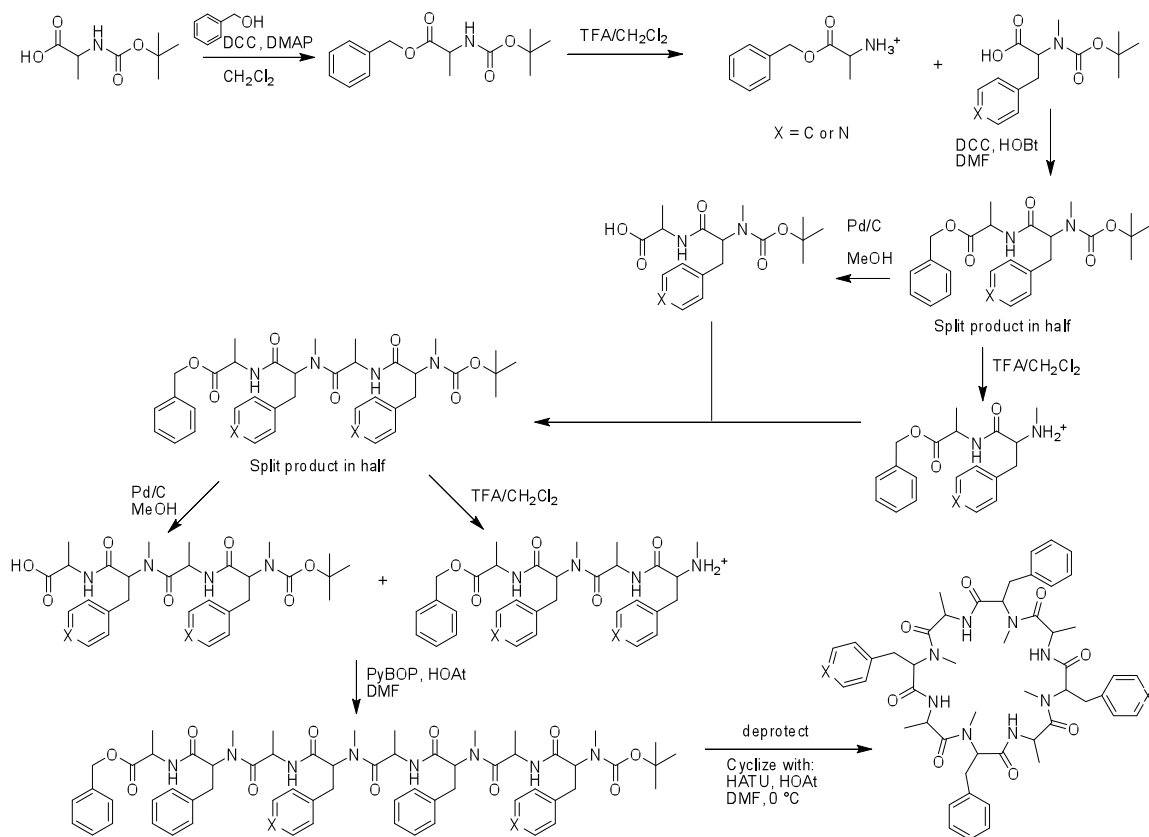


**Figure 2.3** Initial solution phase synthetic scheme (compound 3)

The initial solution phase synthetic scheme is shown in Figure 2.3 above. Since compound 3 is symmetric, one tetrapeptide can be made to shorten the synthetic route. By making the sequence alanine-phenylalanine-alanine-pyridylalanine the two ends could be joined easily together by splitting the product in half, deprotecting the C-terminus of

one portion, deprotecting the N-terminus of the other portion, and then joining the peptide together to create the linear octapeptide. The above synthetic route was simplified, where the X represents either a carbon or a nitrogen to make a phenylalanine or a pyridylalanine respectively. Thus, the first step is done twice and one di-peptide with phenylalanine is deprotected on one end and one dipeptide with pyridylalanine is deprotected on the opposite end such that coupling makes the desired tetra-peptide. This route was also used in tandem for the mono-substituted pyridylalanine. However that peptide is not symmetric thus more peptide coupling steps were needed to create the cyclic peptide. Looking closely at this route, the only commercially non-available peptide was the N-methylated-L-4-pyridylalanine, which should be available via a retro Diels-Alder reaction. However Warren Gerhardt determined this reaction did not produce the desired product under these conditions.

After this route failed, a new route was investigated that utilized two N-methylated positions, still hoping to block one face of the cyclic peptide from hydrogen bonding, thus still creating dimers. The two positions chosen to be non-methylated were phenylalanines directly across from one another, as shown in Figure 2.4. In compound 4, all phenylalanine positions were methylated, leaving the non-methylated positions to the pyridylalanine and alanine positions. This route was difficult in the beginning because coupling the third amino acid in the sequence did not always result in a tripeptide. Rather the diketopiperazine, a stable 6-membered lactam, was formed. Overcoming this obstacle involved using a syringe pump to slowly add the deprotected amino acid into the reaction vessel that contained the activated amino acid to be coupled. This was probably not seen in the first synthetic route because the second amino acid in the chain was N-methylated, which slows down couplings and intramolecular interactions.

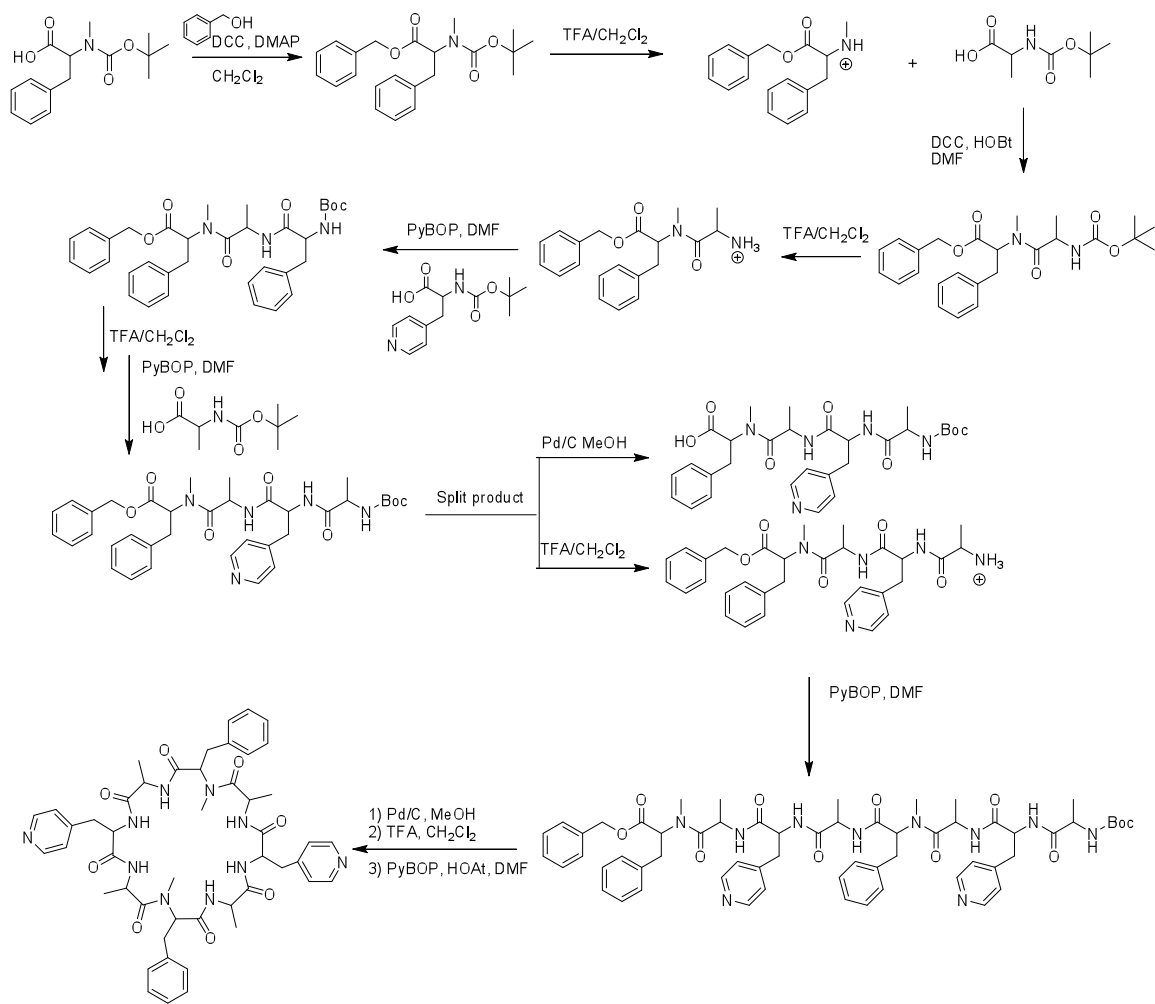


**Figure 2.4** Di-substituted pyridylalanine cyclic octapeptide route containing two N-methylated phenylalanines (compound 4)

It was also noted during this synthesis that the peptide product needed to be kept from light once the L-4-pyridylalanine was in the sequence. Since the peptide needed to be chromatographed over silica gel to remove impurities it was noticed that a degradation product was being formed when exposed to light. When the product mixture was spotted on TLC, it would show one product, however if a TLC plate remained exposed to light for a brief amount of time the spot would turn yellow. This spot would also break into two spots once the TLC plate was exposed to the eluting solvent. Using preparatory high

performance liquid chromatography (HPLC) overcame this degradation of the peptide and the degradation products were not further investigated.

A collaboration with Warren Gerhardt resulted in the successful synthesis of the mono-pyridyl cyclic octapeptide. Unfortunately, due to an impurity, the cyclic octapeptide work could not be published. However, Warren Gerhardt did demonstrate in preliminary results that the cyclic octapeptide and pincer compounds could metal-coordinate with one another.

### **Solid Phase**

The solid phase approach to peptide chemistry involves the use of a resin suspended in the reaction reagents to synthesize the linear peptide. This approach can be very beneficial in many aspects, most notably the ease of purification and overcoming solubility issues. The drawbacks of this method include limitation to milligram scale, the need for addition equivalents of reagent, lower yields, and more steps. However, since purification of the linear peptide had been the most difficult aspect of the project when using solution phase chemistry, it was thought that this route was the most beneficial route to complete this thesis' goal of synthesizing the cyclic peptide.

There are various types of resins available for peptide chemistry.<sup>66-68</sup> The Wang resin was utilized throughout this thesis' work. Each type of resin enables different reagents to be used without cleaving the peptide from the resin itself. The Wang resin shown in the Figure 2.5 below is cleaved by trifluoroacetic acid once the linear peptide has been synthesized. Since the peptide is cleaved from the resin using TFA, the Boc protecting group chemistry is not suitable for this approach. An acceptable protecting group strategy on Wang resin is Fmoc (9-fluorenylmethyl carbamate).



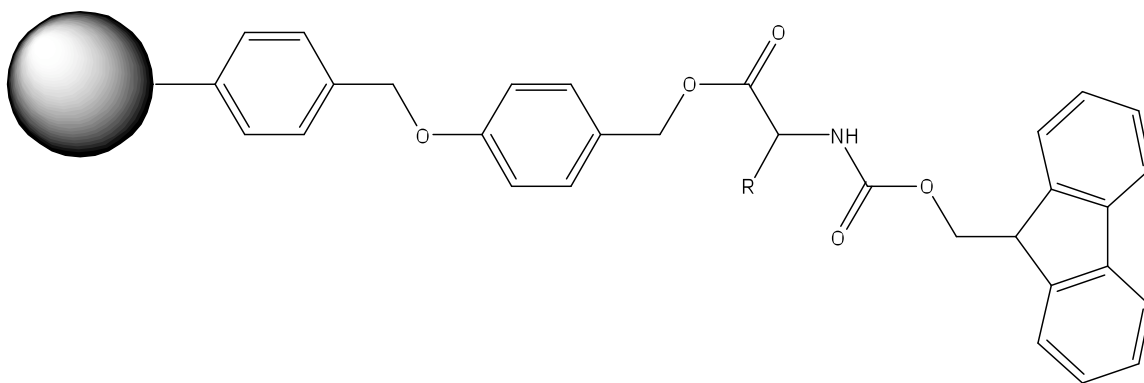


**Figure 2.5** Wang resin (R= starting amino acid side-chain)

The spherical ball in Figure 2.5 represents the resin, followed by the Wang linker, the first amino acid in the series, and lastly on the far right the Fmoc protecting group. The Fmoc protecting strategy is very popular and all amino acids were purchased with the Fmoc protecting group already intact on the amino acid.<sup>69</sup> Removal of the Fmoc is facile using a 20% solution of piperidine in N,N-dimethylformamide. The Fmoc group was washed away as 9-methylene-9H-fluorene and did not need any further purification.

A solid-phase approach was based on N-methylated alanine in which the alanine would be coupled to the resin as the first step to avoid cyclizing with a terminal N-methylated amino acid, Figure 2.6. Since the first step in this synthesis was coupling the resin and the amino acid together it was imperative for the subsequent steps to have a known amino acid loading on the resin. This can be done by cleaving the Fmoc protecting group from the amino acid and using a UV/Vis spectrometer to obtain an absorbance reading. Once the absorbance reading is known and taking into account the dilution factor the amino acid loading can be determined. Unfortunately, the Fmoc loadings were inconsistent and the amino acid did not seem to load onto the resin consistently so after checking for compound 5, as shown in Figure 2.6, this route was reevaluated.

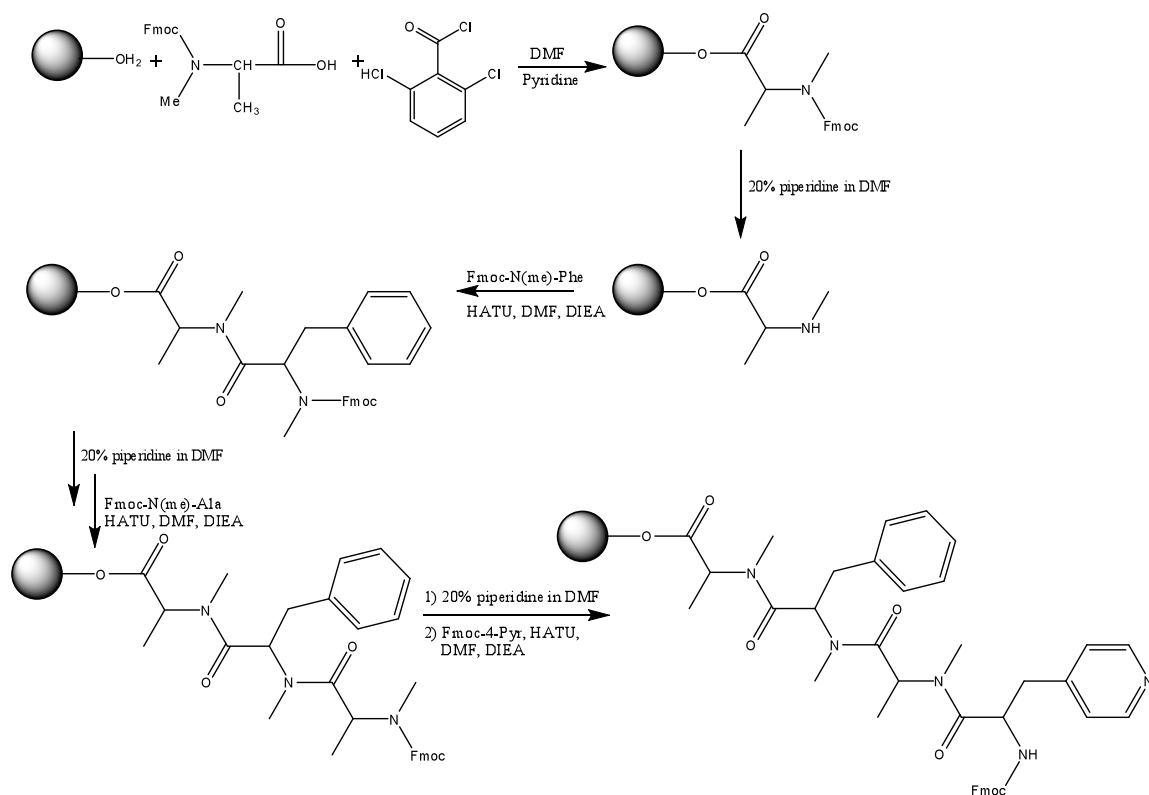
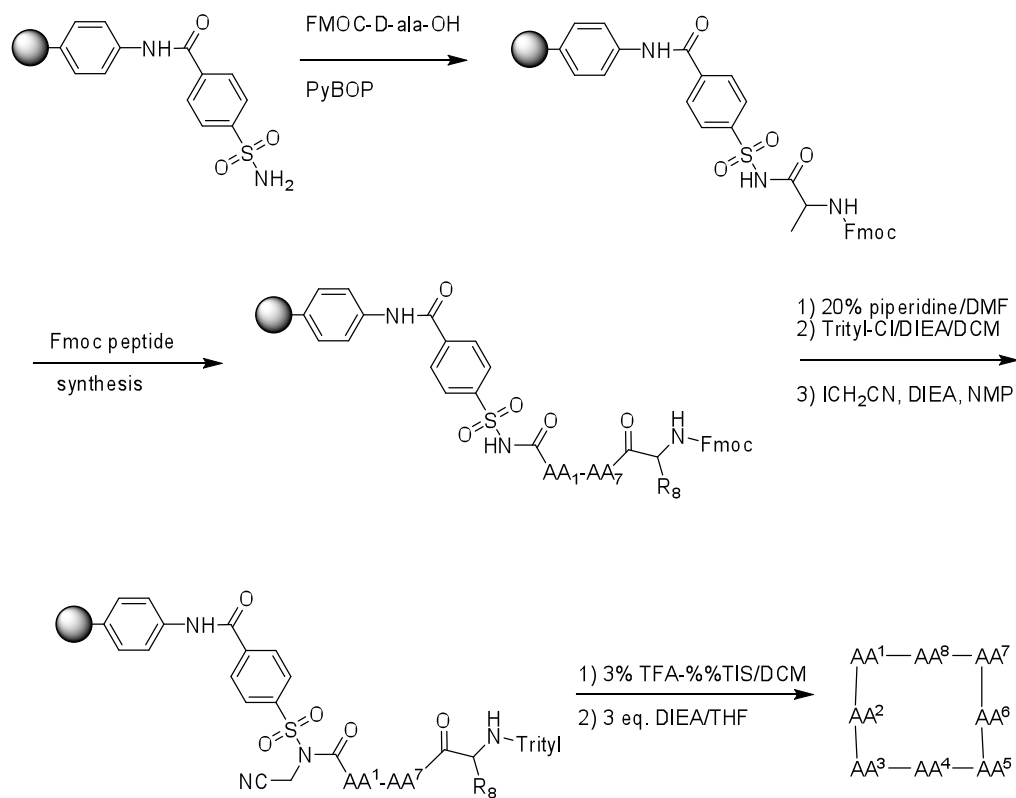


**Figure 2.6** Solid-phase approach with N(methylated) alanines and phenylalanines (compound 5)

Upon consent of Dr. Arora at New York University, some time on his peptide synthesizer was obtained in late spring of 2008. The peptide synthesizer is an automated machine that used microwave radiation to speed up the coupling processes. This machine did in a day what typically took two days by hand, with higher purity than what can be obtained by using bench top chemistry methods. However, only one round of linear peptides were made during the trip to NYU. It was a very beneficial time and allowed for the non-methylated cyclic peptide to be synthesized. As discussed previously, this was not the ideal peptide to synthesize however it was the easiest given time constraints. The linear (Ala-Pyr-Ala-Phe)<sub>2</sub> was purified; however, cyclization of the purified linear peptide yielded 20 mg which did not show any cyclized product once submitted to reaction conditions. The product may have just been insoluble in the solvents used to

obtain the mass spectrum and using MALDI-MS probably would have been too harsh and broken the cyclic peptide apart.

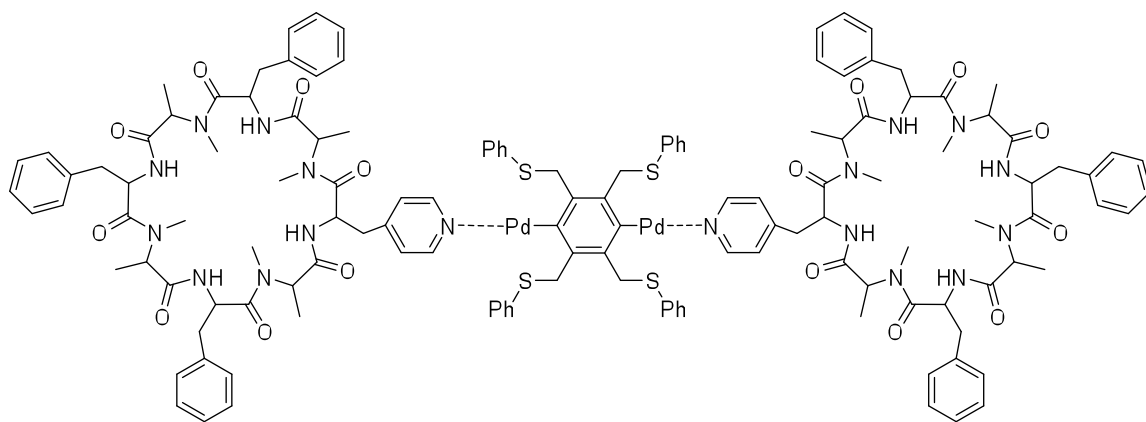
While in New York, a different resin than the one that was being used initially was suggested that would enable cyclization to occur on the resin, by-passing the peptide cleavage step from the resin. This new resin was a Kenner “safety-catch” resin and allows for the amino acid to be coupled to the polymer resin via a sulfonamide which once activated by iodocyanomethane the peptide can cyclize off the resin, leaving the cyclic peptide.<sup>70</sup> The synthetic scheme is shown below in Figure 2.7. This was a very promising route that would enable the peptide to be made from start to finish much faster.



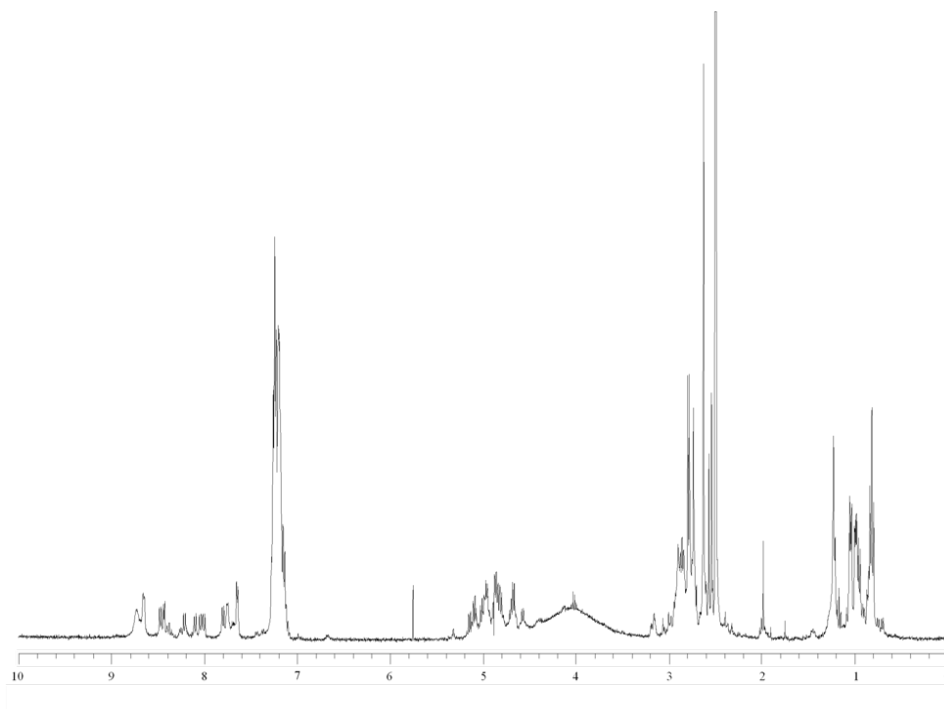
**Figure 2.7** Kenner “Safety-catch” Resin synthesis (AA represents an amino acid)

This strategy also had the prospect of obtaining a purer peptide species because it would be cleaved off the resin as a cyclic peptide, which could precipitate out of solution. The

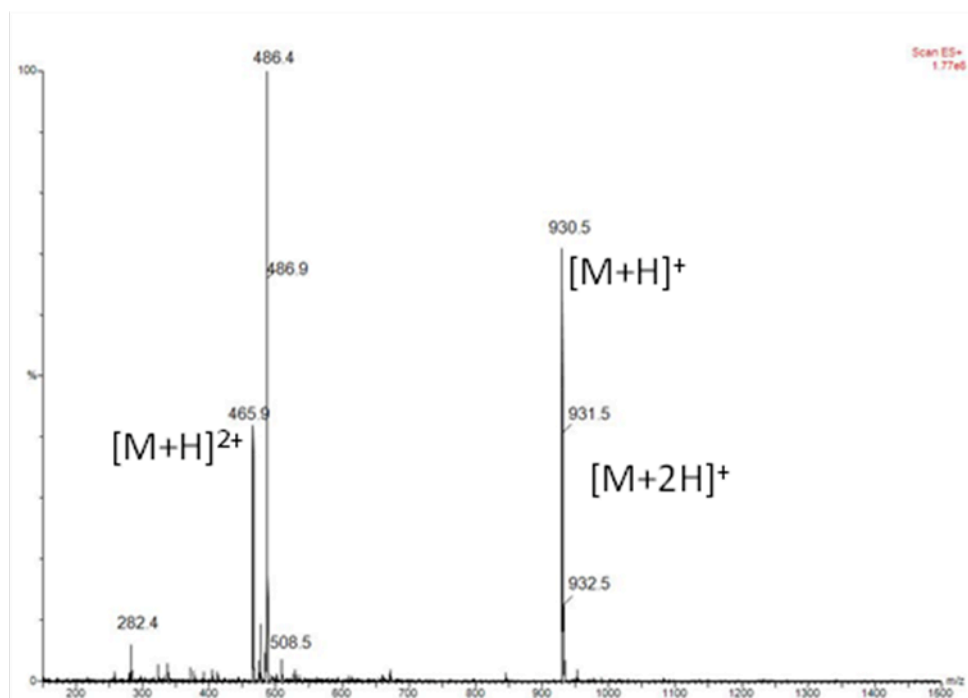
first step was to take the Kenner resin and couple it to the first amino acid, or load the resin with the amino acid. This seemed to have worked and gave consistent amino acid loading estimates at 0.5357 mmol/g. The problem with this resin was the cleavage of the peptide from the resin. Activating the resin for cleavage did not seem to work since there was never a product indicated by mass spectrum analysis. While this route seemed to be promising, in the end it was abandoned for a different solid-phase route on the initial Wang resin. At this time, Dr. Madhavan had begun the synthesis of the mono-substituted pyridylalanine cyclic peptide (Figure 2.8), compound 6, and was using N-methylated D-alanine at every other position. She successfully showed that the cyclic octapeptide could metal-coordinate with the bis-pincer. Figure 2.9 shows the proton NMR spectrum of compound 6, however even after an extended period of time a  $^{13}\text{C}$  NMR spectrum could not be obtained for the compound. A mass spectrum was obtained and has a molecular ion peak at 930 m/z and 465 m/z corresponds to the doubly charged species as well.



**Figure 2.8** Monosubstituted pyridylalanine (compound 6) coordinated to bis-pincer compound.

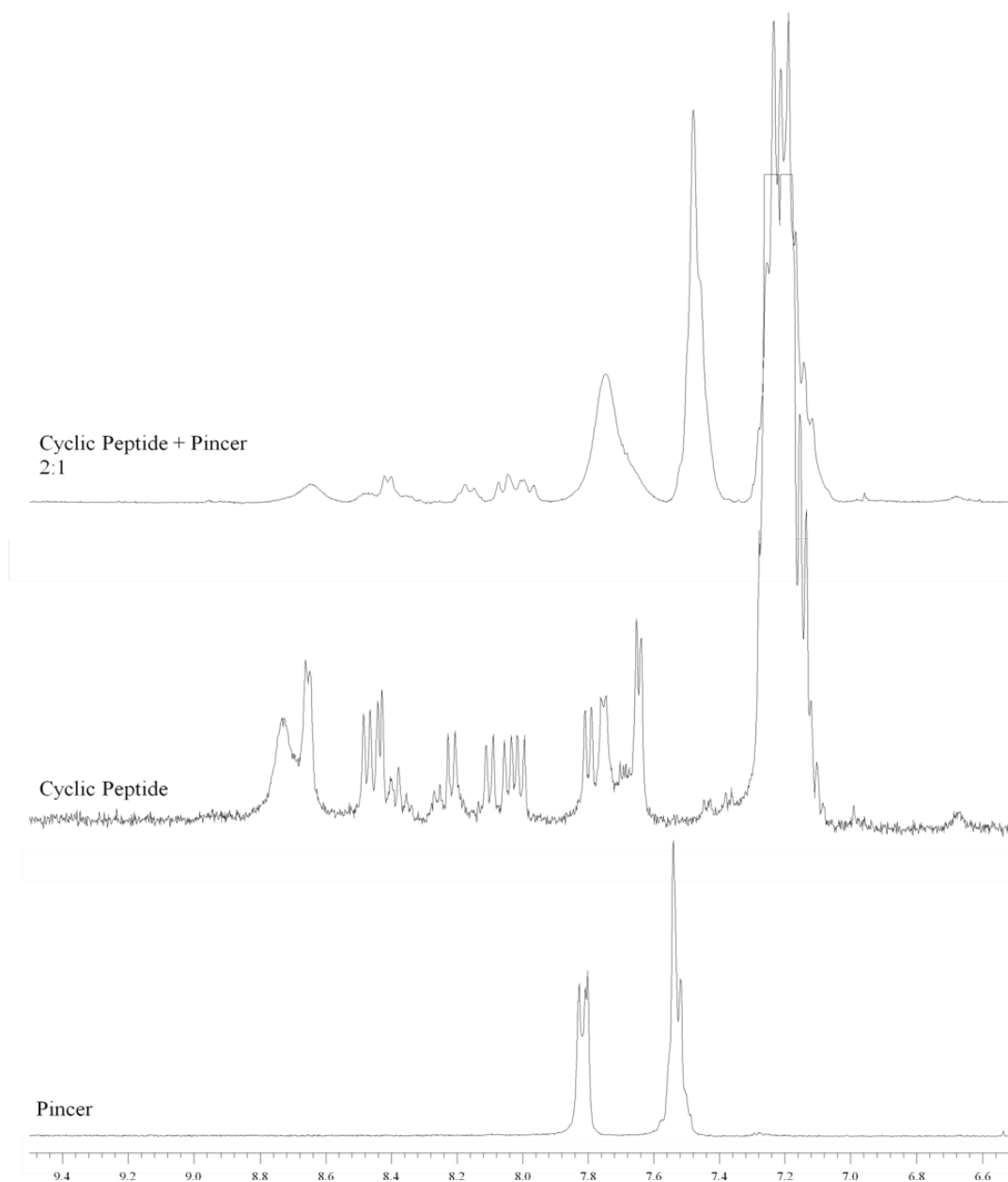


**Figure 2.9**  $^1\text{H}$  NMR spectrum of compound 6



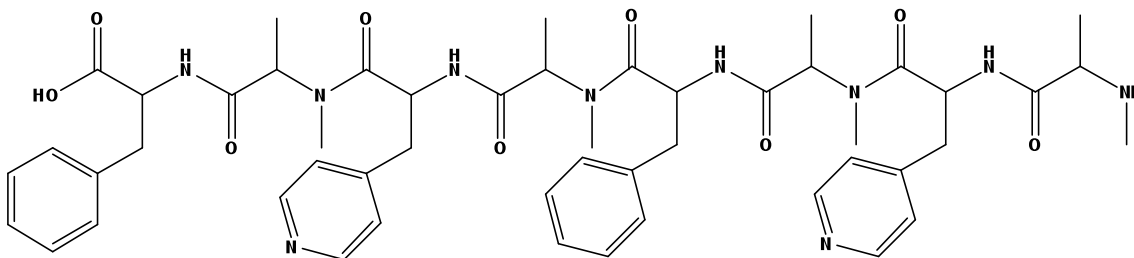
**Figure 2.10** Mass Spectrum of compound 6

Figure 2.11 shows the aromatic region of the proton NMR spectrum for the coordination with the pincer complex. It shows a shift in the peaks that corresponds to the pyridylalanine hydrogens, while the pincer signals become broader upon complexation. In addition, the peaks belonging to the phenylalanine hydrogens do not shift, thus the phenylalanine does not interfere with the metal-coordination of the pincer and the cyclic octapeptide.



**Figure 2.11**  $^1\text{H}$  NMR spectrum of cyclic peptide and bis-pincer complex (2:1 ratio)

To have a good comparison study with the mono-substituted peptide the following synthesis for the di-substituted peptide was completed (Figure 2.12).



**Figure 2.12** Linear octapeptide containing N-methylated alanines (compound 7)

This was the last synthetic scheme explored. This route still deals with a very little linear product cleaved from the resin and after purification via HPLC there is typically about 50 mg that can be cyclized using the appropriate scale for the peptide reaction vessel. The cyclization product has not been obtained in a high enough purity to obtain the necessary characterization data for publication and studies with the pincer complex. However, a mass spectrum of the cyclized octapeptide shown in Figure 2.13 was obtained that shows an  $[M+H]^+$  peak at 931m/z and the  $[M+2H]^+$  at 932m/z. A proton NMR spectrum of the disubstituted pyridyl cyclic octapeptide was obtained and is shown in Figure 2.14. A carbon NMR spectrum was also attempted, however, as Dr. Madhavan experienced relaxation times were too long to obtain a complete spectrum given overnight data acquisition.

Two-dimensional NMR studies were carried out for both cyclized peptide compounds. The first study completed for compound 6 was COReLation SpectroscopY (COSY). This method shows which protons are spin-spin coupled and for peptides this can help to assign the 1D proton NMR spectrum since these spectra are often complex. This was a very useful method since the monopyridylalanine cyclic peptide is not symmetric like its disubstituted counterpart. The COSY spectrum (Figure A.1) was most

helpful in differentiating the pyridylalanine aromatic signals at 8.60 ppm and 7.68 ppm from the phenylalanine peaks at 7.20 ppm. The second 2D NMR experiment was TOtal Correlation SpectroscopY (TOCSY) (Figure A.5) which shows the signals from the COSY but also protons that are spin-spin coupled further than three bonds away. The TOCSY was helpful in determining the position of the N-methyl groups at 2.48 ppm from the CH<sub>2</sub> groups on the phenylalanine and pyridylalanine. Since these CH<sub>2</sub>'s are so close together it differentiated between the pyridylalanine CH<sub>2</sub> at 2.81 ppm from the phenylalanine CH<sub>2</sub> at 2.61 ppm. Unfortunately, given the overlap in the spectra, the alanine spin-spin systems could not be distinguished. A ROESY experiment (Figure A.7) was also completed, however it did not provide any more insight than the previous 2D studied did.

Two dimensional NMR studies for the compound 7 were also completed. However, due to impurities there is not as much information gained from them. The first 2D NMR study was a COSY experiment (Figure A.8) which showed the connectivity between the pyridylalanine aromatic protons at 7.73 and 8.76 ppm. While the mass spectrum showed the molecular weight of the cyclic compound to be correct (Figure 2.13), the 2D NMR experiment shows that an impurity is present, possibly an incorrect peptide sequence. Initially, it was thought that there was an extra CH<sub>3</sub> alanine peak due to different conformations of the cyclic peptide species, however further investigation of the spin-spin correlations makes it appear that not all of the alanines are N-methylated. There are clear CH<sub>3</sub> correlations between a CH<sub>3</sub> at 1.22 ppm and a CH at 4.7 ppm, which also correlates to an NH proton at 8.60 ppm. A structural discrepancy was not apparent in the MS but is clearly evident by the NMR data. One possibility for the discrepancy lies in an impure starting material, however one would expect that more positions would show up non-methylated since coupling an alanine would be greater and thus give inaccurate MS results. Therefore, a second hypothesis is that during cyclization the terminal methyl group was cleaved before cyclization could be completed. It would not



make sense for a degradation route to be a problem since the MS and NMR spectra were taken so close together. The second 2D NMR experiment began was a Heteronuclear Single Quantum Coherence (HSQC) study (Figure A.14) which shows carbon to proton spin-spin connectivity. However, due to slow carbon relaxation times the study was abandoned. A larger sample and much longer times on the instrument would be needed to obtain useful HSQC data. Even without the carbon spectra present it is still possible to see the peaks and gain some carbon NMR data from the spectra. The 2D NMR data suggests that next round of cyclic peptide synthesized needs to be purified better in order to determine what has lead to the additional peak that was found in the NMR data, unfortunately the DMSO used for characterization prevents further purification methods from being explored.

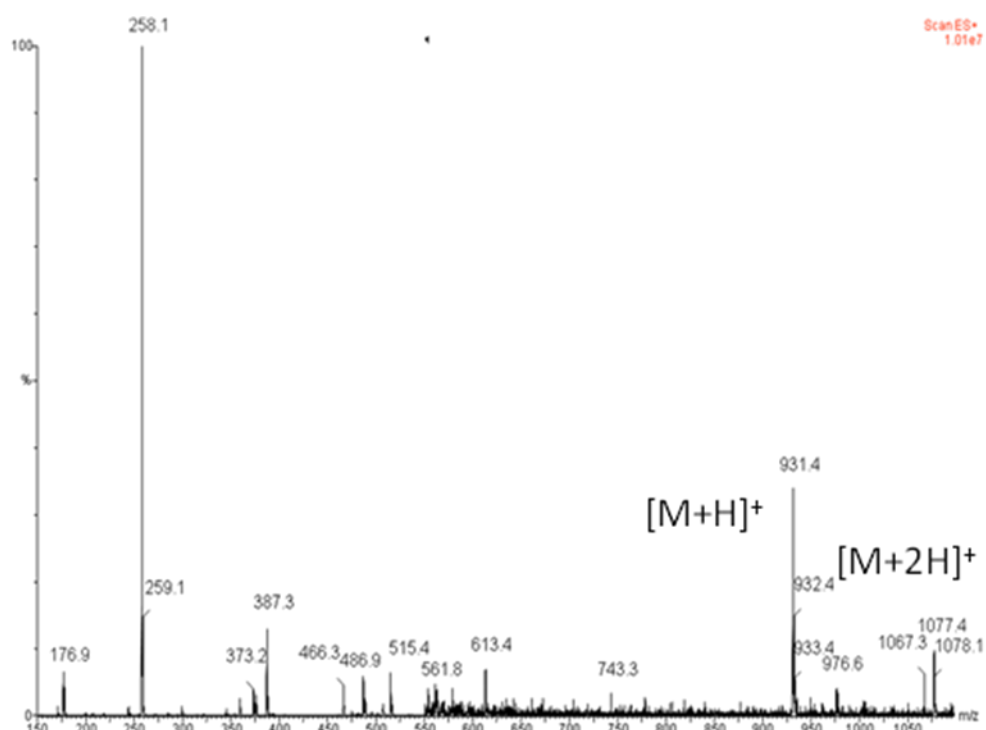


**Figure 2.13** Mass Spectrum for compound 7

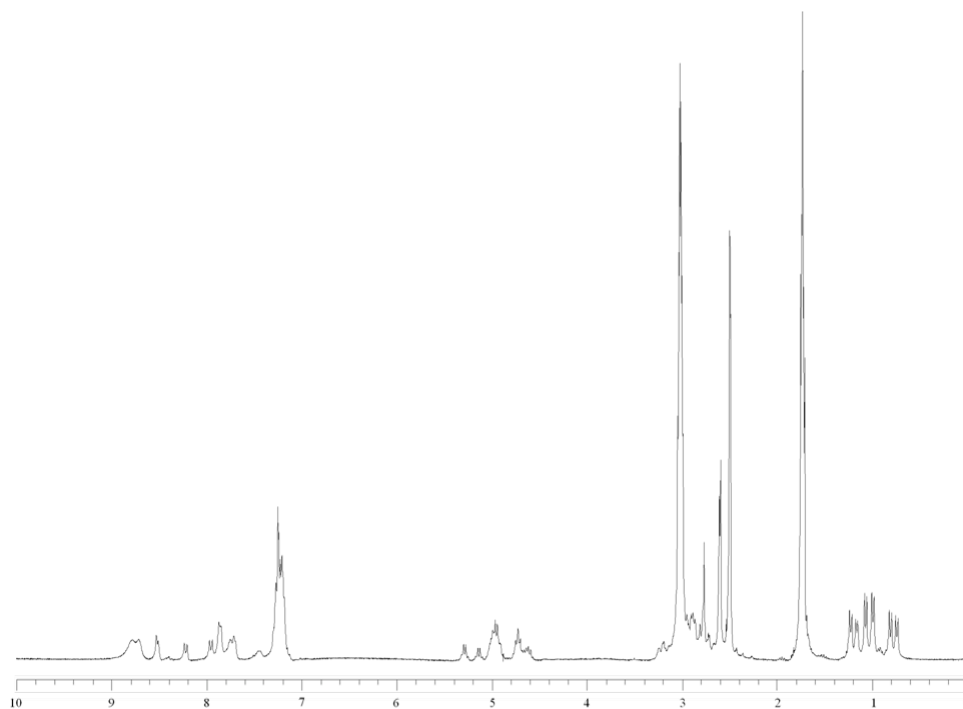


**Figure 2.14** Proton NMR spectrum of compound 7

## Experimental Section

### *Materials and Methods:*

All peptides were commercially available from Peptech Corp. and Peptides International. DIEA was distilled over calcium hydride and the DCM was dried by passing it through a  $\text{Cu}_2\text{O}$  and alumina column. DMF, pyridine, and piperidine were purchased dry from Alfa Aesar. NMR spectra were acquired on a Bruker DSX 300 at 298 K ( $^1\text{H}$  NMR: 300 MHz,  $^{13}\text{C}$  NMR: 75MHz). All chemical shifts are reported in parts per million (ppm), using the solvent as an internal standard. Data are reported as follows: chemical shift, multiplicity, coupling constant, and integration.

### *Benzylation method for protecting amino acid carboxylic acids:*

Boc-alanine (10.026 g, 52.9 mmol) was added to a solution of DMAP (1.292 g, 0.032 mmol), DCC (10.924 g, 53 mmol), and benzyl alcohol (5.5 mL, 211 mmol) was

added to a 100 mL round bottom flask with 10 mL of DCM on ice. A precipitate formed immediately and the reaction was worked up the following day by filtering over celite using ethyl acetate to wash the precipitate. The excess solvent was removed via reduced pressure and the solid was redissolved in ethyl acetate and placed in the fridge. If more precipitate crashed out of solution then it was filtered over celite, otherwise the solution was washed with 0.5M HCl and 0.5M NaOH. Afterwards excess benzyl alcohol was removed using a kugelrohr yielding a white solid (17.46 g, 88.5%).

***Method for removing the Boc protecting group:***

Benzyl 2-(*tert*-butoxycarbonylamino)propanoate (4.513 g, 16.2 mmol) was dissolved in a round bottom with 20 mL of DCM and 10 mL of TFA under argon. After an hour and a half the solvent was removed under vacuum and then placed under vacuum overnight to dry thoroughly. This solid was used without further purification.

***General method for coupling amino acids via solution phase:***

Benzyl (2-methylamino)propanoate (4.78 g, 15.2 mmol) and 2 mL of DIEA were added to 30 mL of DMF. Fmoc-L-4-pyridylalanine (2.08 g, 7.79 mmol), HOBt (1.05 g, 7.7 mmol), PyBOP (4.45 g, 8.5 mmol), and 2 mL of DIEA were added into 20 mL of DMF to activate. The second reaction mixture turned yellow upon addition of the DIEA to solution and was subsequently added to the first reaction mixture. After six hours, the DMF was removed under vacuum using an extra trap. The solid was redissolved in ethyl acetate and washed with saturated sodium bicarbonate solution and dried over magnesium sulfate. The ethyl acetate was then removed under reduced pressure and dried overnight, if necessary a column using silica gel and 1:1 EtOAc and hexanes can be used to purify, to yield a white solid (3.25 g, 96%).

***General method for debenzylation of peptide:***

The benzyl protected linear peptide was dissolved in ethanol (15 mL) in a pressure flask, a catalytic amount of Pd/C (10%) was added and secured in the Parr hydrogenation apparatus. The mixture was pressurized in a hydrogen atmosphere to 50 PSI and shaken for 24 hours, after which it was filtered over celite and the solvent removed under reduced vacuum to give a white solid, used without further purification.

***General method for coupling amino acid onto resin:***

Wang resin (517 mg) was added to a peptide vessel containing 5 mL of DMF. This mixture was allowed to swell under argon for 15 minutes. N(Me)-alanine (1eq, 450 mg), 2,6-dichlorobenzoyl chloride (1.1 eq, 0.25 mL), and pyridine (1.1 eq, 0.25 mL) was added into the reaction vessel and reacted overnight. The next morning the resin was rinsed three times with DMF and DCM. The resin loading was tested using the method from Gude.<sup>71</sup>

***General method for linear octapeptide by solid-phase synthesis:***

The linear octapeptide was synthesized via a solid phase peptide synthesis strategy using an Fmoc-phenylalanine functionalized Wang resin. The synthesis was carried out in a solid phase synthesis vessel where the resin was first swelled with CH<sub>2</sub>Cl<sub>2</sub> for 45 min., following which it was washed with DMF. The Fmoc groups were deprotected by treating the resin with a 20% solution of piperidine in DMF to give a free amine. A solution of three equivalents each of Fmoc-D-N(me)-alanine, HATU and 15 equivalents of DIEA in 5 mL of DMF was added to the vessel and allowed to react with the resin for 30 min. Argon was bubbled through the flask in order to ensure mixing of the resin and the reagents. After the resin was thoroughly washed, the Fmoc protecting group was removed and another round of peptide couplings could progress according to the synthetic scheme. Following ever N(methylated)-alanine the coupling was done

twice to ensure proper loading of the subsequent amino acid. After the linear octapeptide sequence was completed, the resin was rinsed well with DMF, DCM, and MeOH. Following the washes the peptide was cleaved from the resin using 5% TFA in DCM. The liquid was then removed under reduced pressure to yield an impure solid which was purified by reverse phase HPLC using a gradient of water containing 1% TFA and acetonitrile.

#### ***Cyclization procedure:***

Monosubstituted pyridylalanine octapeptide (compound 7) (84 mg, 0.079 mmol) was added to a round bottom flask with 115 mL of DMF. PyAOP (123.6 mg, 0.237 mmol) and DIEA (82  $\mu$ L, 0.475 mmol) was added and allowed to react under argon for three hours. Afterwards, a secondary trap was used to remove the solvent and the residue was purified by reverse phase HPLC using a gradient of acetonitrile and water with 1% TFA. The fractions were collected and the HPLC solvents were removed under reduced pressure and the remaining liquid was lyophilized off to give a solid (45 mg, 61%).  $^1\text{H}$  NMR (300 MHz, DMSO)  $\delta$ : 0.81 (t,  $J$ = 36.0, 3H), 0.99 (dd,  $J$ = 5.8, 11.2, 3H), 1.05 (dd,  $J$ = 9.3, 17.4, 3H), 2.54 (s, 3H), 2.57 (s, 3H), 2.63(s, 6H), 2.79 (m, 12H), 4.57-5.14 (m, 8H), 7.14-7.28 (m, 15H), 7.71 (m, 2H), 8.04-8.45 (m, 2H), 8.69 (m, 2H); MS (ESI) positive mode 930.6m/z.

#### **Future Work**

There is still much work to be done on the cyclic octapeptide project. Most of the time spent on this project involved synthesizing and purification of the linear and cyclic octapeptides. If time was available on the automated peptide synthesizer at New York University larger amounts of the peptide could be obtained and purified at a much faster rate. However, the synthetic route is effective at synthesizing the linear peptide and reverse phase HPLC is helpful in the purification of both the linear and cyclic peptide

products. Unfortunately, the target molecule for this thesis, the disubstituted pyridylalanine, while being in hand, is present as a mixture with impurities that HPLC has not been able to resolve. Perhaps recrystallization could be used to purify the compound further.

Once the purified peptide is obtained and characterized the metal-coordination step with the pincer, both mono- and bis- can be evaluated. The Weck group has extensively synthesized and studied metal-coordination interactions using pincer molecules so this aspect of the project should not cause a stumbling block.<sup>72, 73</sup> The mono-palladium pincer is used to show the binding constant, however comparison to the mono-substituted pyridylalanine cyclic octapeptide will give the best data since the binding ratio of pincer to peptide would be 1:1. The use of the bis-palladium pincer enables the supramolecular structure to be elongated along the horizontal axis and with multiple pyridines and a bis-pincer the binding constants may get difficult to fully determine. The solubility of the cyclic octapeptide with the bis-pincer also makes characterization difficult. If it precipitates from solution upon coordination then electron microscopy may be the only route to characterization. However, if it remains soluble then possibly gel permeation chromatography, MALDI-MS, dynamic light scattering, x-ray crystallography, and proton NMR spectroscopy may help to characterize the system.

After the characterization of the disubstituted pyridylalanine and fully N-methylated alanine cyclic octapeptide, the non-methylated cyclic octapeptide can be synthesized. The peptide brings with it its own set of challenges, which include significant characterization hurdles. Since the methyl groups will no longer be present to block one face of the molecule the cyclic peptides can hydrogen bond with one another to form the peptide nanotubes that Ghadiri's group has explored significantly. After metal-coordination of the non-methylated cyclic octapeptide the peptide project would then have met its primary long-term goal synthetically. The nanotubes can be placed into lipid bilayers and hopefully show that the alignment of the peptide nanotubes benefits from the

metal-coordination. This will be difficult to prove, however using a control flow study that shows the difference in directional flow across the lipid bilayer with and without metal-coordination could be key. It is hoped that the metal-coordination will align the peptide nanotubes in a vertical fashion together, and if this is achieved once placed into the lipid bilayer the flow across the membrane with the metal-coordination should be greater.

Over the course of this thesis, we have learned much about peptide chemistry. Specifically, the two approaches of solid and solution phases were explored. The benefits of each route are now understood. For this cyclic peptide purification is the most significant issue; therefore the solid-phase synthesis is the optimal route due to the peptide being purer once cleaved from the resin. Both routes struggled with the diketopiperazine by-product and reaction conditions had to be optimized to avoid this by-product.

In conclusion, the goal of this thesis was to synthesize a disubstituted pyridylalanine cyclic octapeptide. Full characterization has not been accomplished due to impurity, solubility, and extremely long carbon nuclei relaxation times. It is hoped that by the work in and leading up to this thesis that the application of cyclic octapeptides will find use in biomaterials such as transport across lipid membranes.

## APPENDIX A

### 2-DIMENSIONAL NMR DATA OF CYCLIC PEPTIDES

**Figure A.1** COSY data of mono-substituted pyridylalanine cyclic peptide compound 6

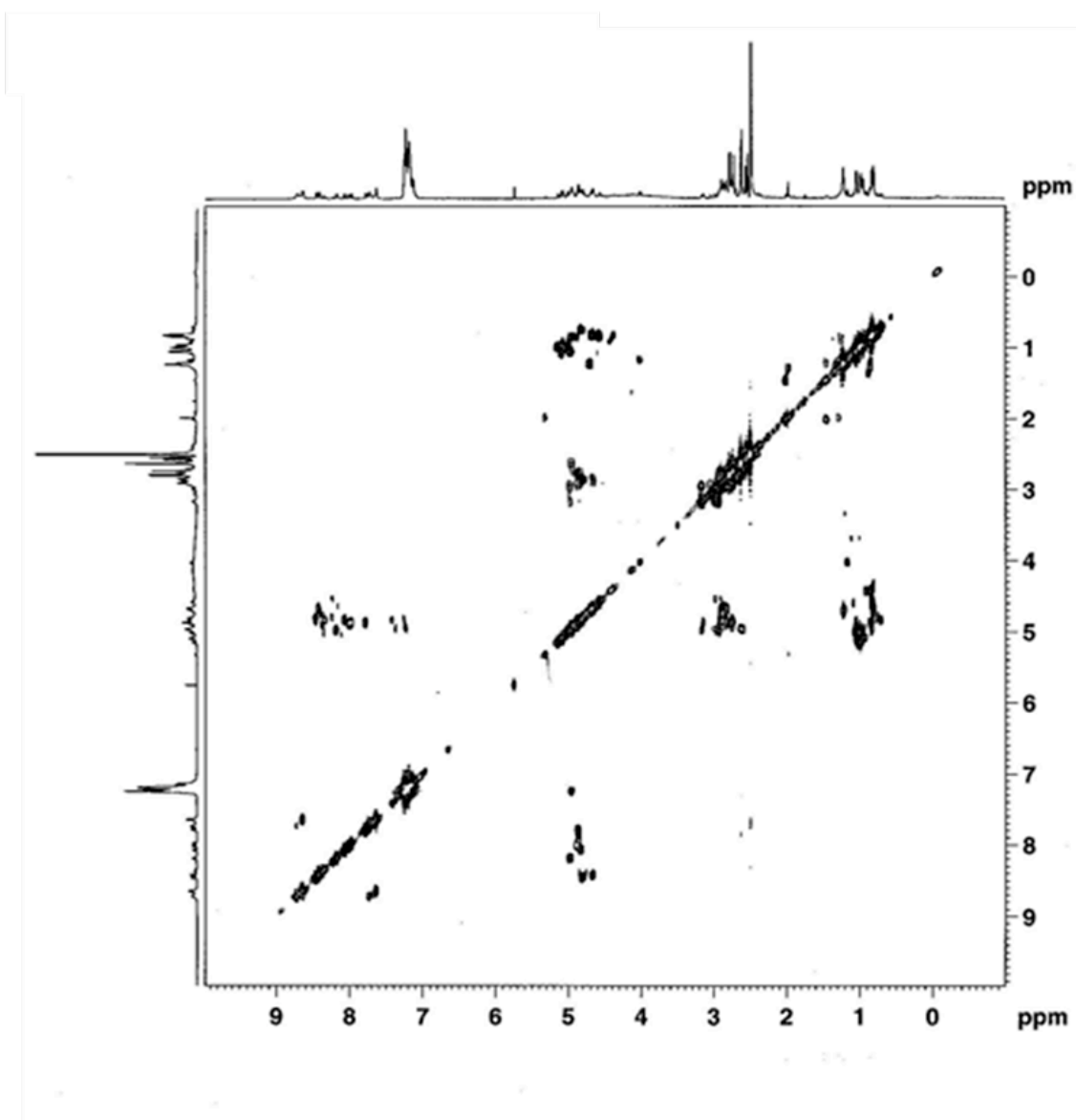
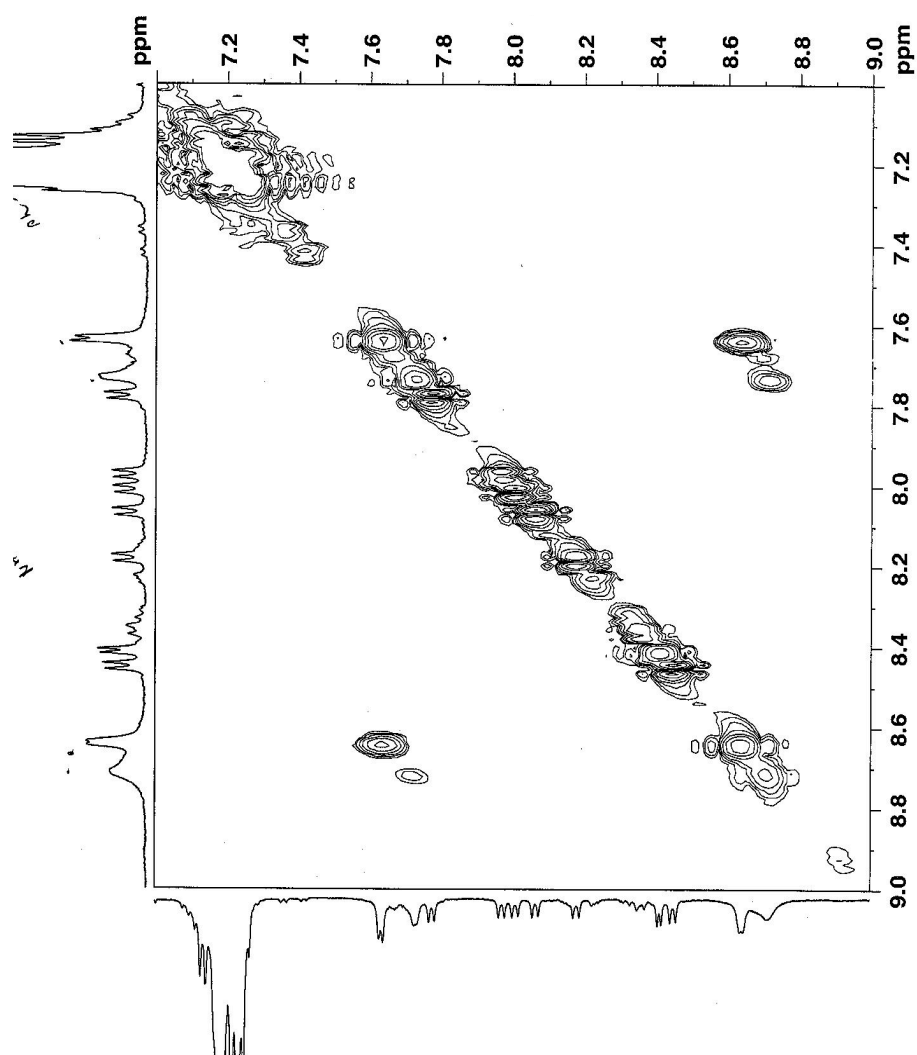




Figure A.2 COSY 7.2-9.0 ppm range



**Figure A.3** COSY 7.2-9.0, 4.0-5.5 ppm

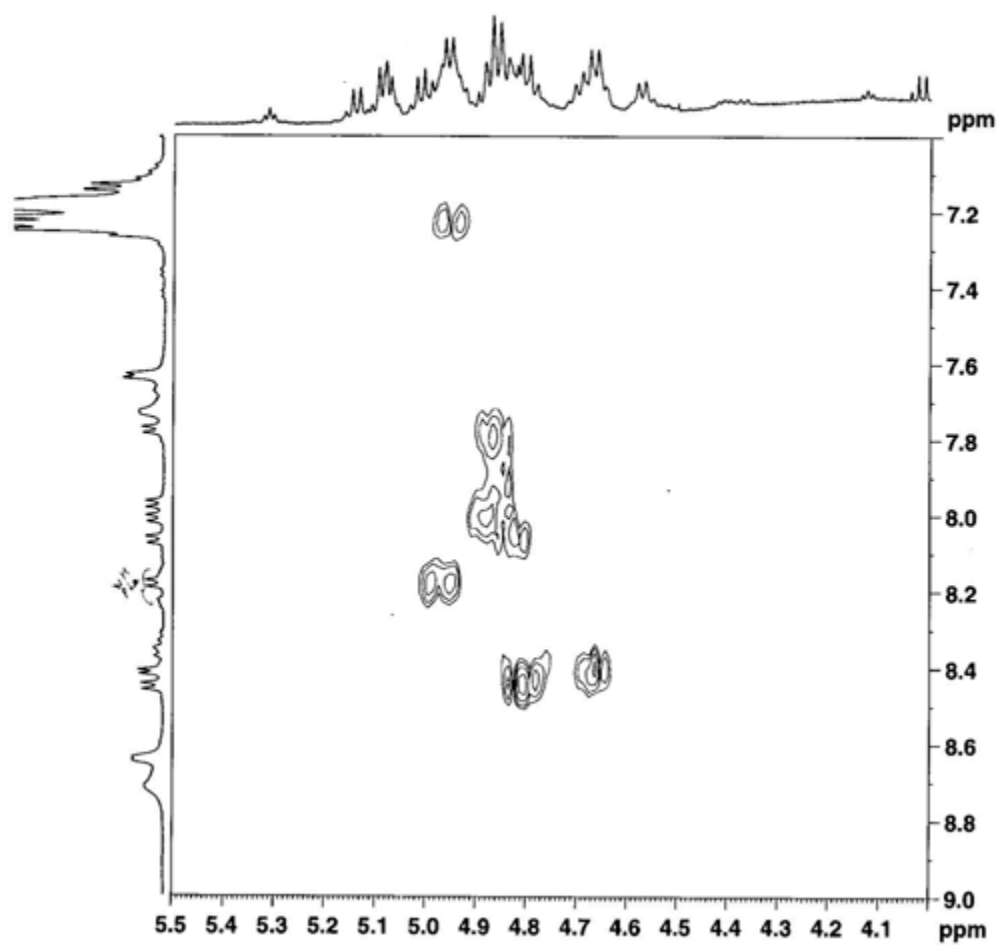


Figure A.4 COSY 1.0-6.0 ppm

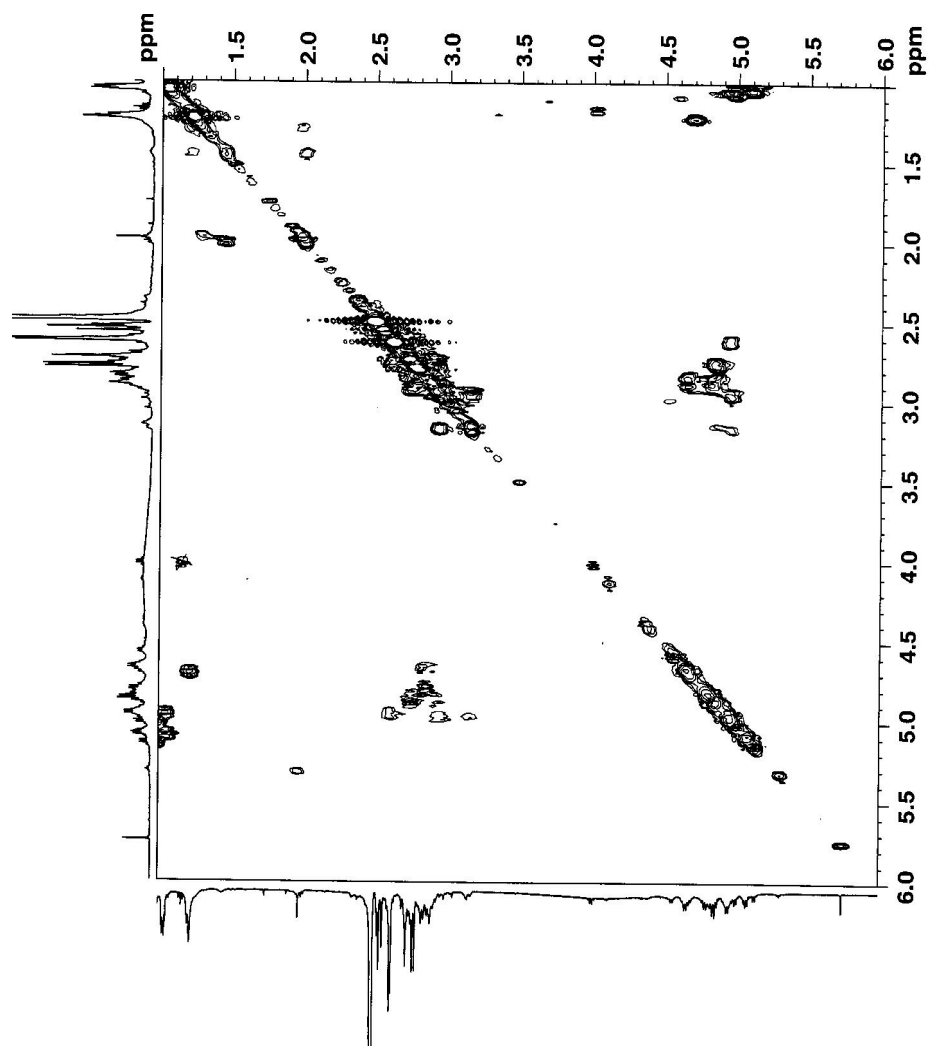


FIGURE A.5 TOCSY data of compound 6

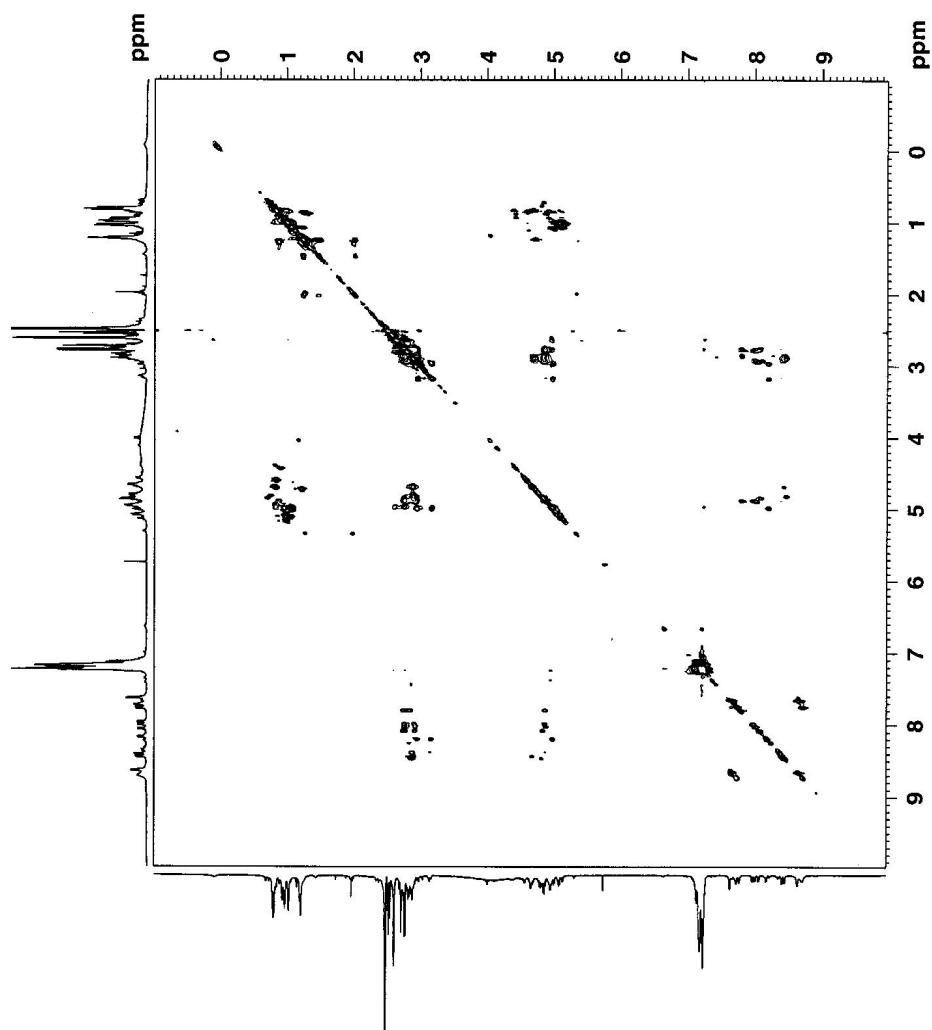
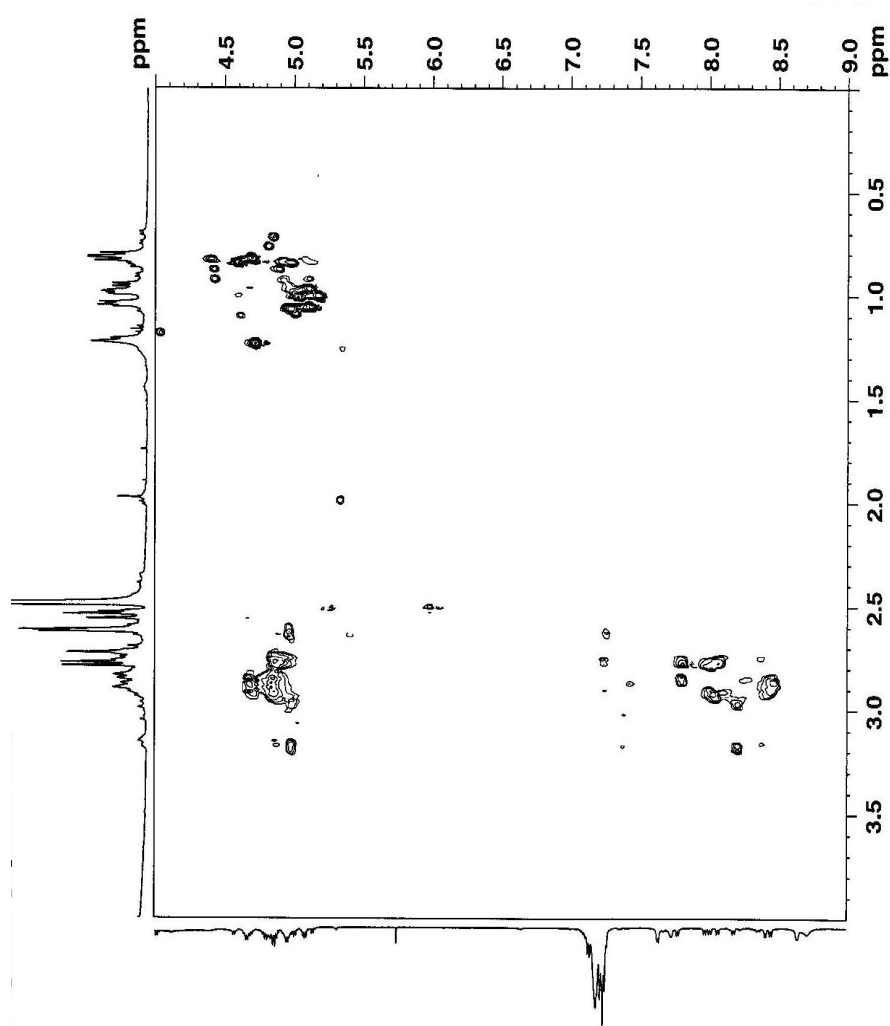
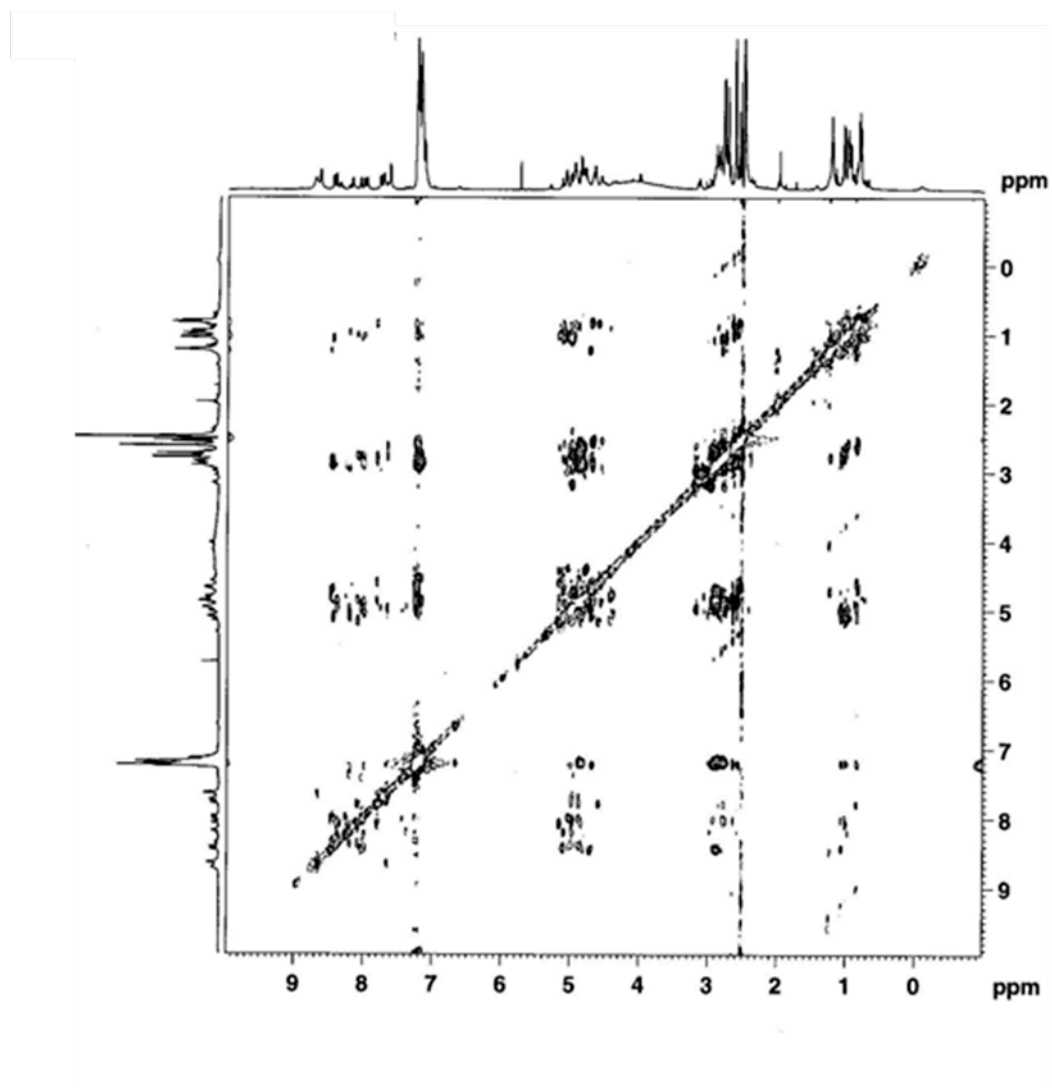


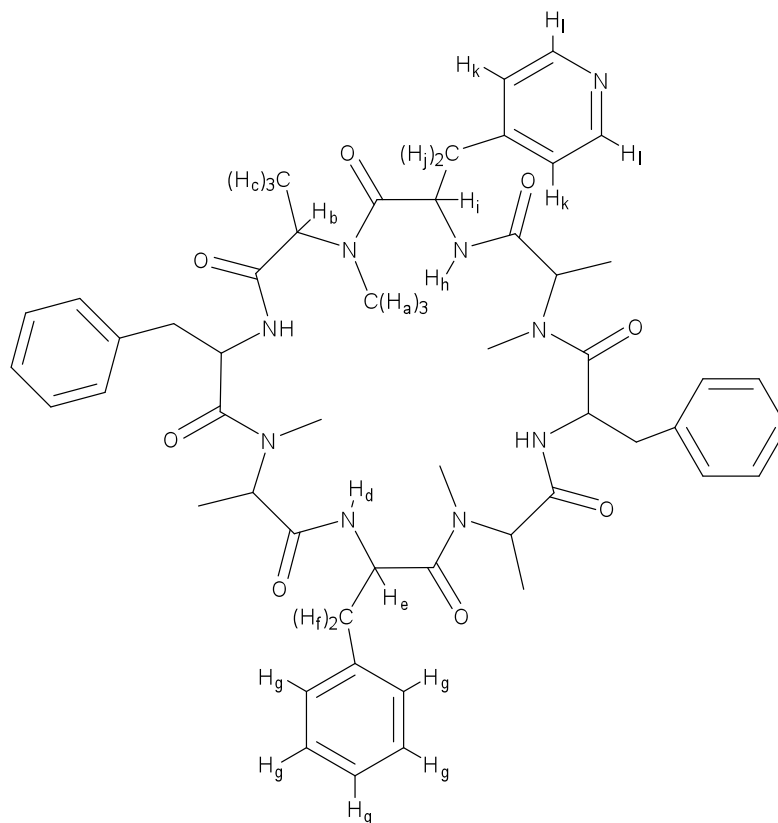
Figure A.6 TOCSY 4.0-9.0, 4.0-0.0ppm



**FIGURE A.7** ROESY data of compound 6



2D NMR data assigned to compound 6



Even though all the alanine, phenylalanine, NH's, and N-methyl groups are not equivalent to each other the signals could not be conclusively assigned for each individual amino acid in the cyclic octapeptide.

N(me)-Alanine signals:

$H_a$ = 2.48 ppm	N-Me $CH_3$
$H_b$ = 4.50-5.20 ppm	CH
$H_c$ = 0.80, 0.90, 1.00, 1.30 ppm	$CH_3$

Phenylalanine signals:

$H_d$ = 7.75-8.42 ppm	NH (overlapping with pyridylalanine NH)
$H_e$ = 5.13 ppm	CH
$H_f$ = 2.61 ppm	$CH_2$
$H_g$ = 7.20 ppm	aromatic protons

Pyridylalanine signals:

$H_h$ = 7.75-8.42 ppm	NH (overlapping with phenylalanine NH)
$H_i$ = 4.81 ppm	CH
$H_j$ = 2.81 ppm	$CH_2$
$H_k$ = 7.68 ppm	aromatic protons
$H_l$ = 8.60 ppm	aromatic protons

**FIGURE A.8** COSY data of di-substituted pyridylalanine cyclic peptide (compound 7)

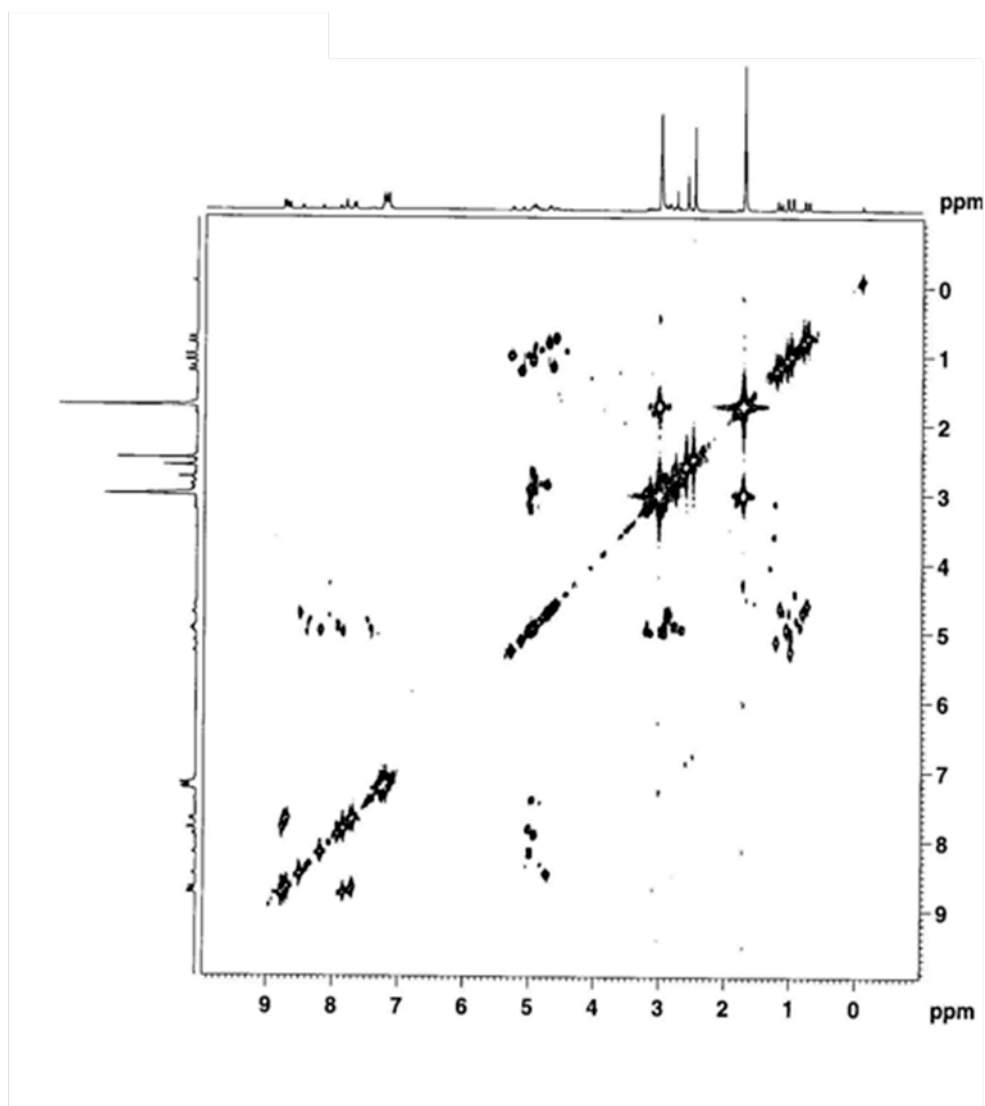
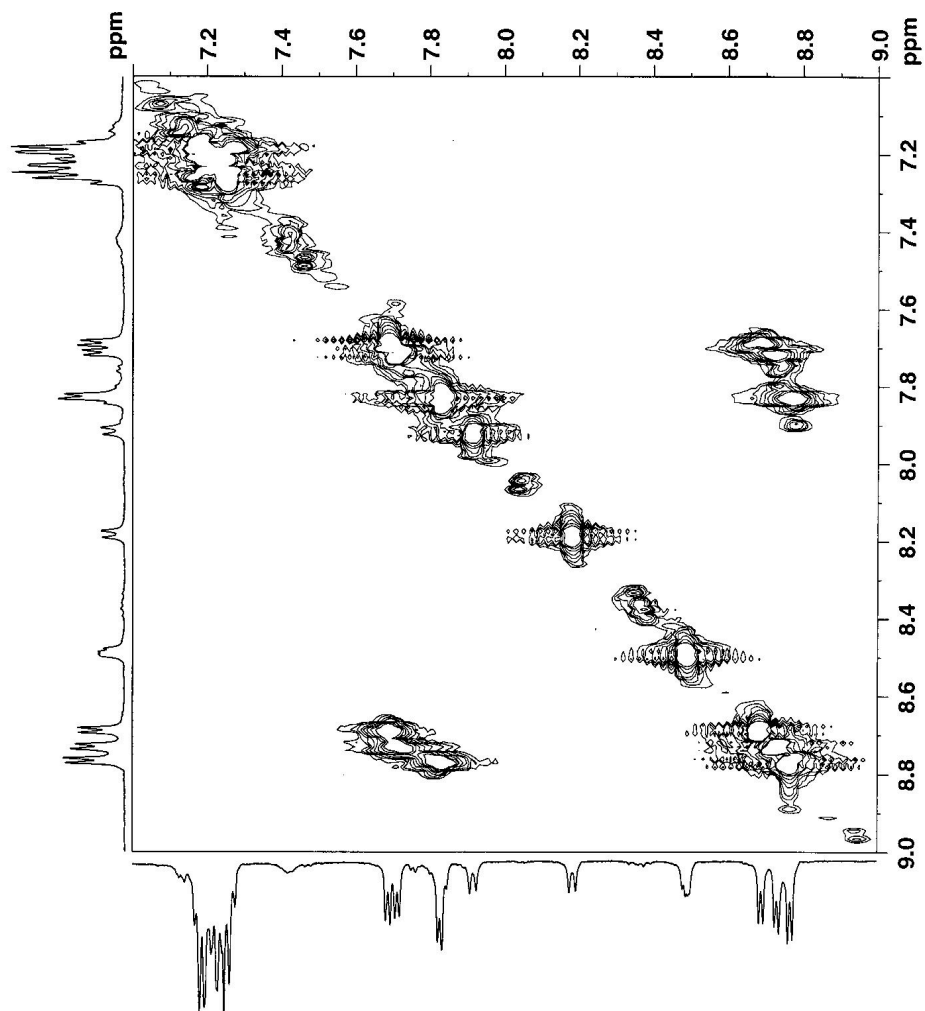




Figure A.9 COSY 7.0-9.0ppm



**Figure A.10** COSY 5.5-0.0ppm

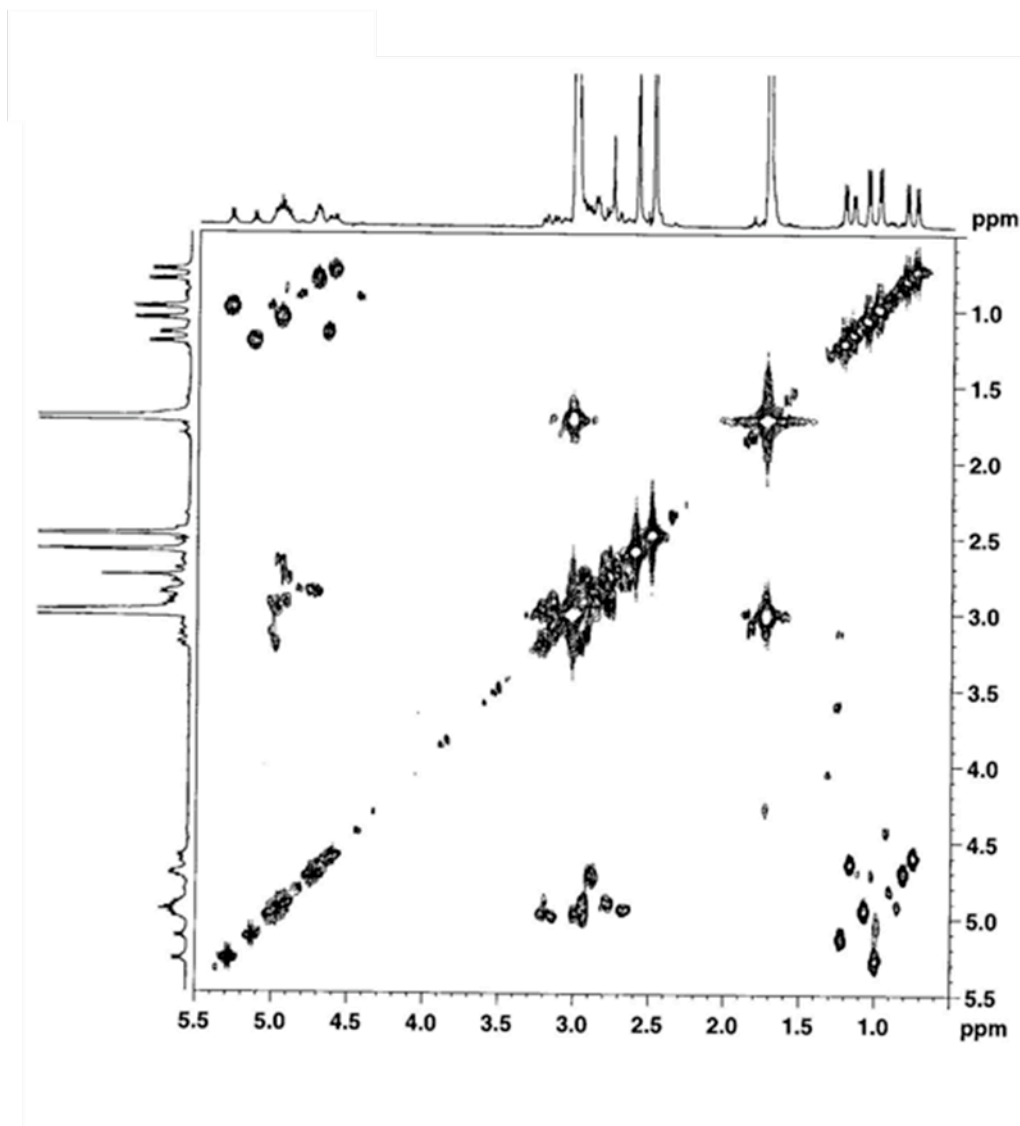
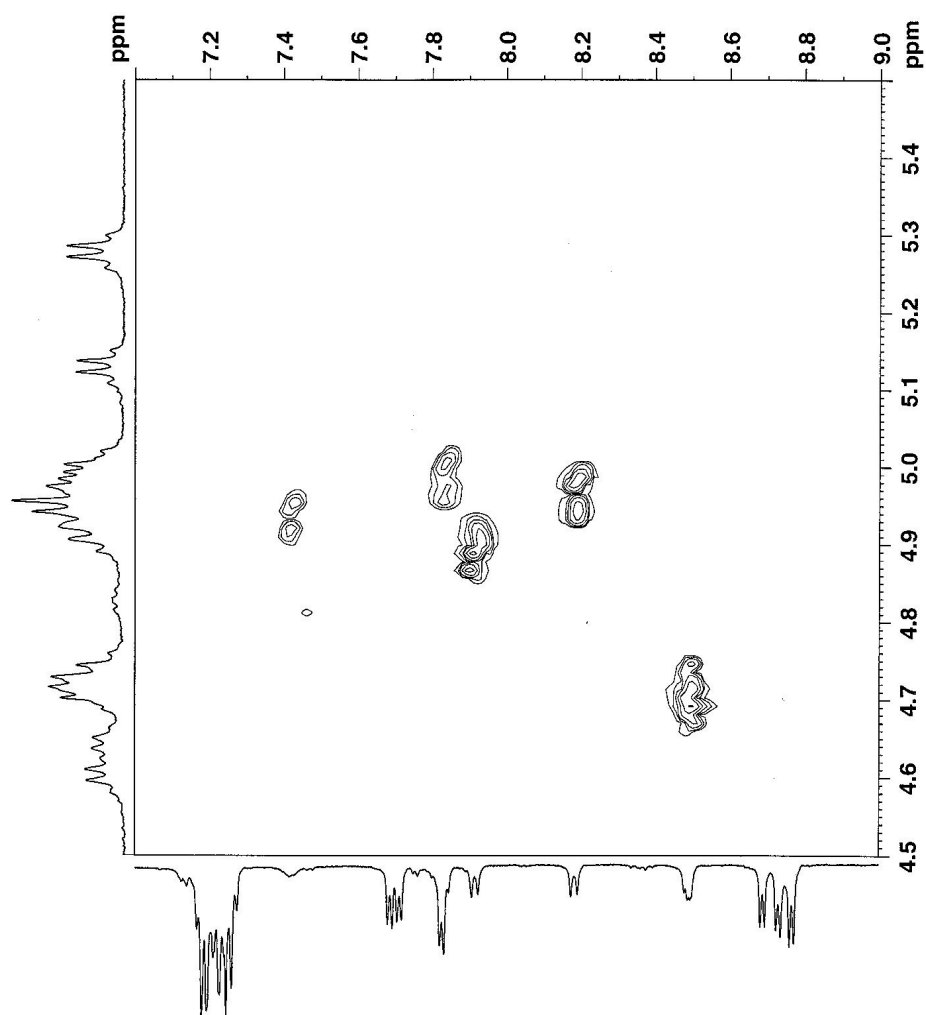


Figure A.11 COSY 9.0-7.0, 5.5-4.5ppm



**Figure A.12** COSY 5.5-4.3, 2.4-3.4ppm

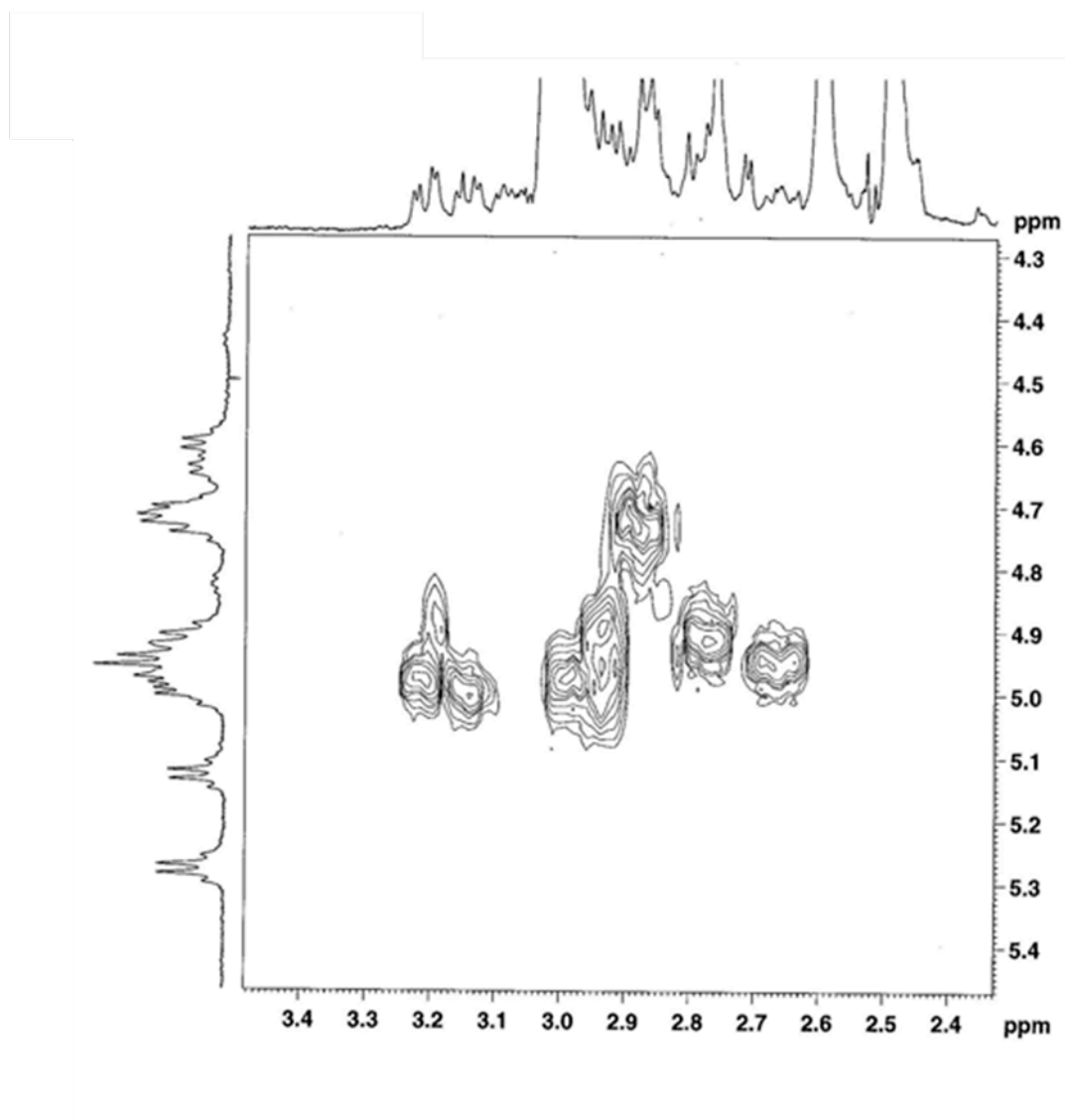
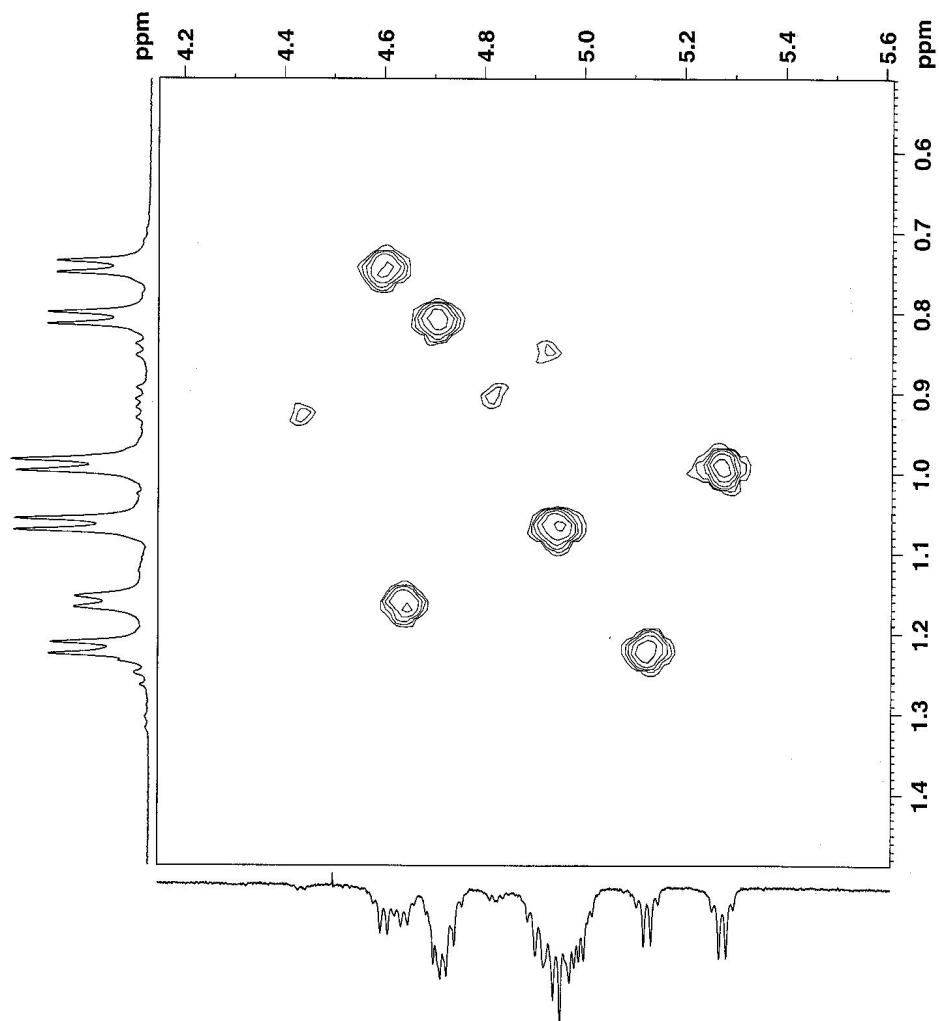
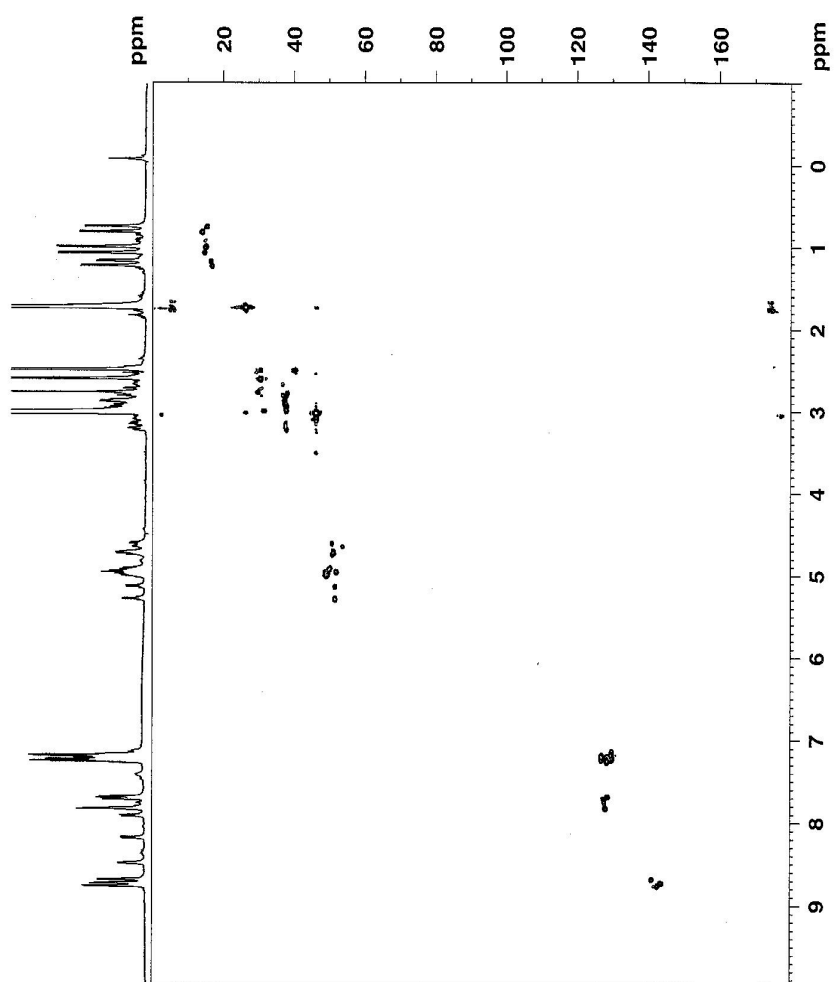


Figure A.13 COSY 5.6-4.2, 0.5-1.5ppm



**FIGURE A.14** HSQC data of di-substituted pyridylalanine cyclic peptide



**Figure A.15** HSQC 150-120, 7.0-9.0 ppm

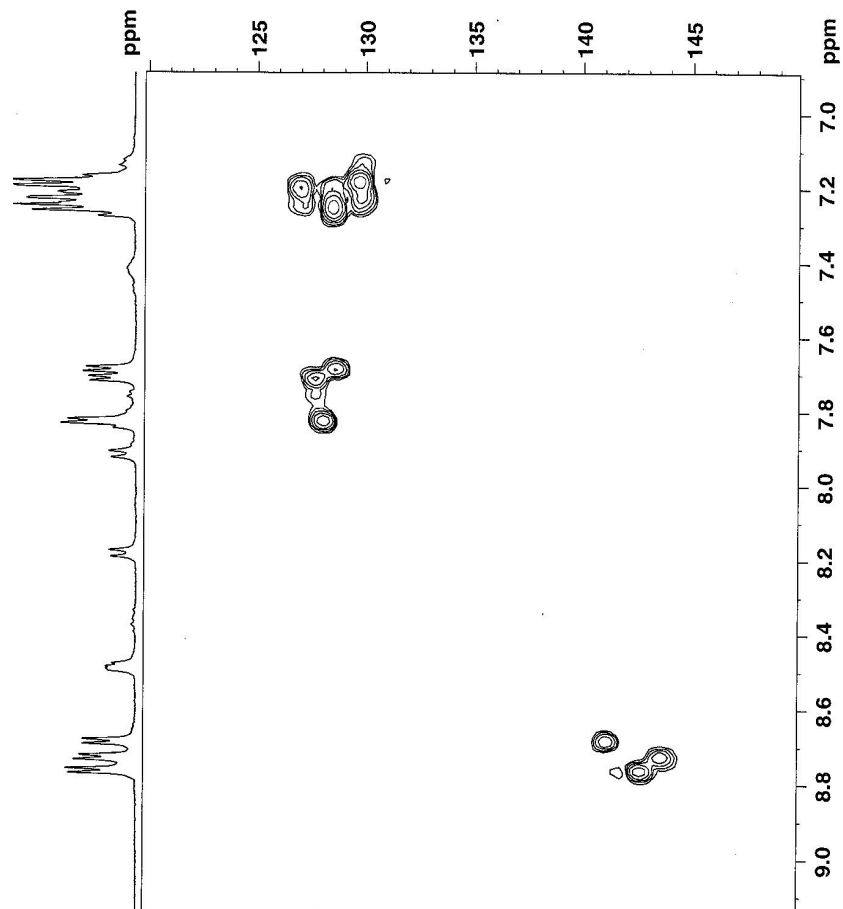


Figure A.16 HSQC 57-44, 4.3-5.7 ppm

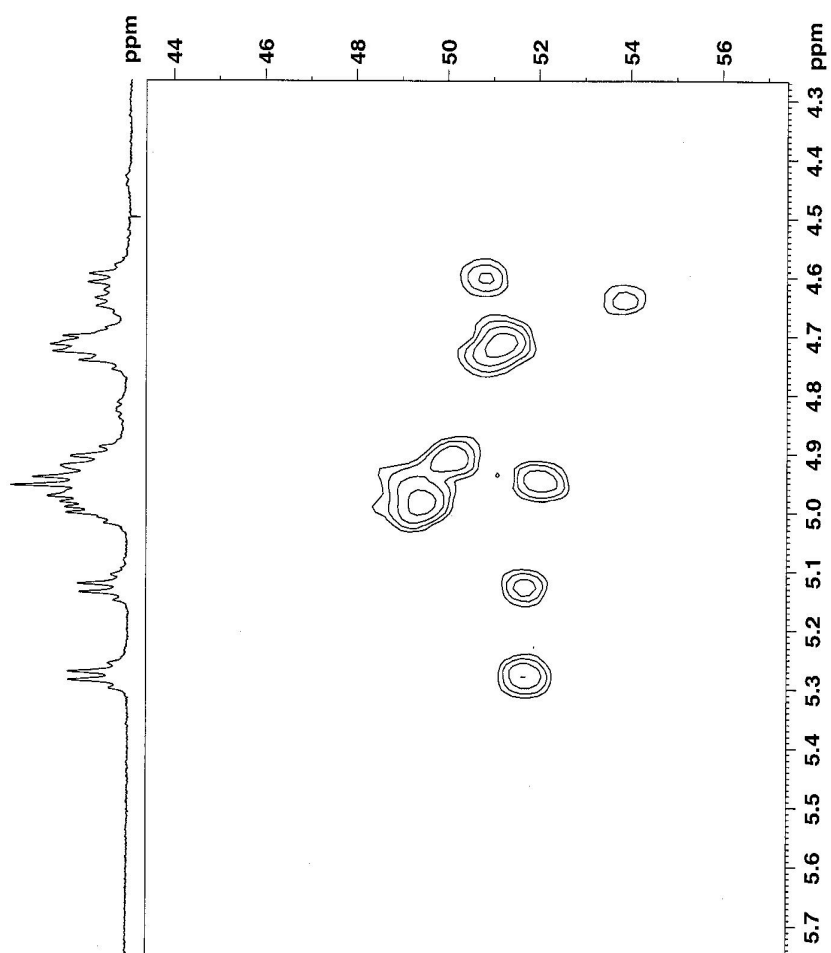
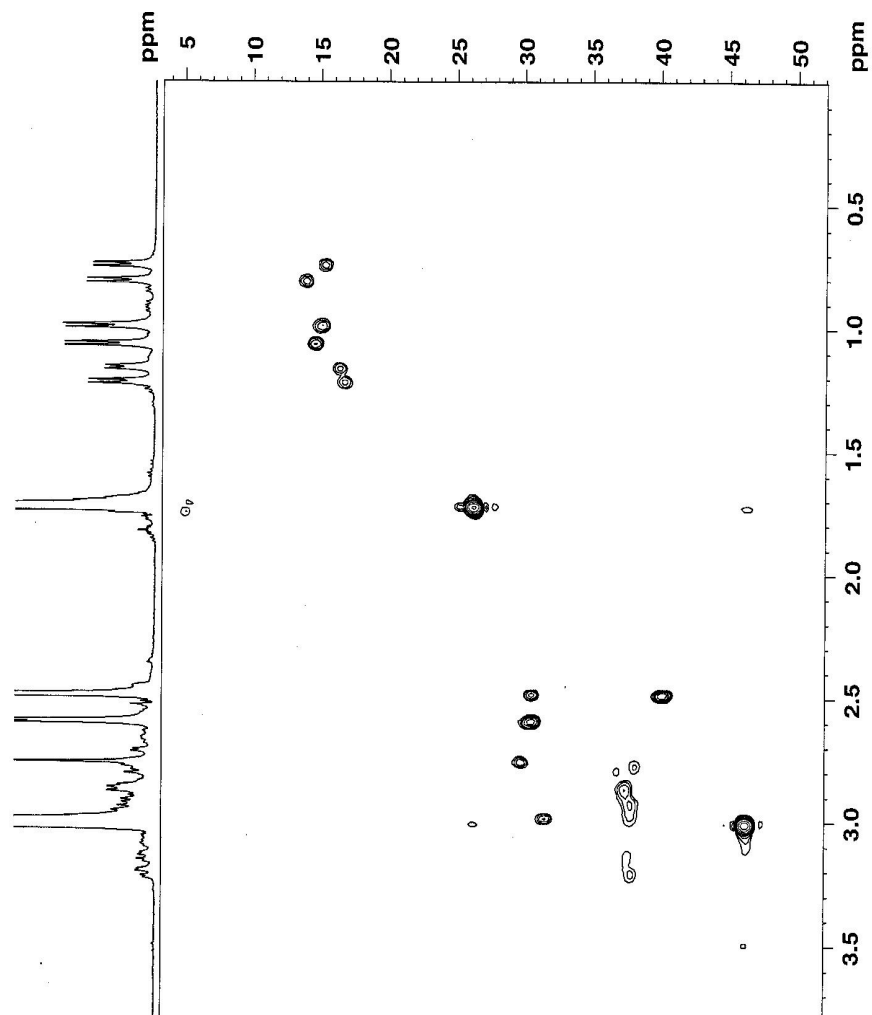
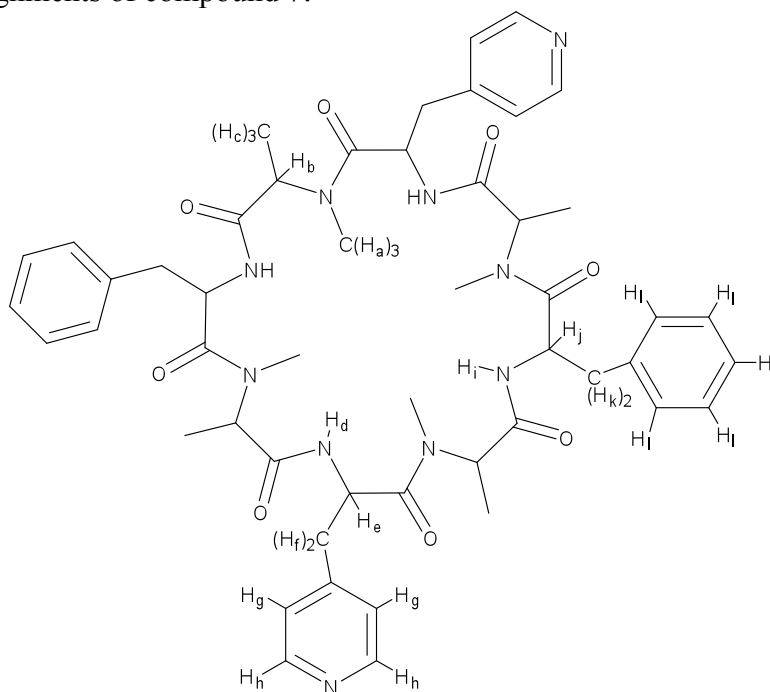




Figure A.17 HSQC 50-5, 0-3.5 ppm



2D NMR assignments of compound 7:



The HSQC was not complete; therefore the proton-carbon assignments could not be assigned.

N-(methyl)-Alanine Signals: Theoretically there are 2 equivalent alanines per cyclic peptide but these NMR studies cannot distinguish them from one another

$H_a = 2.50$ ppm	N-CH <sub>3</sub>
$H_b = 4.70$ ppm, $5.14$ ppm	CH
$H_c = 0.77$ ppm, $1.02$ ppm	CH <sub>3</sub>

Pyridylalanine Signals:

$H_d = 7.90$ or $8.18$ ppm	NH cannot distinguish from phenylalanine NH signal
$H_e = 4.91$ - $5.05$ ppm	CH overlap with phenylalanine CH signal
$H_f = 2.82$ - $3.04$ ppm	CH <sub>2</sub> overlap with phenylalanine CH <sub>2</sub> signal
$H_g = 7.73$ ppm	Aromatic proton
$H_h = 8.76$ ppm	Aromatic proton

Phenylalanine Signals:

$H_i = 7.90$ or $8.18$ ppm	NH cannot distinguish from pyridylalanine NH signal
$H_j = 4.91$ - $5.05$ ppm	CH overlap with pyridylalanine CH signal
$H_k = 2.82$ - $3.04$ ppm	CH <sub>2</sub> overlap with pyridylalanine CH <sub>2</sub> signal
$H_l = 7.20$ - $7.35$ ppm	Aromatic proton

Non N-(Me)-Alanine

$1.22$ ppm	CH <sub>3</sub>	
$4.70$ ppm	CH	
	$8.60$ ppm	NH

## APPENDIX B

### AN ALKYNE FUNCTIONALIZED LACTIDE MONOMER

#### Introduction

Poly(lactic acid), (PLA), has gained popularity in recent years due to it being a biorenewable resource and its potential applications in the medical community by being biocompatible and biodegradable.<sup>74</sup> Proposed and current medical applications of PLA include sutures, stents, drug delivery, among others, however. This appendix of the thesis targets the use of functionalized PLA-based polymeric systems as novel materials for bone scaffolding.

The need to functionalize lactide monomers stems from the fact that without such modification there is little that can alter the polymer in terms of biocompatibility, tissue adhesion, hydrophobicity, degradation rates, and mechanical strength.<sup>75</sup> Also, it allows for the post-polymerization functionalization with of biological moieties. Previously functionalized lactide monomers by the Weck and Collard groups have focused on serines or lactides functionalized with sugars. This project proposed a lactide monomer (Figure B.1) that is functionalized with an alkyne group that can undergo post-polymerization reactions including 1,3 dipolar cycloadditions.

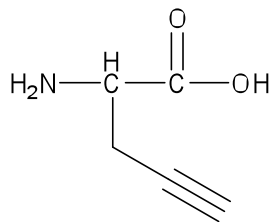


**Figure B.1:** Lactide monomer

#### Results and Discussion

The synthesis of the alkyne lactide monomer is shown in Figure B.2 below. The starting product is a commercially available amino acid that is available in racemic and enantiomerically pure forms. However, to reduce costs, the racemic starting material was always used. Overall, the functionalized lactide monomer is made with an overall yield of 21% from start to finish. The starting material being an amino acid allows for the synthetic scheme to be opened to a larger library of lactides, each bringing with it its own properties and benefits.

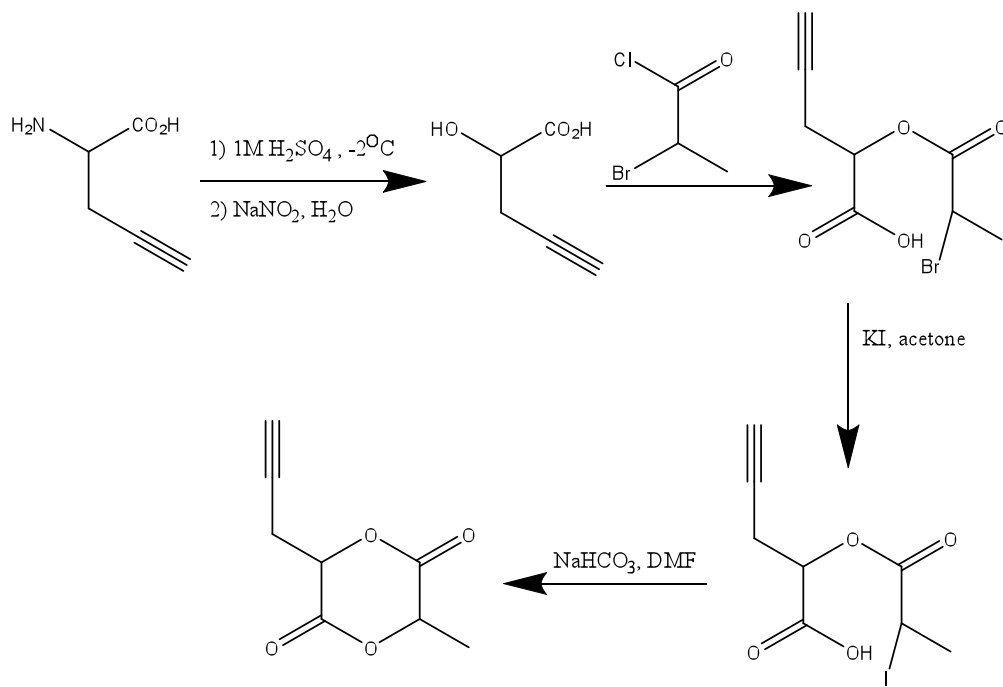


**Figure B.2:** Synthesis of lactide monomer

Polymerization of the functionalized lactide occurs through a ring-opening polymerization using stannous octoate as catalyst and *t*-butyl benzyl alcohol as the initiator. Stannous octoate offers the benefit of being an approved catalyst for medical applications.<sup>76</sup> Another initiator besides the *t*-butyl benzyl alcohol is a norbornene polymer chain with an alcohol group on one end. The benefits of using the norbornene polymer initiator is that it can provide rigidity to the polymer chain and help to alter the properties of the overall co-polymer for the target bone scaffolding application. Wang *et*

*al.* recently published the use of a norbornene initiator for use with lactide monomers to form highly porous scaffolds that could be beneficial for bone scaffolding.<sup>77</sup> After the copolymerization of the functionalized lactide monomer with the norbornene initiator the foaming process is based on thermally induced phase separation (TIPS) to successfully create the necessary and reproducible pore size.<sup>78</sup> By dissolving the polymer in a solvent followed by freeze-drying endows the remaining material with the desired porous structure. After creating the pores the cross-linking can be done using a photo cross-linkable agent to further set the polymer.

This post-polymerization occurs through a 1,3-dipolar cycloaddition with an azide functionalized moiety that can be a PEG chain for solubility, peptide sequences for cell adhesion, or even biotin for binding studies. Figure B.3 below shows the monomer polymerization and a simplified view of the products after the 1,3-dipolar cycloaddition.

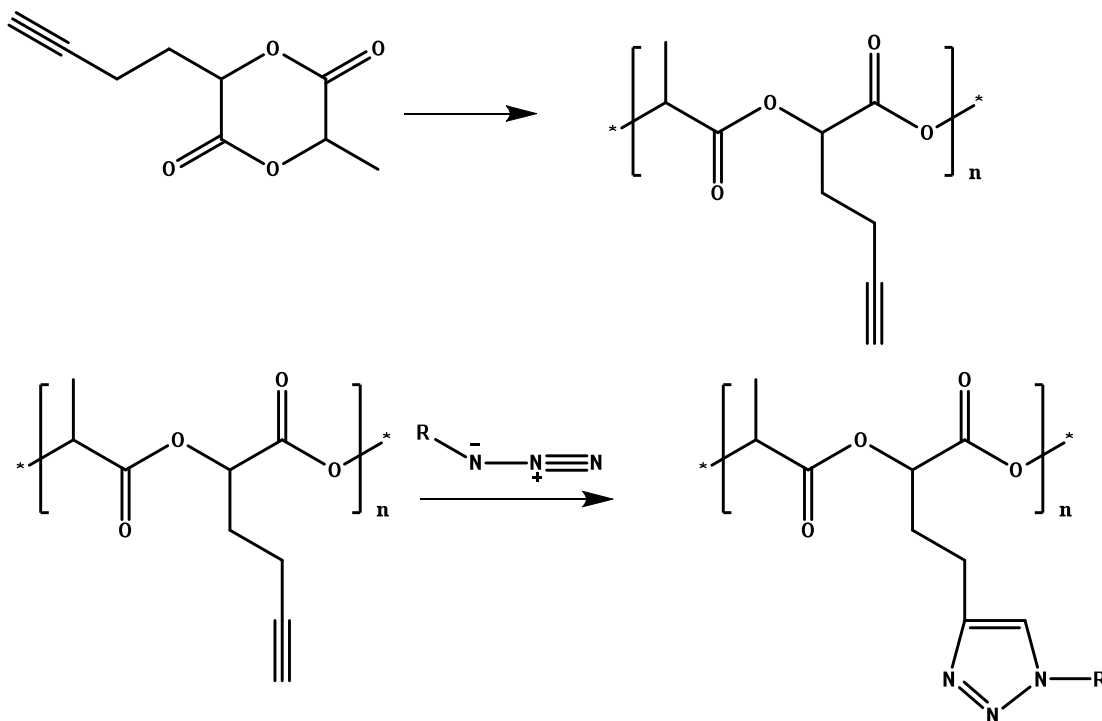


**Figure B.3:** Ring-opening polymerization of functionalized monomer and subsequent post-polymerization reaction.

The copolymerization of this monomer with lactic acid maintains the biodegradation needed for bone scaffolding applications and minimizes the amount of functionalized lactide monomer needed. As stated before, the azide for the 1,3-dipolar cycloadditions can contain a library of different biological moieties, but we were mostly interested in peptides, sugars, and biotin. A small poly(ethylene glycol) chain could be used as well but this does not affect how the polymer works biologically except for altering its hydrophilicity. The 1,3-dipolar cycloaddition is often referred to as “click” chemistry and offers benefits of being widely applicable due to mild reaction conditions, high yield, and byproducts that are easily removed.<sup>79</sup> In this case it enables the polymer to undergo various different routes of functionalization through the same chemical route. The high yielding post-polymerization step is also a necessity because the monomer is made in such a low yielding synthesis and was copolymerized with lactide that it must be high yielding to achieve the maximum results desired.

Synthesis of the alkyne functionalized lactide monomer has been the most difficult process of this project. Over the years, each step in the synthesis of the alkyne functionalized lactide monomer has resulted in the reevaluation of the synthetic strategy. Buying new reagents, trying different water sources and many other synthetic steps have been taken to provide what little monomer has actually been made. Different solvents, acids, and bases were also explored, but did not offer any further insight into how the reaction scheme could be optimized. Using different proton sources, like acetic acid, TFA, or even sulfuric acid, during the alpha hydroxyl acid synthesis also did not provide any insight into the yields, however the -2 °C ice water bath for the reaction did seem to provide the optimal results for the product synthesis. Using an amine to sequester the HCl formed *in situ* during the coupling step of the alpha hydroxy acid to the acid chloride did not seem to affect the yield of the product and in turn made the purification more difficult. Trying to cyclize the monomer without switching the halogen to iodine did not

provide the desired cyclized product. Longer reaction times also did not seem to give rise to higher yields. Lactide monomers from Dr. Collard's group are often dimerized at high temperature for so long, however the alkyne functionality may not survive such harsh conditions for that long of a time. Also, the dimerized product may interfere with the 1,3-dipolar cycloaddition post-polymerization reaction. However, a small amount of the alkyne functionalized lactide monomer was made through the synthetic route. While not enough to complete all the characterization and desired experiments, it was adequate for a test polymerization reaction. A test polymerization was carried out using 10% of the alkyne functionalized monomer and 90% lactide. The reaction was complete in less than 30 minutes using stannous octoate as the catalyst and *t*-butyl benzyl alcohol as the initiator. A molecular weight determination was attempted by GPC, however, the GPC data were inconclusive. However, end group analysis carried out by NMR spectroscopy suggests a molecular weight between 25,000 and 30,000 g/mol.

Another goal of the project is to reinforce the PLA block by using a norbornene polymer as the initiator. This alters the mechanical strength of the final material and has shown to be useful for making the necessary porosity of the foamed polymer.<sup>2</sup> Not only does the norbornene polymer provides a rigid polymer backbone but can also contain functional groups that can alter the physical and mechanical properties of the final copolymer. Such is the case with Wang's system where a cross-linkable unit off of the norbornene was used to photo cross-link the material after the foaming process took place. Since there was not enough of the alkyne monomer synthesized and purified the polymerizations off of the norbornene and 1,3-dipolar cycloaddition reactions were not carried out. However, based on a recent publication from Baker's group there is nothing to suggest that it would not undergo the 1,3-dipolar cycloaddition reaction.<sup>80</sup>

## Conclusions

Since taking over this project in early 2006 many advances have been made. A different synthetic scheme was chosen other than the previous one used. In addition the alkyne functionalized monomer has been synthesized, although in very low quantities, and has shown to polymerize with racemic lactide in a short period of time. Continued success on this project will come once the monomer can be synthesized in greater quantity. After synthesis of the monomer is completed the polymerization reactions need to be fully evaluated. Potentially changing the monomer from an alkyne to an azide would help in overcoming this obstacle, however the monomer and the corresponding dimer have been made; therefore possibly further exploring different reaction routes and conditions would be more helpful than doing a total monomer switch. In addition, post-polymerization reactions using the 1,3-dipolar cycloaddition reaction can be carried out with various biological moieties. Then, polymer samples, both before and after post-polymerization need to be given to Dr. García's group to ensure biocompatibility.

In the long term, the alkyne functionalized monomer can be copolymerized with other monomers that our group has previous published to provide two functional handles on the PLA backbone.<sup>4</sup> However, the deprotection of the benzyl groups uses hydrogenation and may hydrogenate the alkyne if the alkyne does not undergo the 1,3-dipolar cycloaddition reactions prior to hydrogenation. The degradation rates and biocompatibility need to be evaluated. The use of the norbornene initiator also needs to be explored which would lead to various mechanical tests to determine the physical properties of the overall polymer and working to optimize the results.

## **Experimental**

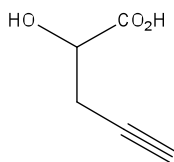
### ***Materials and Methods:***

Propargylglycine was purchased from Chem-Impex. 2-Bromopropionyl chloride, dry DMF and acetone were purchased from Aldrich. D,L-Lactide was purchased from Aldrich and recrystallized in dry EtOAc, dissolved in benzene, lyophilized, and stored in



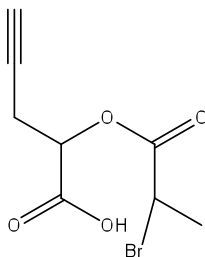
a nitrogen filled glovebox. NMR spectra acquired on a Bruker DSX 300 at 298 K ( $^1\text{H}$  NMR: 300 MHz,  $^{13}\text{C}$  NMR: 75MHz). All chemical shifts are reported in parts per million (ppm), using the solvent as an internal standard. Data is reported as follows: chemical shift, multiplicity, coupling constant, and integration.

***Synthesis of 2-hydroxypent-4-ynoic acid***



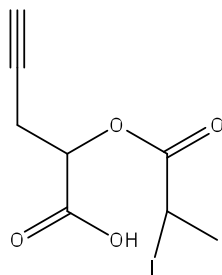
Propargylglycine (3.495 g, 30.9 mmol) was dissolved in ~120 mL of 1M  $\text{H}_2\text{SO}_4$  and cooled to  $-2\text{ }^\circ\text{C}$ .  $\text{NaNO}_3$  (6.40 g, 92.8 mmol) was dissolved in 60 mL of deionized water and added dropwise to the reaction mixture over 45 minutes under argon, allowing the reaction temperature to not exceed  $0\text{ }^\circ\text{C}$ . The ice bath was removed 9 hours later and the reaction was stirred at room temperature for another 16 hours. Then the water was washed with ethyl acetate, dried over magnesium sulfate, and excess solvent was removed under reduced pressure. Upon removal of the solvent a yellow crystalline solid appeared. Purification was completed using column chromatography (silica gel,  $\text{CH}_2\text{Cl}_2$ , MeOH,  $\text{CH}_3\text{COOH}$ ,  $\text{H}_2\text{O}$ ; 42.5:5:2.5:1). Yield: 2.6 g (74%).  $^1\text{H}$  NMR (300MHz,  $\text{CDCl}_3$ )  $\delta$  2.15(s, 1H), 2.79 (t,  $J=5$ , 2H), 4.42 (t,  $J=3$ , 1H);  $^{13}\text{C}$  NMR (300MHz,  $\text{CDCl}_3$ )  $\delta$  24.6, 70.3, 74.9, 78.2, and 176.5; MS (ESI) negative mode 112.8

***Synthesis of 2-(2-bromopropanolyoxy)pent-4-ynoic acid***



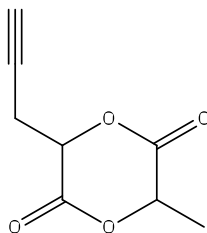
2-Hydroxypent-4-ynoic acid (2.6 g, 22.8 mmol) was dissolved in 2-bromopropanoyl chloride and heat to 40 °C. *n*-Methyl morpholine (4.5 mL, 48.4 mmol) was added dropwise to the reaction mixture. The reaction was then filtered over celite using ethyl acetate, dried over magnesium sulfate, and excess solvent was removed under reduced pressure. Excess acid chloride was removed using a Kugelrohr. Purification of the brown oil was completed using column chromatography (silica gel, CH<sub>2</sub>Cl<sub>2</sub>, MeOH, CH<sub>3</sub>COOH; 46.5:2.5:1). Residual acetic acid was removed using a Kugelrohr. Yield 3.89 g (68.5%). <sup>1</sup>H NMR (CDCl<sub>3</sub>) δ 1.85(m, *J*=6, 3H), 2.07 (m, 1H), 2.83(m, 2H), 4.50(m, 1H), 5.23(m, *J*=5, 1H), 9.25(b, 1H); MS (ESI) negative mode 248.7

***Synthesis of 2-(2-iodopropanolyoxy)pent-4-ynoic acid***



2-(2-Bromopropanolyoxy)pent-4-ynoic acid (3.89 g, 15.6 mmol) was dissolved in 40 mL of dry acetone and potassium iodine (15.0 g, 90.3 mmol) was added and the reaction mixture was closed under argon and heated to 75 °C overnight. Residual solid was removed by filtration and acetone was removed under reduced pressure. The resulting solid was dissolved in diethyl ether and washed with a solution of saturated thiosulfate (200 mL), dried over magnesium sulfate, and excess solvent was removed under reduced pressure. Yield 3.69 g (79.9%). <sup>1</sup>H NMR (CDCl<sub>3</sub>) δ 1.98 (m, *J*=6, 3H), 2.09 (m, 1H), 2.81 (m, 2H), 4.58 (m, 1H), 5.22 (m, *J*= 5, 1H), 9.50 (b, 1H)

***Synthesis of 3-methyl-6-(pro-2-ynyl)-1,4-dioxane-2,5-dione***



2-(2-iodopropanolyoxy)pent-4-ynoic acid (103 mg, 0.348 mmol) was dissolved in 2 mL of DMF. The solution was added to 10 mL of DMF (dry and degassed) and  $\text{NaHCO}_3$  (55 mg, 0.654 mmol) heated to 40 °C, via a syringe pump with an addition rate of 0.5 mL/h. The reaction was left overnight, DMF was removed under reduced pressure, and was purified by dissolving in diethyl ether and precipitating in methanol three times. Yield 30 mg (52%).  $^1\text{H}$  NMR ( $\text{CDCl}_3$ )  $\delta$  1.69 (d,  $J=6$ , 3H), 2.16 (t,  $J=4$ , 1H), 2.98 (m, 2H), 5.07(m, 2H); Elemental Analysis calcd. for  $\text{C}_8\text{H}_8\text{O}_4$ : C, 57.14; H, 4.80; O, 38.06. found C, 56.76; H, 4.82; O, 38.35.

#### ***SnOct<sub>2</sub> Catalyst Stock Solution:***

In a nitrogen-filled glovebox the stannous octoate (0.32 g, 0.8 mmol) was added to a 10 mL volumetric flask and filled with dry, degassed benzene. The resulting solution was 0.8 M and stored in the glovebox contained in a Schlenk flask.

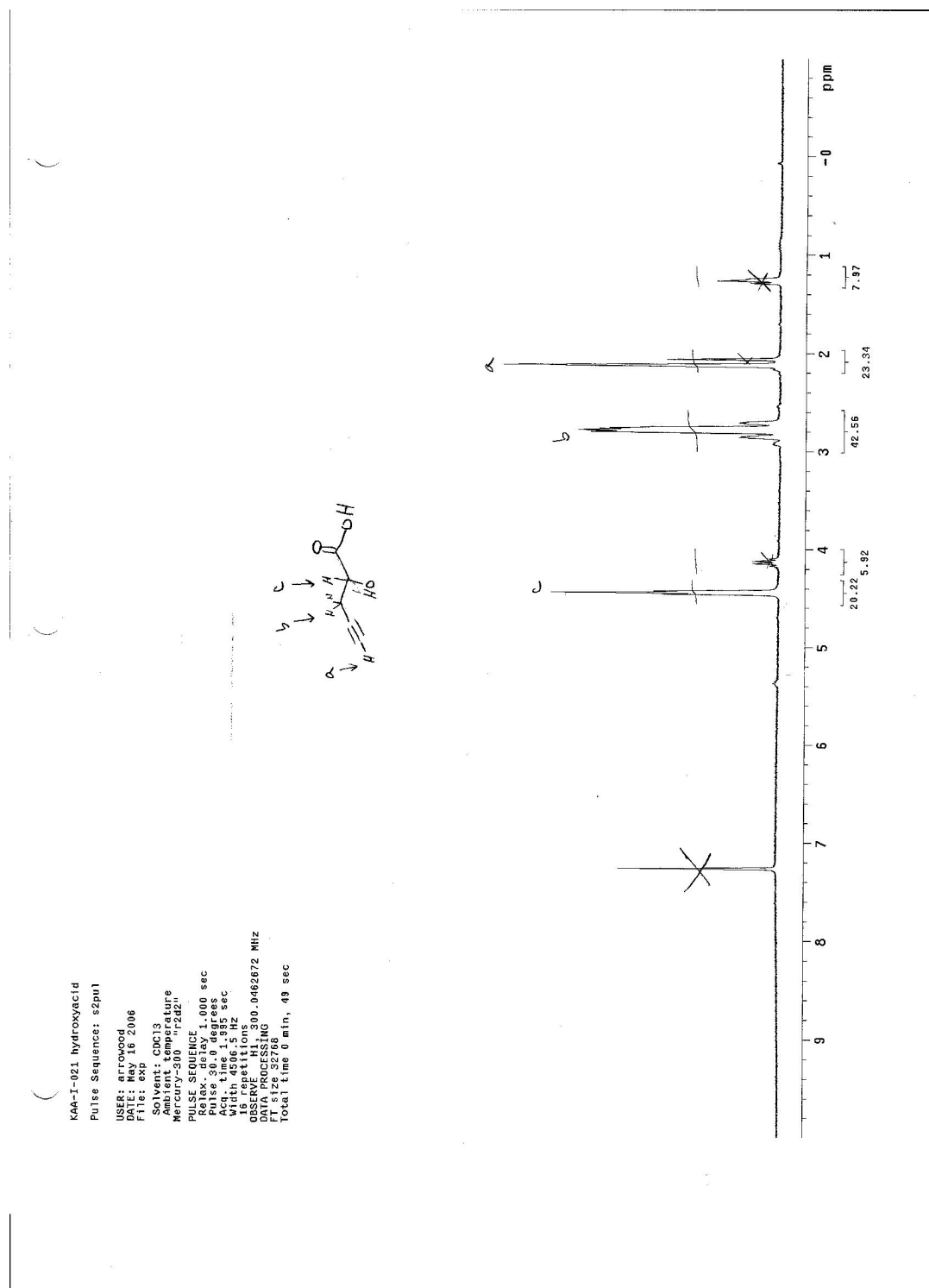
#### ***Copolymerization procedure:***

In a nitrogen filled glovebox, 13.5 mg(0.08 mmol) of alkyne lactide monomer, 107 mg (0.72 mmol), 100  $\mu\text{L}$  (0.0008 mmol) of 0.004 M  $\text{Sn}(\text{oct})_2$  catalyst, and 71  $\mu\text{L}$  of *t*-butyl benzyl alcohol were added to a reaction vessel along with a small amount of benzene (less than 1 mL) to get the solid into the bottom of the vessel. The sample was then removed from the glovebox and lyophilized prior to polymerization. Under argon, the reaction mixture was then heated to 110 °C and stirred for 1 hour. The solid was dissolved in methylene chloride and precipitated out using cold methanol three times.

$^1\text{H}$  ( $\text{CDCl}_3$ )  $\delta$  1.59 (d,  $J=3$ , multiple H's) , 2.05 (m, 1H), 2.85 (m, 2H), 5.11(q,  $J=1,3$ , multiple H's);  $^{13}\text{C}$  NMR racemic (300MHz,  $\text{CDCl}_3$ )  $\delta$  169.17, 169.04, 168.83, 167.22, 166.98, 168.81, 71.43, 70.51, 70.39, 69.49, 69.35, 69.08, 68.95, 68.79, 66.68, 31.22, 21.47, 20.46, 16.80, 16.58.

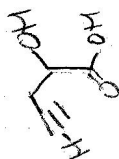
### Raw Data

**Figure B.4**  $^1\text{H}$  NMR spectrum for 2-hydroxypent-4-ynoic acid (300 MHz)



CC#CC(=O)O

13C NMR SPECTRUM  
 1 15927.235 211.106 31.0  
 Pulse Seq 4408-4861 194.957 21.2  
 3 14070.300 186.502 -20.9  
 USER: arrow 6245.038 177.013 -23.4  
 5 13338.026 176.526 -27.9  
 7 13181.036 157.343 20.3  
 Solvent: CDCl3 83.445  
 Ambient temperature 22.4  
 Mercury-300 75.271 98.871 -22.1  
 PULSE SEQUENCE 4408 92.085 25.4  
 Relaxation delay 1.000 85.082 21.9  
 Acq. time 5.000146 77.418 456.6  
 Width 1875.600146 77.418 478.3  
 256 repetitions 38.655087 74.955 -20.6  
 DECUPLE HET 7306 60726.000 Hz  
 Power 38 dB 555.087 74.955 67.0  
 continuous 60726.000 Hz  
 Lock 1875.600146 77.418 59.8  
 DATA PROCESSING 70.309 41.0  
 Lk 4408 194.957 44.0  
 FT 2048 6550884.090 56.783 22.4  
 Total time 2.0714288 55.304 22.7  
 22 2611.360 31.612 24.4  
 23 1853.893 24.652 54.1  
 24 984.521 13.049 21.4  
 25 654.105 8.670 22.7  
 26 74.730 0.990 32.7



13C NMR	FREQUENCY	PPM	HEIGHT
CDCl <sub>3</sub> solvent	132.7, 125.35	21.106	31.0
Pure 1	132.7, 125.35	184.957	21.2
Pure 2	132.7, 125.35	184.957	21.2
Pure 3	132.7, 125.35	184.957	21.2
Pure 4	132.7, 125.35	184.957	21.2
Pure 5	132.7, 125.35	184.957	21.2
Pure 6	132.7, 125.35	184.957	21.2
Pure 7	132.7, 125.35	184.957	21.2
Pure 8	132.7, 125.35	184.957	21.2
Pure 9	132.7, 125.35	184.957	21.2
Pure 10	132.7, 125.35	184.957	21.2
Pure 11	132.7, 125.35	184.957	21.2
Pure 12	132.7, 125.35	184.957	21.2
Pure 13	132.7, 125.35	184.957	21.2
Pure 14	132.7, 125.35	184.957	21.2
Pure 15	132.7, 125.35	184.957	21.2
Pure 16	132.7, 125.35	184.957	21.2
Pure 17	132.7, 125.35	184.957	21.2
Pure 18	132.7, 125.35	184.957	21.2
Pure 19	132.7, 125.35	184.957	21.2
Pure 20	132.7, 125.35	184.957	21.2
Pure 21	132.7, 125.35	184.957	21.2
Pure 22	132.7, 125.35	184.957	21.2
Pure 23	132.7, 125.35	184.957	21.2
Pure 24	132.7, 125.35	184.957	21.2
Pure 25	132.7, 125.35	184.957	21.2
Pure 26	132.7, 125.35	184.957	21.2
Pure 27	132.7, 125.35	184.957	21.2
Pure 28	132.7, 125.35	184.957	21.2
Pure 29	132.7, 125.35	184.957	21.2
Pure 30	132.7, 125.35	184.957	21.2
Pure 31	132.7, 125.35	184.957	21.2
Pure 32	132.7, 125.35	184.957	21.2
Pure 33	132.7, 125.35	184.957	21.2
Pure 34	132.7, 125.35	184.957	21.2
Pure 35	132.7, 125.35	184.957	21.2
Pure 36	132.7, 125.35	184.957	21.2
Pure 37	132.7, 125.35	184.957	21.2
Pure 38	132.7, 125.35	184.957	21.2
Pure 39	132.7, 125.35	184.957	21.2
Pure 40	132.7, 125.35	184.957	21.2
Pure 41	132.7, 125.35	184.957	21.2
Pure 42	132.7, 125.35	184.957	21.2
Pure 43	132.7, 125.35	184.957	21.2
Pure 44	132.7, 125.35	184.957	21.2
Pure 45	132.7, 125.35	184.957	21.2
Pure 46	132.7, 125.35	184.957	21.2
Pure 47	132.7, 125.35	184.957	21.2
Pure 48	132.7, 125.35	184.957	21.2
Pure 49	132.7, 125.35	184.957	21.2
Pure 50	132.7, 125.35	184.957	21.2
Pure 51	132.7, 125.35	184.957	21.2
Pure 52	132.7, 125.35	184.957	21.2
Pure 53	132.7, 125.35	184.957	21.2
Pure 54	132.7, 125.35	184.957	21.2
Pure 55	132.7, 125.35	184.957	21.2
Pure 56	132.7, 125.35	184.957	21.2
Pure 57	132.7, 125.35	184.957	21.2
Pure 58	132.7, 125.35	184.957	21.2
Pure 59	132.7, 125.35	184.957	21.2
Pure 60	132.7, 125.35	184.957	21.2
Pure 61	132.7, 125.35	184.957	21.2
Pure 62	132.7, 125.35	184.957	21.2
Pure 63	132.7, 125.35	184.957	21.2
Pure 64	132.7, 125.35	184.957	21.2
Pure 65	132.7, 125.35	184.957	21.2
Pure 66	132.7, 125.35	184.957	21.2
Pure 67	132.7, 125.35	184.957	21.2
Pure 68	132.7, 125.35	184.957	21.2
Pure 69	132.7, 125.35	184.957	21.2
Pure 70	132.7, 125.35	184.957	21.2
Pure 71	132.7, 125.35	184.957	21.2
Pure 72	132.7, 125.35	184.957	21.2
Pure 73	132.7, 125.35	184.957	21.2
Pure 74	132.7, 125.35	184.957	21.2

**Figure B.6**  $^1\text{H}$  NMR spectrum for 2-(2-bromopropanolyoxy)pent-4ynoic acid (300 MHz)

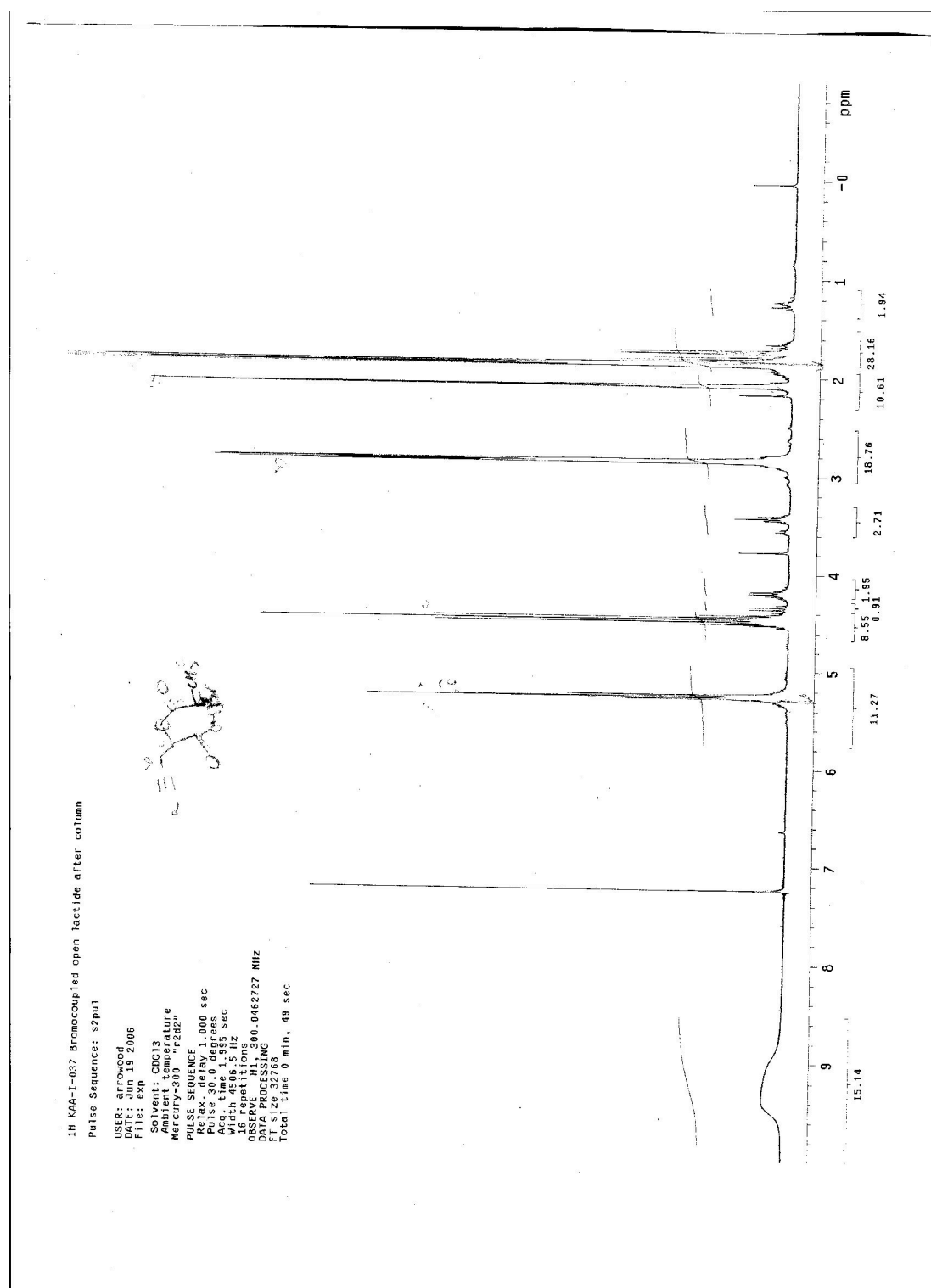


**Figure B.7**  $^1\text{H}$  NMR spectrum for 2-(2-iodopropanolyoxy)pent-4ynoic acid (300 MHz)

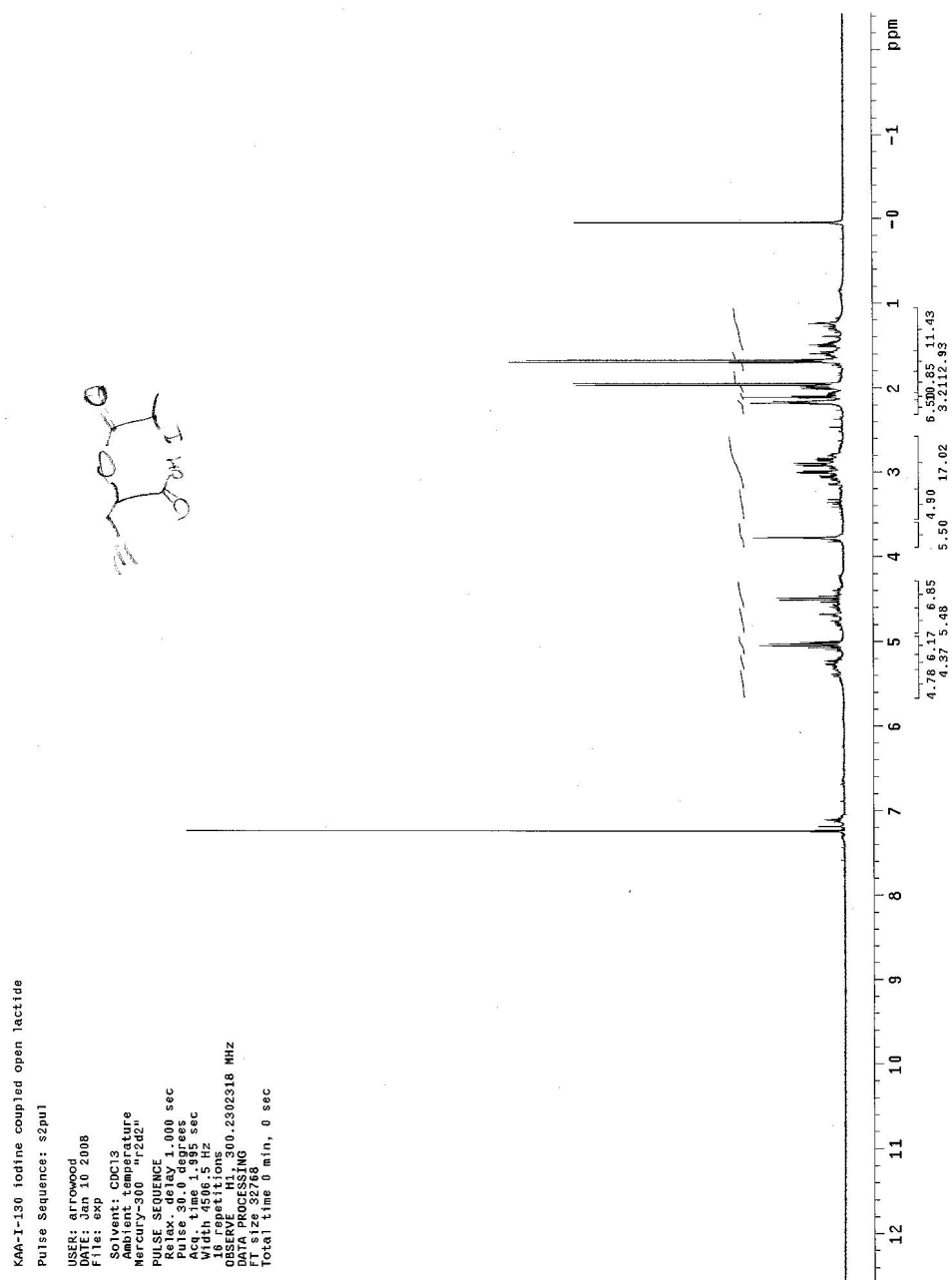




**Figure B.8**  $^1\text{H}$  NMR spectrum of 3-methyl-6-(pro-2-ynyl)-1,4-dioxane-2,5-dione (300 MHz)

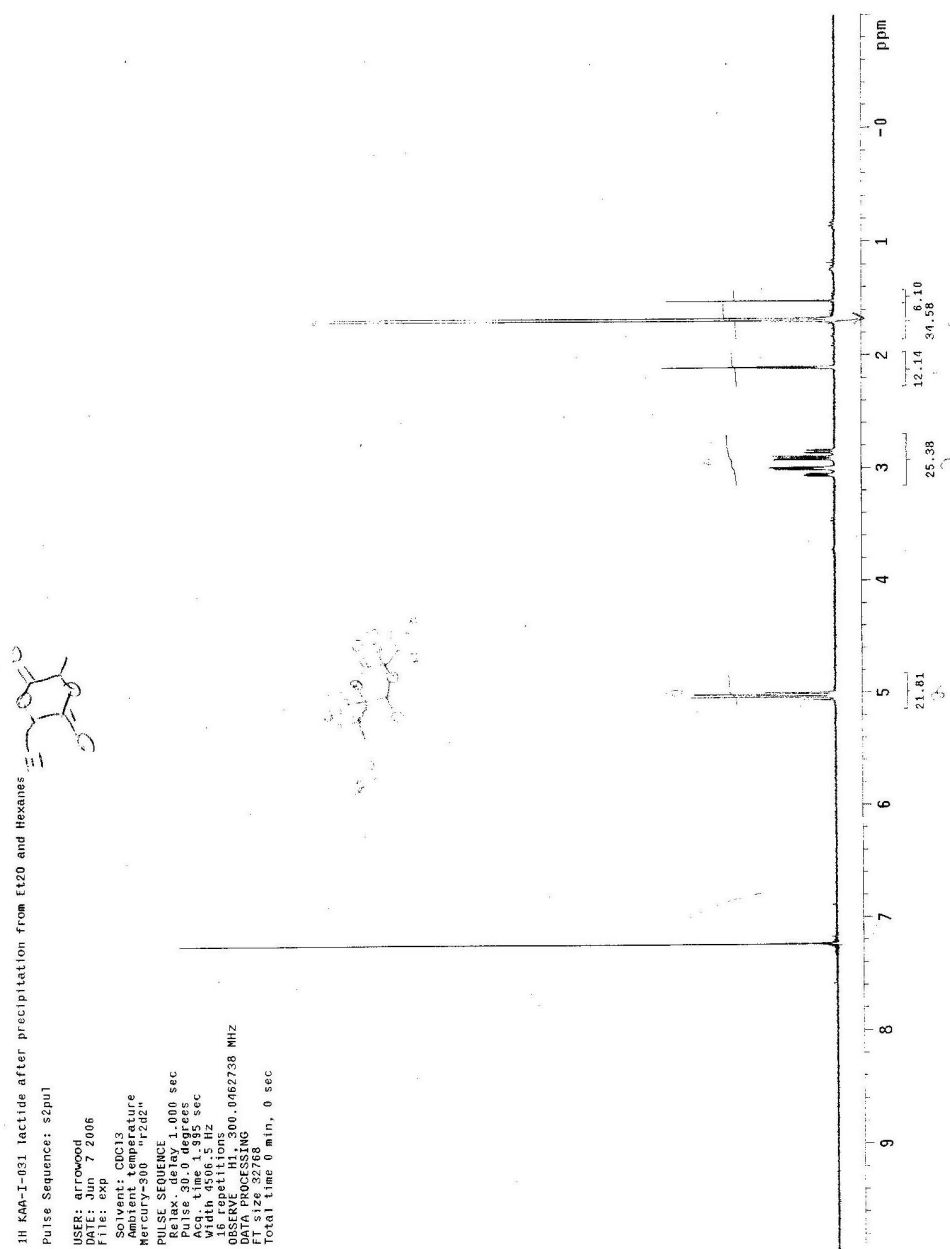


**Figure B.9**  $^{13}\text{C}$  NMR spectrum for 3-methyl-6-(pro-2-ynyl)-1,4-dioxane-2,5-dione (300 MHz)

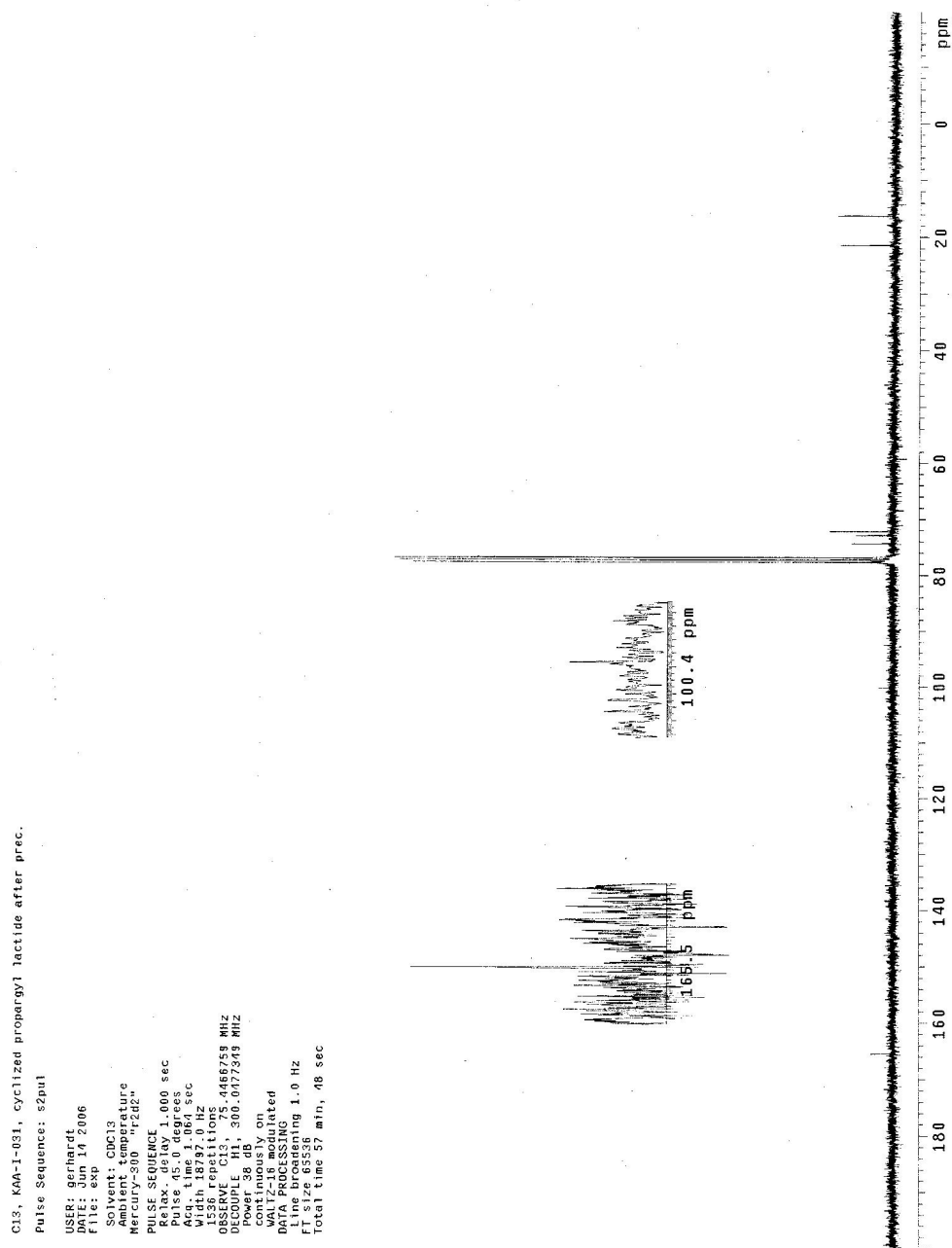


**Figure B.10**  $^{13}\text{C}$  NMR spectrum for 3-methyl-6-(pro-2-ynyl)-1,4-dioxane-2,5-dione  
10ppm-170ppm (300 MHz)

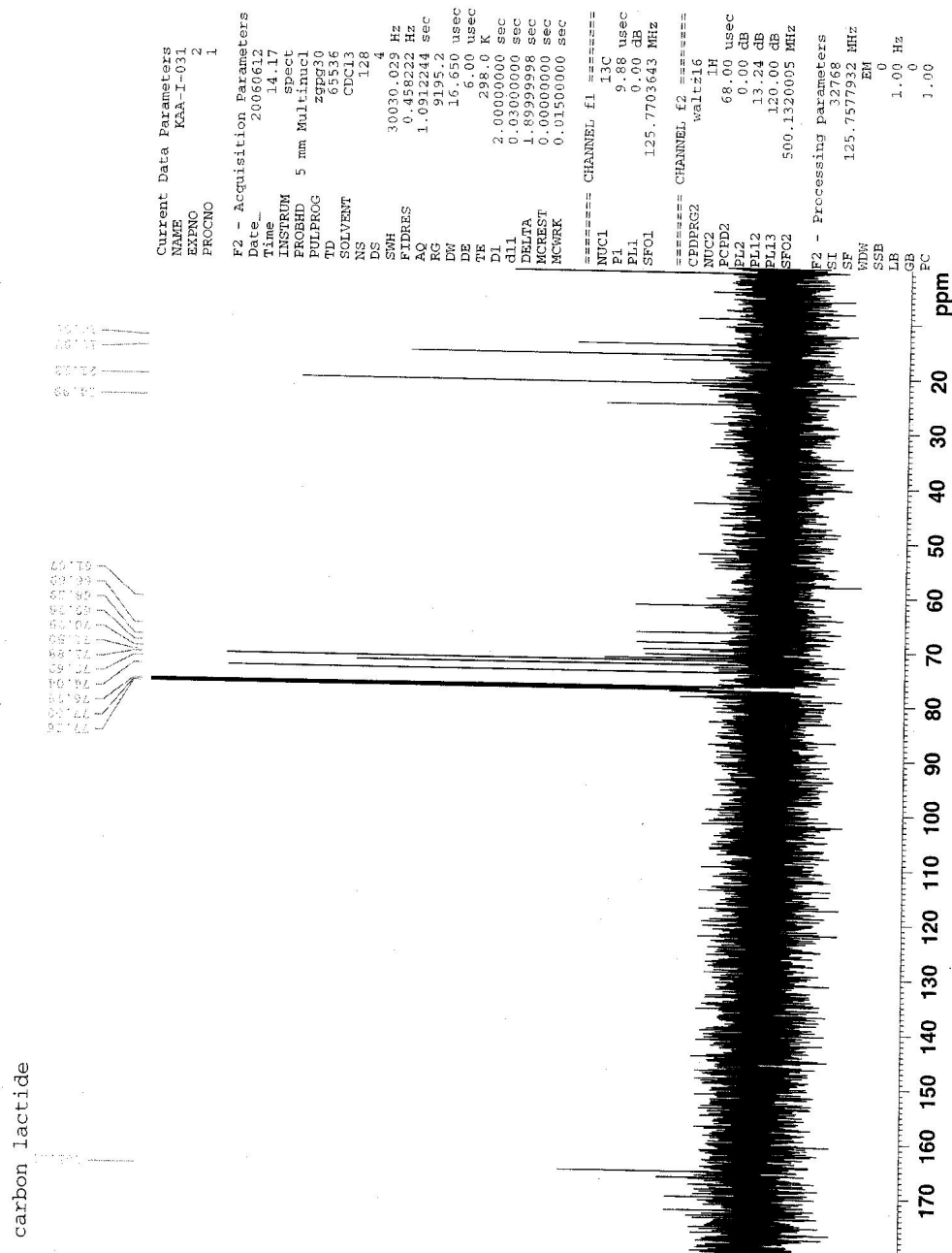


Figure B.11  $^1\text{H}$  NMR spectrum of lactide copolymer

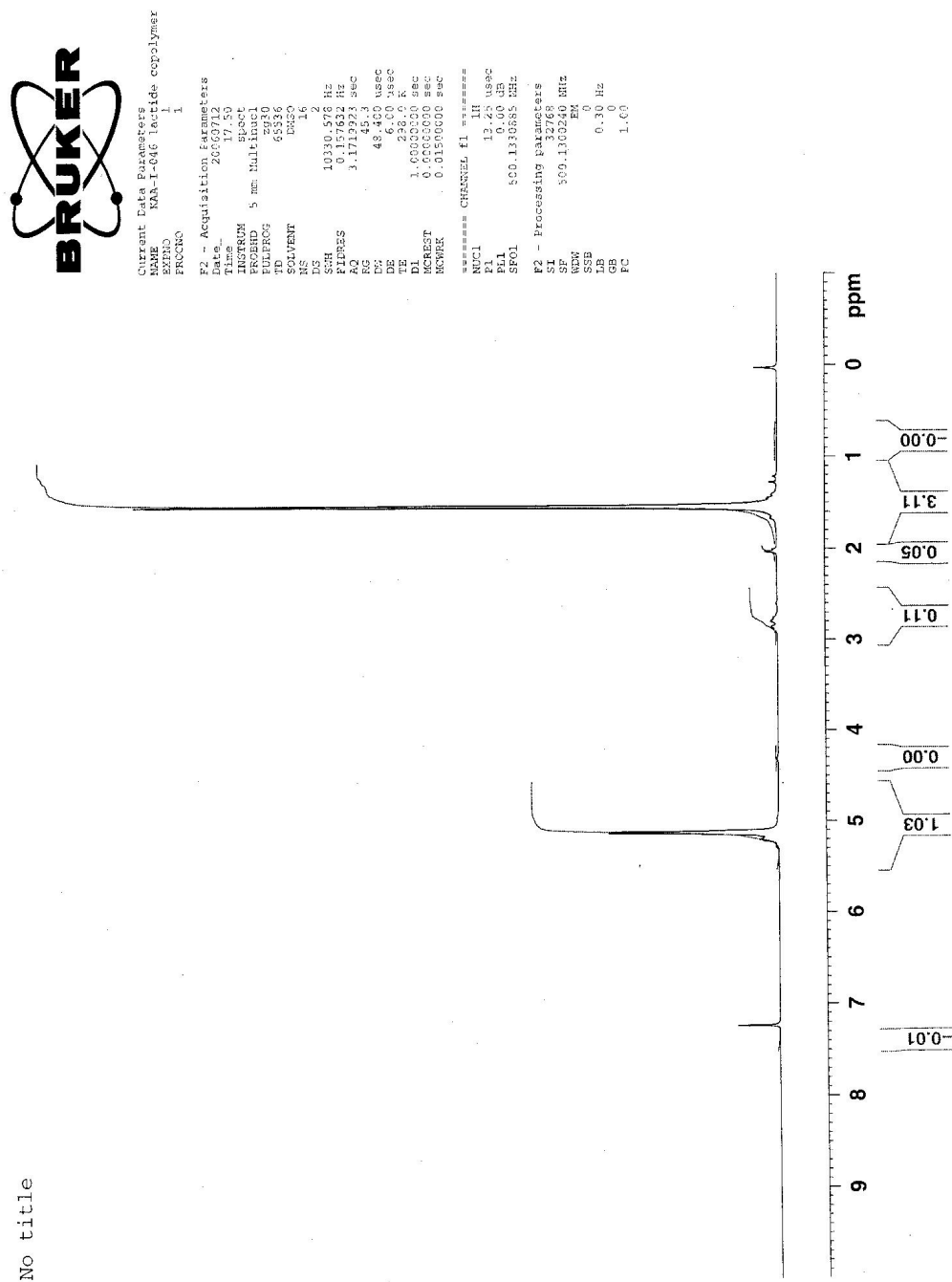


Figure B.12  $^{13}\text{C}$  NMR spectrum of lactide copolymer (300 MHz)

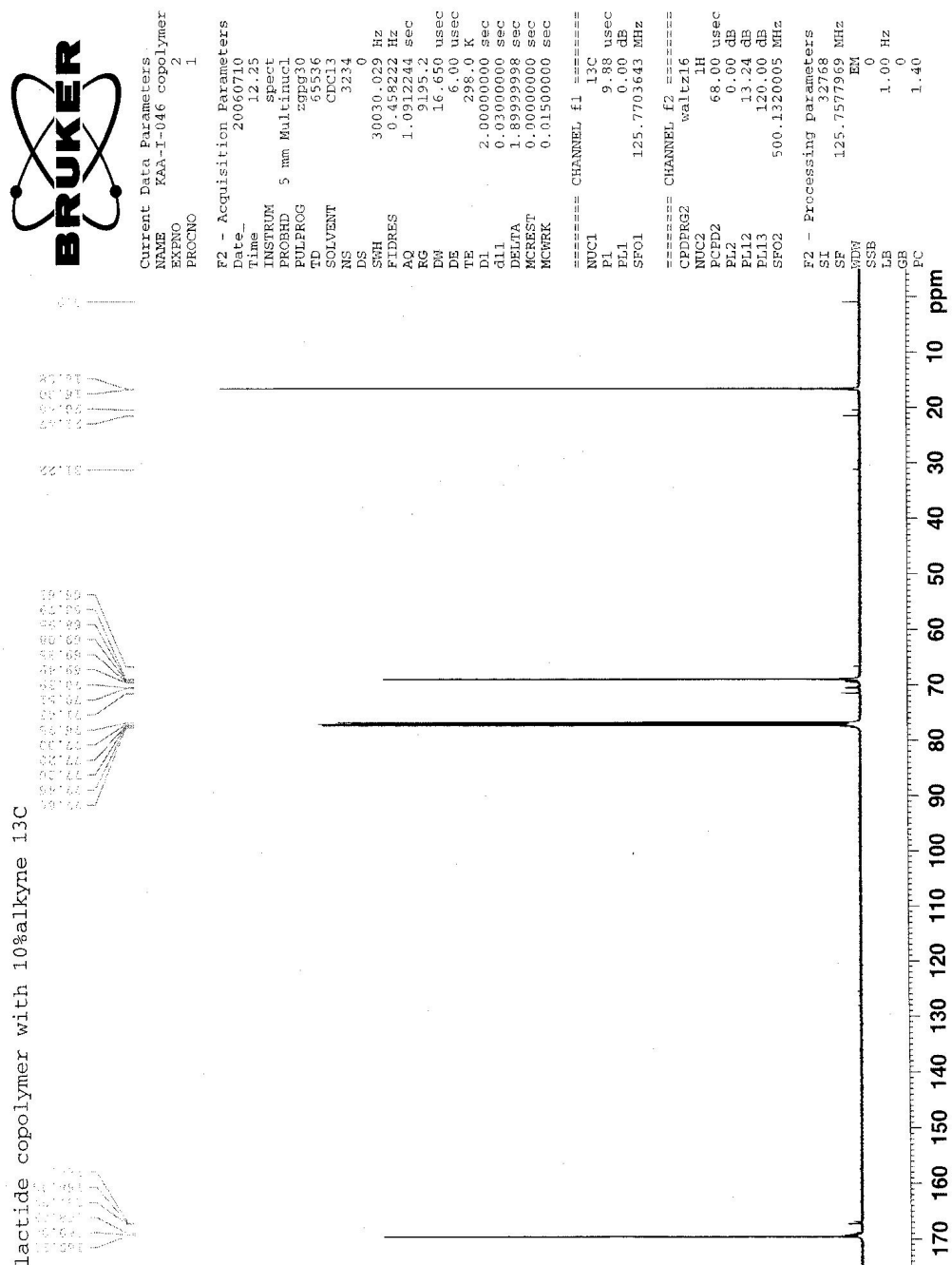


Figure B.13  $^{13}\text{C}$  NMR spectrum of lactide copolymer region 15ppm-31ppm (300 MHz)

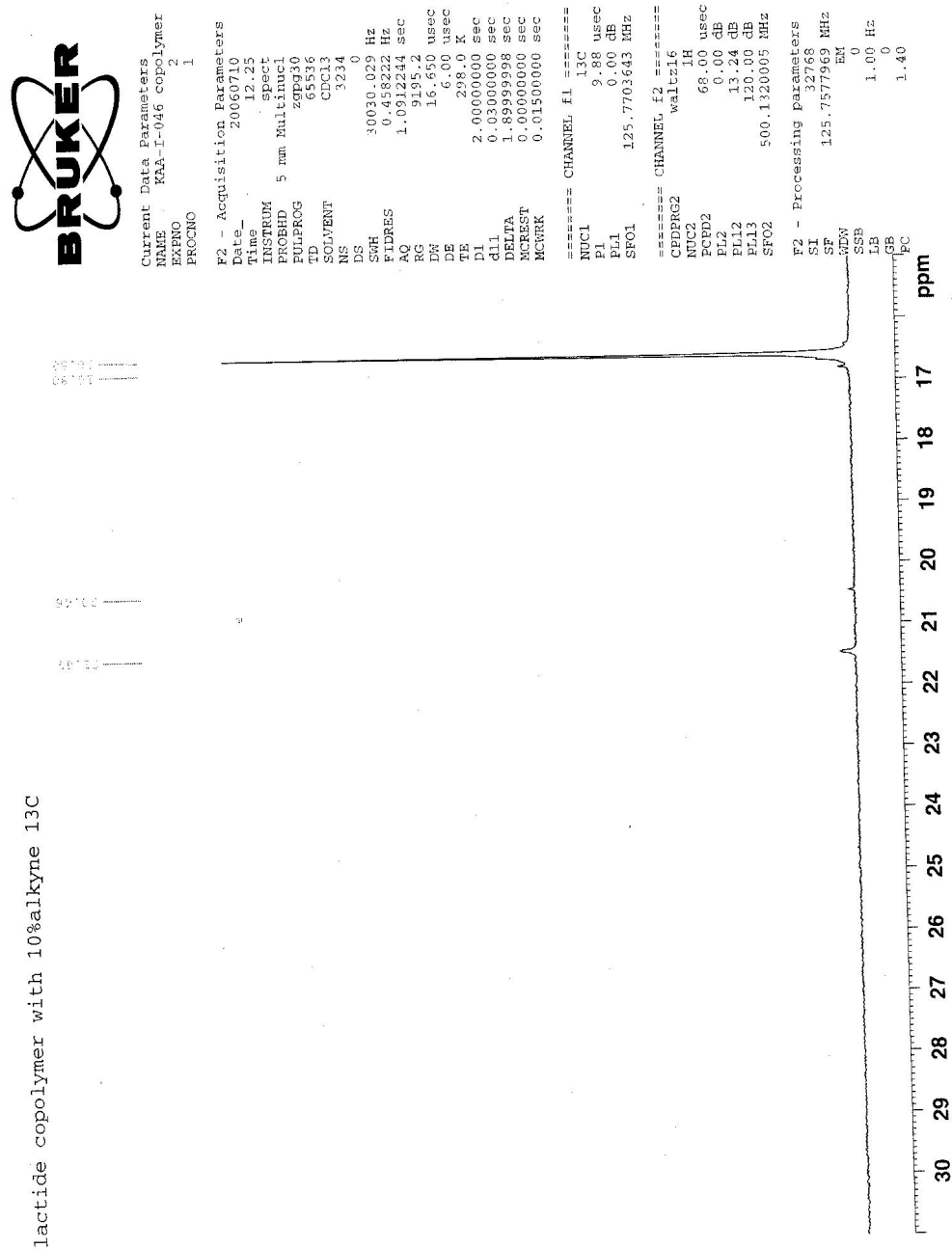


Figure B.14  $^{13}\text{C}$  NMR spectrum Lactide Copolymer region 66-80ppm (300 MHz)

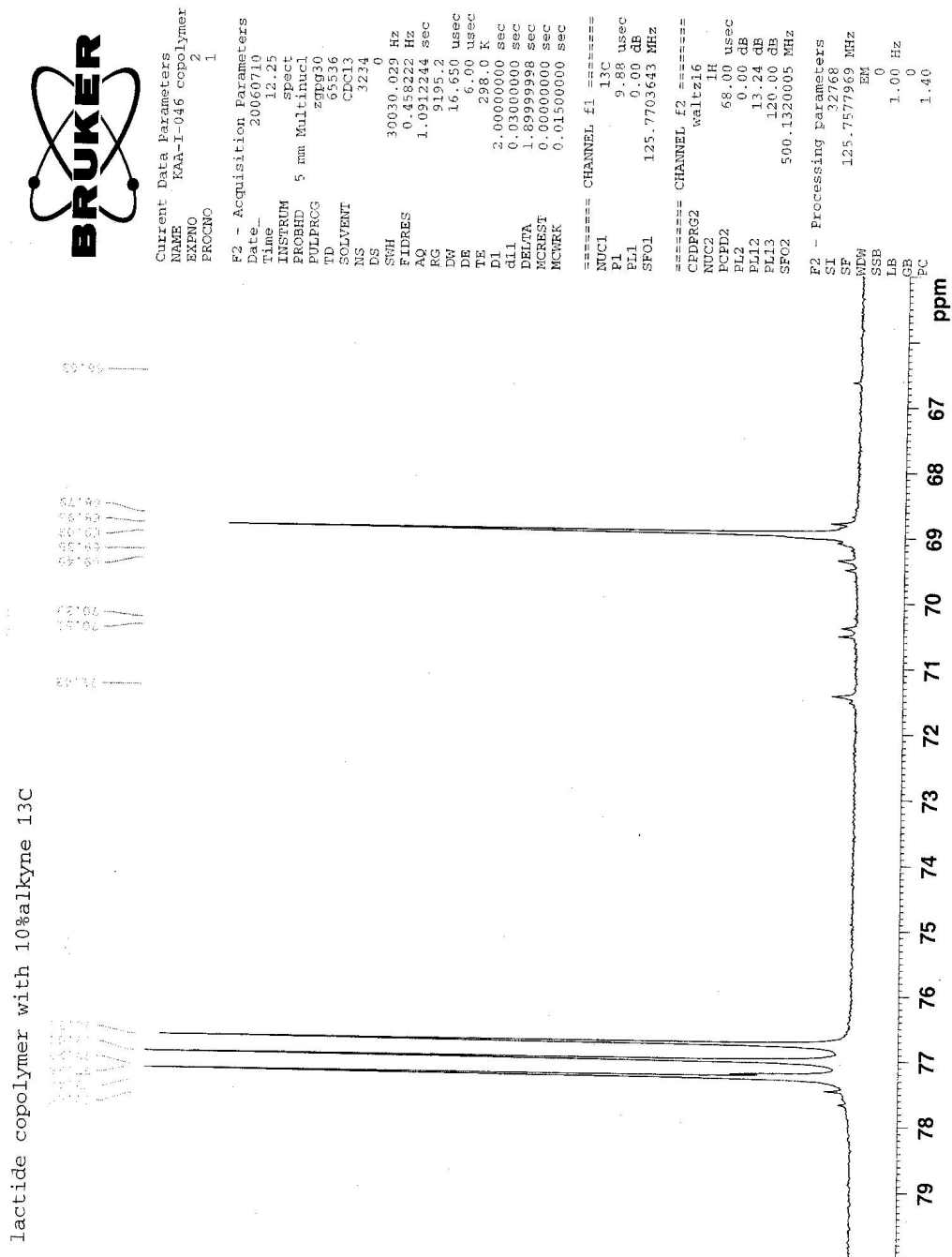
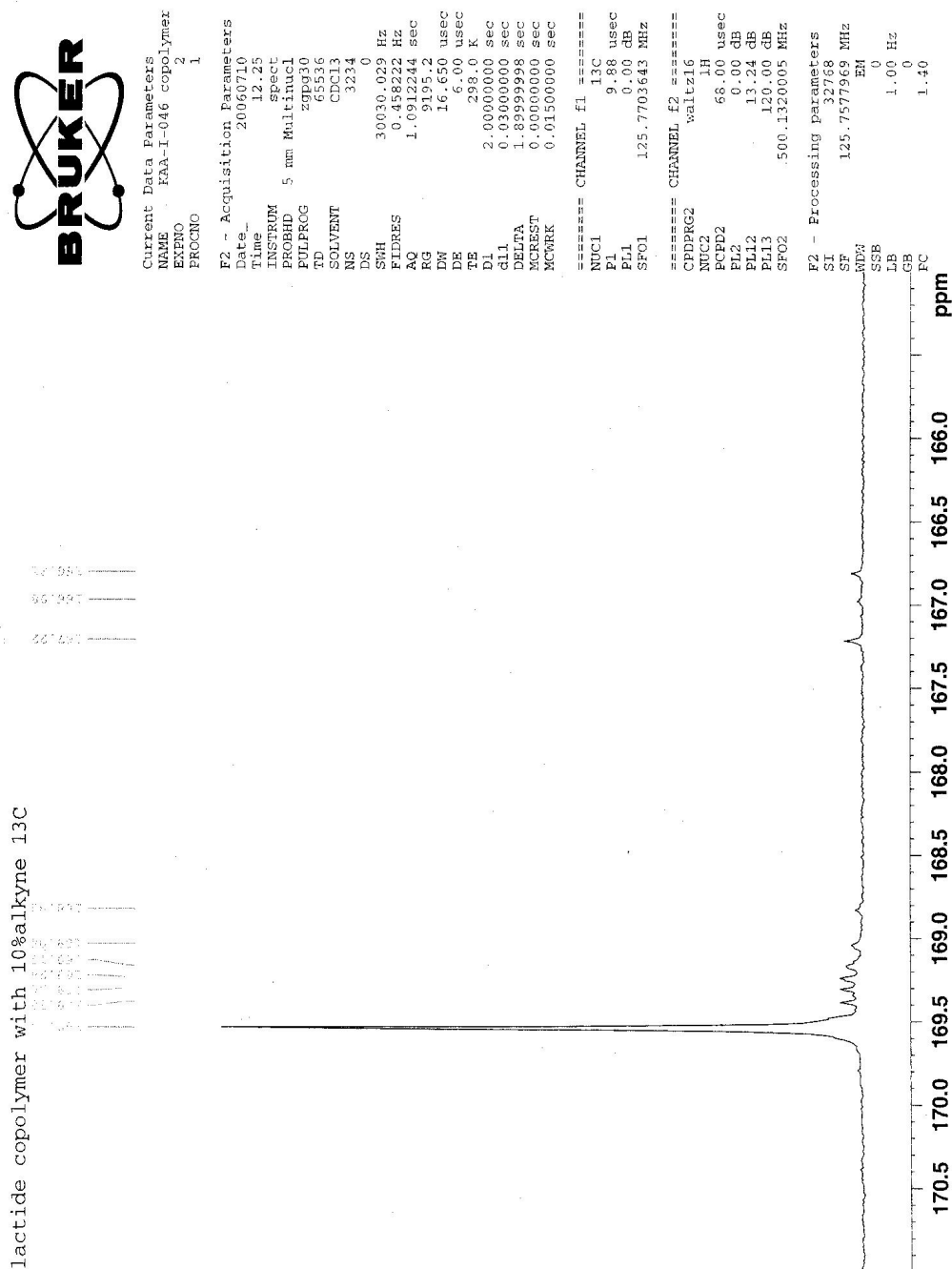


Figure B.15  $^{13}\text{C}$  NMR spectrum Lactide Copolymer 165-171ppm (300 MHz)





## REFERENCES

1. Lehn, J. M., Supramolecular Chemistry. *Science* **1993**, 260, (5115), 1762-1763.
2. Jorgensen, W. L., Supramolecular Chemistry. *Pro. Natl. Acad. Sci* **1993**, 90, (5), 1635-1636.
3. Sakurai, K.; Mizu, M.; Shinkai, S., Polysaccharide-Polynucleotide Complexes. 2. Complementary Polynucleotide Mimic Behavior of the Natural Polysaccharide Schizophyllan in the Macromolecular Complex with Single-Stranded RNA and DNA. *Biomacromolecules* **2001**, 2, (3), 641-650.
4. Lim, Y.; Moon, K.; Lee, M., Recent Advances in the Functional Supramolecular Nanostructures Assembled from Bioactive Building Blocks *Chem. Soc. Rev.* **2009**, 38, (4), 925-934.
5. Yang, Z.; Liang, G.; Wang, L.; Xu, B., Using a Kinase/Phosphatase Switch to Regulate a Supramolecular Hydrogel and Forming the Supramolecular Hydrogel in Vivo. *J. Am. Chem. Soc.* **2006**, 128, (9), 3038-3043.
6. Li, J.; Loh, X. J., Cyclodextrin-based Supramolecular Architectures: Synthesis, Structures, and Applications for Drug and Gene Delivery. *Adv. Drug Delivery Rev.* **2008**, 60, (9), 1000-1017.
7. Smith, D. K., A Supramolecular Approach to Medicinal Chemistry: Medicine Beyond the Molecule. *J. Chem. Educ.* **2005**, 82, (3), 393-400.
8. Koide, T.; Homma, D. L.; Asada, S.; Kitagawa, K., Self-complementary Peptides for the Formation of Collagen-like Triple Helical Supramolecules. *Bioorg. Med. Chem. Lett.* **2005**, 15, (23), 5230-5233.

9. Zhang, S., Fabrication of Novel Biomaterials Through Molecular Self-Assembly. *Nat. Biotechnol.* **2003**, 21, (10), 1171-1178.
10. Sanderson, J. M.; Yazdani, S., The Design, Synthesis and Characterisation of Channel-forming Peptides. *Chem. Commun.* **2002**, 10, 1154-1155.
11. Mart, R. J.; Osborne, R. D.; Stevens, M. M.; Ulijn, R. V., Peptide-based Stimuli-responsive Biomaterials. *Soft Matter* **2006**, 2, (10), 822-835.
12. Horton, H. R.; Moran, L. A.; Ochs, R. S.; Rawn, J. D.; Scrimgeour, K. G., *Principles of Biochemistry*, 3rd ed.; Prentice Hall: New Jersey, **2002**.
13. Schmidt, B.; Ho, L.; Hogg, P. J., Allosteric Disulfide Bonds. *Biochemistry* **2006**, 45, (24), 7429-7433.
14. Stendahl, J. C.; Rao, M. S.; Guler, M. O.; Stupp, S. I., Intermolecular Forces in the Self-Assembly of Peptide Amphiphile Nanofibers. *Adv. Funct. Mater.* **2006**, 16, (4), 499-508.
15. Zhao, X.; Zhang, S., Designer Self-Assembling Peptide Materials. *Macromol. Biosci.* **2007**, 7, (1), 13-22.
16. Wang, K.; Keasling, J. D.; Muller, S. J., Effects of the Sequence and Size of Non-polar Residues on Self-assembly of Amphiphilic Peptides. *Int. J. Biol. Macro.* **2005**, 36, (4), 232-240.
17. Nagai, Y.; Unsworth, L. D.; Koutsopoulos, S.; Zhang, S., Slow Release of Molecules in Self-assembling Peptide Nanofiber Scaffolds. *J. Controlled Release* **2006**, 115, (1), 18-25.
18. Hell, A. J. v.; Costa, C. I. C. A.; Flesch, F. M.; Sutter, M.; Jiskoot, W.; Crommelin, D. J. A.; Hennink, W. E.; Mastrobattista, E., Self-Assembly of

- Recombinant Amphilic Oligopeptides into Vesicles. *Biomacromolecules* **2007**, 8, (9), 2753-2761.
19. Palmer, L. C.; Stupp, S. I., Molecular Self-Assembly into One-Dimensional Nanostructures. *Acc. Chem. Res.* **2008**, 41, (12), 1674-1684.
20. Watson, J. D.; Crick, F. H. C., Molecular Structure of Nucleic Acids. *Nature* **1953**, 171, (4356), 737-738.
21. McGhee, A. M.; Kilner, C.; Wilson, A. J., Conformer Independent Heterodimerisation of Linear Arrays using Three Hydrogen Bonds. *Chem. Commun.* **2008**, 3, 344-346.
22. Dankers, P. Y. W.; Meijer, E. W., Supramolecular Biomaterials. A Modular Approach towards Tissue Engineering. *Bull. Chem. Soc. Jpn* **2007**, 80, (11), 2047-2073.
23. Pauling, L.; Corey, R. B., Configuration of Polypeptide Chains. *Nature* **1951**, 168, (4274), 550-551.
24. Pauling, L.; Corey, R. B., Two Hydrogen-Bonded Spiral Configurations of the Polypeptide Chain. *J. Am. Chem. Soc.* **1950**, 72, (11), 5349.
25. Wang, D.-A., Engineering Blood-contact Biomaterials by "H-Bonding Grafting" Surface Modification. *Adv. Poly. Sci.* **2007**, 209, 179-227.
26. Wisse, E.; Spiering, A. J. H.; van Leeuwen, E. N. M.; Renken, R. A. E.; Dankers, P. Y. W.; Brouwer, L. A.; Luyn, M. J. A. v.; Harmsen, M. C.; Sommerdijk, N. A. J. M.; Meijer, E. W., Molecular Recognition of Poly( $\epsilon$ -caprolactone)-Based Thermoplastic Elastomers. *Biomacromolecules* **2006**, 7, (12), 3385-3395.

27. Guan, Y.; Zhang, Y.; Zhou, T.; Zhou, S., Stability of Hydrogen-Bonded Hydroxypropylcellulose/poly(acrylic acid) Microcapsules in Aqueous Media. *Soft Matt.* **2009**, 5, (4), 842-849.
28. Zhao, W.; Chen, H.; Li, Y.; Li, L.; Lang, M.; Shi, J., Uniform Rattle-type Hollow Magnetic Mesoporous Spheres as Drug Delivery Carriers and Their Sustained-release Property. *Adv. Funct. Mater.* **2008**, 18, (18), 2780-2788.
29. Ashkenasy, N.; Horne, W. S.; Ghadiri, M. R., Design of Self-Assembling Peptide Nanotubes with Delocalized Electronic States. *Small* **2006**, 2, (1), 99-102.
30. Berg, J. M., Zinc Finger Domains, Hypotheses and Current Knowledge. *Ann. Rev. Biophys. Chem.* **1990**, 19, 405-421.
31. Constable, E. C., A New Twist to Self-Assembly. *Nature* **1990**, 346, 314-315.
32. Loeb, S. J., Rotaxanes as Ligands: From molecules to Materials. *Chem. Soc. Rev.* **2007**, 79, (2), 201-212.
33. Severin, K., Supramolecular Chemistry with Organometallic Half-sandwich Complexes. *Chem. Commun.* **2006**, 37, 2859-3867.
34. Kim, J. S.; Vicens, J., Progress of Calixcrowns Chemistry. *J. Incl. Phenom. Macrocycl. Chem.* **2009**, 63, (1-2), 189-193.
35. Maeda, H.; Furuta, H., A Dozen Years of N-Confusion: From Synthesis to Supramolecular Chemistry. *Pure Appl. Chem.* **2006**, 78, (1), 29-44.
36. Tsurkan, M. V.; Ogawa, M. Y., Metal-peptide Nanoassemblies. *Chem. Commun.* **2004**, 18, 2092-2093.
37. Pires, M. M.; Chmielewski, J., Self-assembly of Collagen Peptides into Microflorettes via Metal Coordination. *J. Am. Chem. Soc.* **2009**, 131, (7), 2706-2712.

38. Papaioannou, E. H.; Liakopoulou-Kyriakides, M.; Kyriakidis, D. A., Artificial Receptor for Peptide Recognition in Protic Media: The Role of Metal Ion Coordination. *Mater. Sci. Eng. B* **2008**, 152, (1-3), 28-32
39. Ghadiri, M. R.; Choi, C., Secondary Structure Nucleation in Peptides. Transition Metal Ion Stabilized  $\alpha$ -Helices. *J. Am. Chem. Soc.* **1990**, 112, (4), 1630-1632.
40. Ghadiri, M. R.; Fernholz, A. K., Peptide Architecture. Design of Stable  $\alpha$ -Helical Metallopeptides via a Novel Exchange-Inert Ru<sup>III</sup> Complex. *J. Am. Chem. Soc.* **1990**, 112, (26), 9633-9635.
41. Ghadiri, M. R.; Granja, J. R.; Milligan, R. A.; McRee, D. E.; Khazanovich, N., Self-assembling Organic Nanotubes Based on a Cyclic Peptide Architecture. *Nature* **1993**, 366, (6453), 324-327.
42. Khazanovich, N.; Granja, J. R.; McRee, D. E.; Milligan, R. A.; Ghadiri, M. R., Nanoscale Tubular Ensembles with Specified Internal Diameters. Design of a Self-Assembled Nanotube of 13-Å Pore. *J. Am. Chem. Soc.* **1994**, 116, (13), 6011-6012.
43. Ghadiri, M. R., Self-Assembled Nanoscale Tubular Ensembles. *Adv. Mater.* **1995**, 7, (7), 675-677.
44. Sanchez-Quesada, J.; Kim, H. S.; Ghadiri, M. R., A Synthetic Pore-Mediated Transmembrane Transport of Glutamic Acid. *Angew. Chem. Int. Ed.* **2001**, 40, (13), 2503-2506.
45. Engels, M.; Bashford, D.; Ghadiri, M. R., Structure and Dynamics of Self-Assembling Peptide Nanotubes and the Channel-Mediated Water Organization and Self-Diffusion. A Molecular Dynamics Study. *J. Am. Chem. Soc.* **1995**, 117, (36), 9151-9158.

46. Granja, J. R.; Ghadiri, M. R., Channel Mediated Transport of Glucose Across a Lipid Bilayer. *J. Am. Chem. Soc.* **1994**, 116, (23), 10785-10786.
47. Ghadiri, M. R.; Granja, J. R.; Buehler, L. K., Artificial Transmembrane Ion Channels from Self-Assembling Peptide Nanotubes. *Nature* **1994**, 369, (6478), 301-304.
48. Clark, T. D.; Buehler, L. K.; Ghadiri, M. R., Self-Assembling Cyclic  $\beta^3$ -Peptide Nanotubes as Artificial Transmembrane Ion Channels. *J. Am. Chem. Soc.* **1998**, 120, (4), 651-656.
49. Sanchez-Quesada, J.; Ghadiri, M. R.; Bayley, H.; Braha, O., Cyclic Peptides as Molecular Adaptors for a Pore-Forming Protein. *J. Am. Chem. Soc.* **2000**, 122, (48), 11757-11766.
50. Brea, R. J.; Vazquez, M. E.; Mosquera, M.; Castedo, L.; Granja, J. R., Controlling Multiple Fluorescent Signal Output in Cyclic Peptide-Based Supramolecular Systems. *J. Am. Chem. Soc.* **2007**, 129, (6), 1653-1657.
51. Horne, W. S.; Wiethodd, C. M.; Cui, C.; Wilcoxon, K. M.; Amorin, M.; Ghadiri, M. R.; Nemerow, G. R., Antiviral cyclic D,L- $\alpha$ -peptides: Targeting a General Biochemical Pathway in Virus Infections. *Bioorg. Med. Chem.* **2005**, 13, (17), 5145-5153.
52. Dartois, V.; Sanchez-Quesada, J.; Cabezas, E.; Chi, E.; Dubbelde, C.; Dunn, C.; Granja, J. R.; Gritzen, C.; Weinberger, D.; Ghadiri, M. R.; Jr., T. R. P., Systemic Antibacterial Activity of Novel Synthetic Cyclic Peptides. *Antimicrob. Agents Chemother.* **2005**, 49, (8), 3302-3310.

53. motesharei, K.; Ghadiri, M. R., Diffusion-Limited Size-Selective Ion Sensing Based on SAM-Supported Peptide Nanotubes. *J. Am. Chem. Soc.* **1997**, 119, (46), 11306-11312.
54. Yount, W. C.; Loveless, D. M.; Craig, S. L., Strong Means Slow: Dynamic Contributions to the Bulk Mechanical Properties of Supramolecular Networks. *Ange. Chem. Int. Ed.* **2005**, 44, (18), 2746-2748.
55. van Manen, H.-J.; Fokkens, R. H.; van Veggel, F. C. J. M.; Reinhoudt, D. N., Noncovalent Synthesis of Water-Soluble SCS Pd<sup>II</sup> Pincer Assemblies. *Eur. J. Org. Chem.* **2002**, 18, 3189.
56. Albrecht, M.; van Koten, G., Platinum Group Organometallics Based on "Pincer" Complexes: Sensors, Switches, and Catalysts. *Angew. Chem. Int. Ed.* **2001**, 40, (20), 3750-3781.
57. Rapaport, H.; Kim, H. S.; Kjaer, K.; Howes, P. B.; Cohen, S.; Als-Nielsen, J.; Ghadiri, M. R.; Leiserowitz, L.; Lahav, M., Crystalline Cyclic Peptide Nanotubes at Interfaces. *J. Am. Chem. Soc.* **1999**, 121, (6), 1186-1191.
58. Fernandez-Lopez, S.; Kim, H. S.; Choi, E. C.; Delgado, M.; Granja, J. R.; Khasanov, A.; Kraehenbuehl, K.; Long, G.; Weinberger, D. A.; Wilcoxon, K. M.; Ghadiri, M. R., Antibacterial Agents Based on the Cyclic D,L- $\alpha$ -peptide Architecture. *Nature* **2001**, 412, (6845), 452-456.
59. Hartgerink, J. D.; Granja, J. R.; Milligan, R. A.; Ghadiri, M. R., Self-Assembled Peptide Nanotubes. *J. Am. Chem. Soc.* **1996**, 118, (1), 43-50.
60. Fujimura, F.; Kimura, S., Columnar Assembly Formation and Metal Binding of Cyclic Tri- $\beta$ -peptides Having Terpyridine Ligands. *Org. Lett.* **2007**, 9, (5), 793-796.

61. Steinem, C.; Janshoff, A.; Vollmer, M. S.; Ghadiri, M. R., Reversible Photoisomerization of Self-Organized Cylindrical Peptide Assemblies at the Air-Water and Solid Interfaces. *Langmuir* **1999**, 15, (11), 3956-3964.
62. vollmer, M. S.; Clark, T. D.; Steinem, C.; Ghadiri, M. R., Photoswitchable Hydrogen-Bonding in Self-Organized Cylindrical Peptide Systems. *Angew. Chem. Int. Ed.* **1998**, 38, (11), 1598-1601.
63. Clark, T. D.; Buriak, J. M.; Kobayashi, K.; Isler, M. P.; McRee, D. E.; Ghadiri, M. R., Cylindrical  $\beta$ -Sheet Peptide Assemblies. *J. Am. Chem. Soc.* **1998**, 120, (35), 8949-8962.
64. Pollino, J. M.; Nair, K. P.; Stubbs, L. P.; Adams, J.; Weck, M., *Tetrahedron* **2004**, 60, (34), 7205-7213.
65. Gerhardt, W. W.; Weck, M., Invesitigation of Metal-Coordinated Peptides as Supramolecular Synthons. *J. Org. Chem.* **2006**, 71, (17), 6333-6341.
66. Manabe, S.; Ito, Y., Wang Resin-Type Linker Containing a Nitro Group for Polymer Support Oligosaccharide Synthesis: Polymer-Supported Glycosyl Donor. *Chem. Pharm. Bull.* **2001**, 49, (9), 1234-1235.
67. Arshady, R.; Ledwith, A.; Kenner, G. W., Phenolic Resins for Peptide Synthesis. 2. Reactivities of Phenolic and Amino Functional Groups in Styrene Based Resins. *Marcom. Chem. Phys.* **1981**, 182, (1), 41-46.
68. Sarin, V. K.; Kent, S. B. H.; Merrifield, R. B., Properties of Swollen Polymer Networks. Solvation and Swelling of Peptide-Containing Resins in Solid-Phase Peptide Synthesis. *J. Am. Chem. Soc.* **1980**, 102, (17), 5463-5470.



69. Atherton, E.; Fox, H.; Harkiss, D.; Logan, C. J.; Sheppard, R. C.; Williams, B. J., A Mild Procedure for Solid Phase Peptide Synthesis: use of Fluorenylmethoxycarbonylamino-acids. *J.C.S. Chem. Comm.* **1978**, 13, 537-539.
70. Backes, B. J.; Ellman, J. A., An Alkanesulfonamide "Safety-catch" Linker for Solid-Phase Synthesis. *J. Org. Chem.* **1999**, 64, (7), 2322-2330.
71. Gude, M.; J, R.; White, P. D., An Accurate Method for the Quantitation of Fmoc-derivatized Solid-Phase Supports. *Lett. Pep. Sci.* **2002**, 9, 203-206.
72. Gerhardt, W. W.; Zuccherro, A. J.; South, C. R.; Bunz, U. H. F., Controlling Polymer Properties Through Dynamic Metal-Ligand Interactions: Supramolecular Cruciforms Made Easy. *Chem. Eur. J.* **2007**, 13, (16), 4467-4474.
73. South, C.; Weck, M., Bridged Coordination Polymer Multilayers with Tunable Properties. *Langmuir* **2008**, 24, (14), 7506-7511.
74. Cohn, D.; Saloman, A. H., Designing Biodegradable Multiblock PCL/PLA Thermoplastic Elastomers. *Biomaterials* **2005**, 26, (15), 2297-2305.
75. Noga, D. E.; Petrie, T. A.; Kumar, A.; Weck, M.; Garcia, A. J.; Collard, D. M., Synthesis and Modification of Functional Poly(lactide) Copolymers: Toward Biofunctional Materials. *Biomacromolecules* **2008**, 9, (7), 2056-2062.
76. Dechy-Cabaret, O.; Martin-Vaca, B.; Bourissou, D., Controlled Ring-Opening Polymerization of Lactide and Glycolide. *Chem. Rev.* **2004**, 104, (12), 6147-6176.
77. Wang, Y.; Noga, D. E.; Yoon, K.; Wojtowicz, A. M.; Lin, A. S. P.; Garcia, A. J.; Collard, D. M.; Weck, M., Highly Porous Corsslinkable PLA-PNB Block Copolymer Scaffolds. *Adv. Funct. Mater.* **2008**, 18, 3638-3644.

78. Nam, Y. S.; Park, T. G., Biodegradable Polymeric Microcellular Foams by Modified Thermally Induced Phase Separation Method. *Biomaterials* **1999**, 20, (19), 1783-1790.
79. Lutz, J., 1,3-Dipolar Cycloadditions of Azides and Alkynes: A Universal Ligation Tool in Polymer and Materials Science. *Angew. Chem. Int. Ed.* **2007**, 46, (7), 1018-1025.
80. Jiang, X.; Vogel, E. B.; III, M. R. S.; Baker, G. L., "Clickable" Polyglycolides: Tunable Synthons for Thermoresponsive, Degradable Polymers. *Macromolecules* **2008**, 41, (6), 1937-1944.